THESIS

# A COMPARISON OF THE NAVY AEROSOL ANALYSIS AND PREDICTION SYSTEM TO IN SITU AEROSOL MEASUREMENTS IN THE CONTINENTAL U.S.: TRANSPORT VS. LOCAL PRODUCTION OF SOIL DUST AEROSOL

Submitted by

Kelley C. Johnson

Department of Atmospheric Science

In partial fulfillment of the requirements

For the Degree of Master of Science

Colorado State University

Fort Collins, Colorado

Summer 2006

ABSTRACT OF THESIS

A COMPARISON OF THE NAVY AEROSOL ANALYSIS AND PREDICTION SYSTEM TO IN SITU AEROSOL MEASUREMENTS IN THE CONTINENTAL U.S.: TRANSPORT VS. LOCAL PRODUCTION OF SOIL DUST AEROSOL

Atmospheric soil dust aerosol can affect health, air quality, and visibility on both regional and global scales. The Navy Aerosol Analysis and Prediction System (NAAPS) was developed at the Naval Research Laboratory in Monterey, California to predict global concentrations of dust and other atmospheric aerosols, as they can adversely affect U.S. Navy operations throughout the world. Although dust sources in North Africa and Asia are the major contributors to the atmospheric dust burden, dust aerosol sources have also been identified in the western U.S. and northern Mexico (Prospero et al., 2002). Additionally, the impact of Asian dust plumes has been observed throughout the continental U.S. year-round (VanCuren and Cahill, 2002); the presence of Saharan dust has also been observed in the eastern U.S. in summer (Perry et al., 1997). This study combines aerosol data from the Interagency Monitoring of Protected Visual Environments (IMPROVE) network with NAAPS soil dust aerosol predictions to examine observations of soil dust over the continental U.S. from 2001 to 2004. Two model simulations were performed for this entire period: one in which all dust sources were active, and another in which North American dust sources were suppressed.

Comparisons of the 2001-2004 NAAPS predictions of surface dust concentration to IMPROVE [$PM_{10}$-$PM_{2.5}$]+[Soil] measurements were carried out for 28 sites

throughout the U.S. Relative frequencies of the model predictions that fell within a factor of two of the IMPROVE measurements were 39%, 45%, 33% and 30% for winter, spring, summer, and fall, respectively. The correspondence fared best in spring when NAAPS predicted the widest influence of non-North American soil dust at the surface in the U.S. Overall, the model showed good skill at reproducing the timing of Asian dust incursions in the U.S. in spring. However, median ratios of NAAPS-to-IMPROVE surface dust concentrations indicated a persistent bias toward ratios less than one at coastal and some inland sites. Further analyses using speciated IMPROVE $PM_{10}$ data at select sites for 2004 indicated that many of these locations were impacted by sea salt and other sources of coarse-mode particulate matter that biased the IMPROVE soil estimate too high. Ratios greater than one were realized at other sites, depending upon the season and site altitude. An examination of these occurrences suggested agreement between the NAAPS predictions and *in situ* data could be improved by adjusting the model transport and deposition schemes, and by incorporating snow cover data, variable threshold friction velocities, and agricultural sources of dust.

Kelley C. Johnson
Department of Atmospheric Science
Colorado State University
Fort Collins, CO 80523
Summer 2006

ACKNOWLEDGEMENTS

I would like to thank Marcin Witek for running the NAAPS simulations used in this study and for his generous help in processing and analyzing model output. Many thanks also to Dr. Douglas Westphal and Dr. Piotr Flatau for initiating this collaboration and for their many ideas, suggestions, critiques and support. I also thank Dr. Jenny Hand for supplying speciated IMPROVE $PM_{10}$ data and Dr. Bret Schichtel for his suggestions and help in interpreting IMPROVE data flags and reporting procedures.

I thank my committee members, Dr. Richard Johnson and Dr. Jerry Magloughlin, for their expertise and help in refining this work. I extend my utmost thanks also to my advisor, Dr. Sonia Kreidenweis, for her countless ideas, wise guidance, encouragement, and sense of humor. Finally, I thank my family for their continued support and praise, and John for his patience and many sacrifices made for my sake.

This work was supported by the DoD Center for Geosciences/Atmospheric Research at Colorado State University under Cooperative Agreement DAAD19-02-2-0005 with the Army Research Laboratory.

TABLE OF CONTENTS

# LIST OF FIGURES

# 1 Introduction

Atmospheric aerosols can have a marked impact on health, air quality, and visibility on both global and regional scales. Furthermore, the role of aerosols in the global energy budget has been examined in many observational and modeling studies, and their estimated radiative forcing can be similar in magnitude to that of greenhouse gases (IPCC, 2001). While many studies have focused on particulate sulfate and black carbon, natural atmospheric aerosols such as mineral dust compose a large fraction of the total atmospheric aerosol mass loading, and their impact is not as well understood. Between 1000 and 3000 Tg of dust are emitted into the atmosphere each year (Duce, 1995), exerting the largest annual mean direct radiative effect of all aerosol types over ocean at solar wavelengths (Myhre et al., 2004). Additionally, soil dust aerosols typically lie in a larger size mode than anthropogenic species; their larger size enables them to exert a significant longwave radiative effect (Haywood et al., 2005). Dust is frequently transported far from its region of origin, providing a source of nutrients to ocean biota (Duce, 1995) and possibly enhancing the formation of ice clouds at warmer temperatures (Sassen, 2002). At the Earth's surface, dust storms frequently lead to the exceedance of air quality standards in the U.S. (Reid et al., 1994; Prospero et al., 2002) and inhibit U.S. military operations in the Middle East and around the globe.

## 1.1 Overview of Soil Dust Aerosol

### 1.1.1 Production and Characteristics

Atmospheric soil dust aerosol is created primarily through a mechanical process known as saltation. Friction from high surface wind speeds causes soil particles to bounce, resulting in a transfer of momentum through collisions between particles that ultimately leads to their emission from the surface (Gillette, 1978). The size of emitted soil particles can range from about 0.2 to 100 μm in diameter (Duce, 1995), and will vary as a function of many variables such as soil composition, soil moisture content, vegetation, and wind velocity (Ginoux et al., 2001). An aerosol volume distribution derived from optical measurements over the Gobi desert is shown in Figure 1.1 (Eck et al., 1999). This bimodal distribution is commonly observed in measurements of atmospheric aerosols; the peak at particle sizes below 1 μm (radius) is referred to as the fine mode; the peak at larger aerosol sizes is referred to as the coarse mode. Unlike those for anthropogenic and biomass burning aerosols, coarse mode mass concentrations tend to be significantly higher than those in the fine mode for soil dust aerosols over desert surfaces (Figure 1.1), given that large particles exist near dust source regions.

Although very large particles can be emitted from dust sources, particles with diameters larger than 12 μm have very short lifetimes (a few hours or less) due to gravitational settling (Tegen and Fung, 1994). Particles smaller than 12 μm in diameter can, on the other hand, be transported large distances. Saharan dust, for example, has been observed in the U.S. (Perry et al., 1997; Sassen et al., 2003); other studies have confirmed the transport of Asian dust across the Pacific (Duce et al., 1980; Shaw, 1980;

Thulasiraman et al., 2002). The observed size distribution of dust that has been transported large distances tends to be dominated by smaller particles. In the Big Bend Regional Aerosol and Visibility Observational (BRAVO) Study at Big Bend National Park, Texas in 1999, the influence of Saharan dust during the months of July and August resulted in an average coarse mode geometric volume mean diameter of ~2.5 μm. As shown in Figure 1.2, this value increased steadily during the remaining months of the study, corresponding to a diminishing influence of North African dust on the coarse mode properties (Hand et al., 2002) relative to the summer months. The processes leading to the long-range transport of soil dust aerosol will be discussed in the following section.

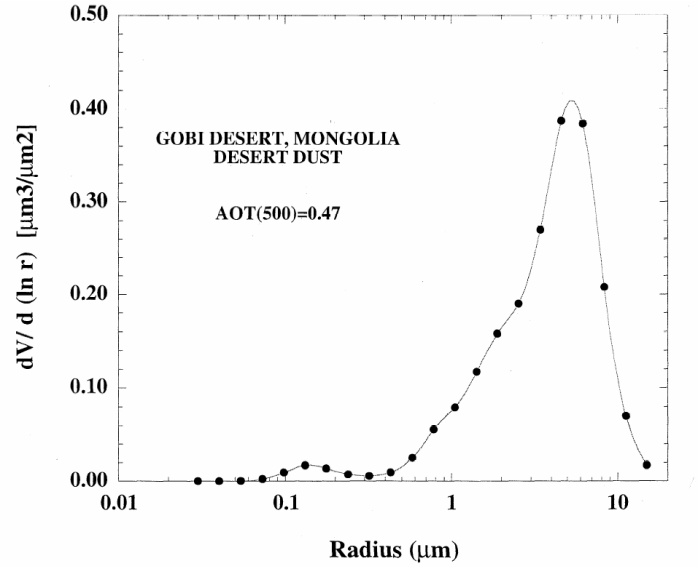


**Figure 1.1: Aerosol volume distribution for desert dust aerosols at Dalanzadgad, Mongolia on 18 April 1998 0955 UTC (Eck et al., 1999).**

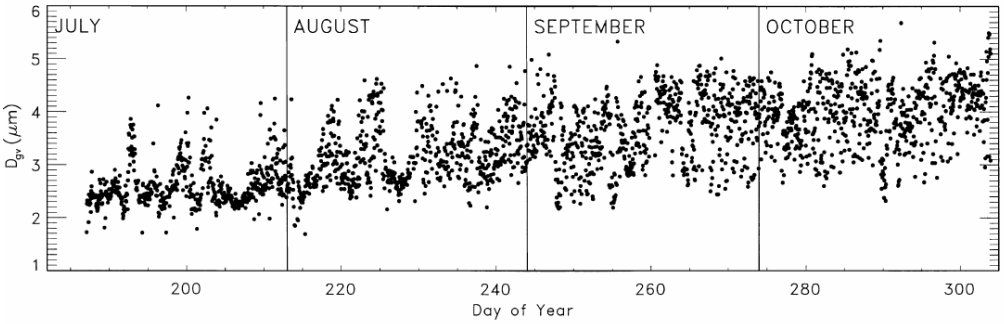


**Figure 1.2: Time series of dry coarse mode geometric volume mean diameter (μm) for Big Bend National Park, Texas (Hand et al., 2002).**

### 1.1.2 Sources and Transport

Although the actual locations and strengths of dust aerosol source regions are not well-defined, data suggest that the majority of airborne dust originates in topographical depressions or closed intermontane basins, where alluvial flow is collected from salt playas and the erosion of dry lake beds, and annual precipitation is low (Prospero et al., 2002). Aridity alone has not been found to be a good indicator of dust source location; for example, dust emissions from Australia are relatively low, despite the fact that the continent is over 1/3 desert (Prospero et al., 2002). Furthermore, some assert that 20-50% of the global atmospheric dust burden is a result of land-use changes such as overgrazing and deforestation (Tegen and Fung, 1995), adding to the uncertainty in dust source characterization.

With the aforementioned caveats in mind, several dust source maps have been constructed for use in modeling studies. Although there is variation among these profiles, the relative locations of major dust-producing regions in each are generally consistent. The global dust emission profile used in the Georgia Tech/Goddard Global Ozone Chemistry Aerosol Radiation and Transport (GOCART) model (Ginoux et al., 2001) is shown in Figure 1.3. Estimations of the contribution of specific source regions using an AGCM are listed in Table 1.1.

| Region | Annual Average Contribution to Global Dust Emission (%) |
|---|---|
| Sahara/Sahel | 50.7 |
| Central Asia | 16.0 |
| Australia | 14.5 |
| North America | 5.2 |
| East Asia | 4.9 |
| Arabia | 4.2 |

**Table 1.1: Annual average regional soil dust emission contributions estimated in an AGCM (Miller et al., 2004).**

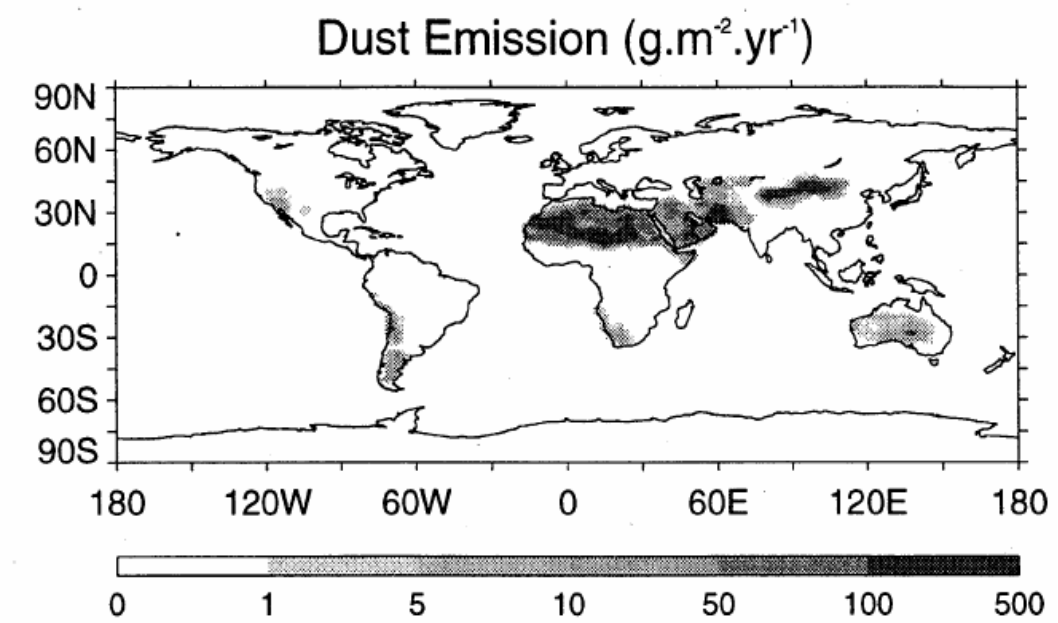

**Figure 1.3: Annual soil dust emission from 1987-1990 in GOCART (Ginoux et al., 2001).**

#### 1.1.2.1 The Global Dust Belt

The vast majority of atmospheric mineral dust is formed and transported in the Northern Hemisphere, in a region referred to by Prospero et al. (2002) as the "Global Dust Belt." The region is composed of dust sources in (and transport from) North Africa, Arabia, the Indian subcontinent, and Asia. Each region is somewhat unique in its source characterization and in the seasonality of its soil dust aerosol production. Since North America's contribution to the total atmospheric dust burden is relatively small, it is not considered to be a source region in the Global Dust Belt.

The largest contributor to the Global Dust Belt is the Sahara/Sahel region in North Africa (Table 1.1). Source regions in eastern Algeria, Tunisia, Libya and Egypt frequently impact the Mediterranean in late spring/early summer, but the most intense dust source in this region (and in the world) is the Lake Chad Basin and the Bodele Depression in central North Africa (Prospero et al., 2002). TOMS Aerosol Index (AI), a

satellite product used as a measure of column aerosol absorption at UV wavelengths (see Section 1.2.1) is consistently at a maximum directly over the lowest portion of the Bodele Depression, and satellite images frequently indicate plumes of dust from this region extending all the way to South America and the eastern U.S. There is evidence that these dust sources are active throughout the year, though their activity reaches a peak from April-September. During this time, rapid daytime convective mixing results in a deep boundary layer (extending to the height of the 600 millibar level on average (Parker et al., 2005)) in which soil dust aerosol can be distributed vertically. The majority of Saharan dust lofting occurs north of 15º N, where annual rainfall is less than 200 mm (Prospero et al., 2002).

Once lofted, North African dust is transported westward along the southern branch of the semi-permanent Bermuda high at an altitude of 3-5 km (Karyampudi et al., 1999), reaching South America in the winter months. This pattern shifts to the north with the displacement of the ITCZ during the Northern Hemisphere summer (Ginoux et al., 2001); North African dust plumes reach the United States during this time as they circulate in a clockwise direction around the Bermuda high. Typical transport pathways of North African dust over the eastern U.S. are shown in Figure 1.4. According to observations, significant Saharan dust incursions occur approximately three times per year in the U.S., generally in July or August. They persist for ~10 days apiece and often lead to 24-hour surface fine ($D_p < 2.5$ μm) soil mass concentrations above 10 μg $m^{-3}$ at sites throughout the eastern U.S. (Perry et al., 1997), and sometimes affecting fine soil mass as far as western Texas (Hand et al., 2002).

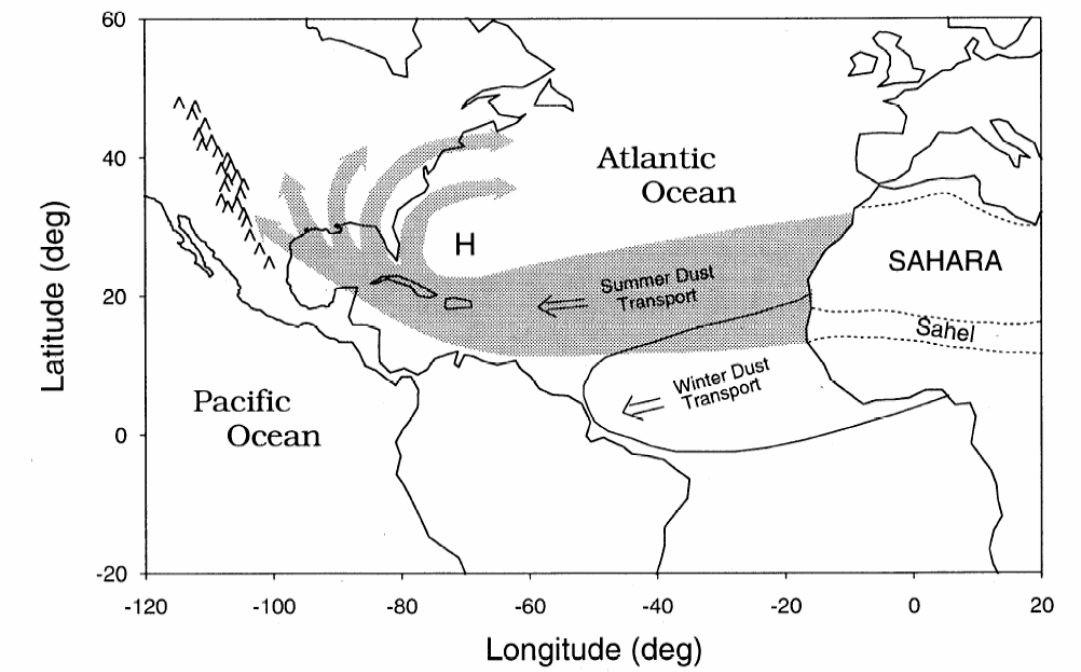


**Figure 1.4: Conceptual model of North African dust transport pathways to the United States (Perry et al., 1997).**

In Asia, the Takla Makan and Gobi deserts are major sources of atmospheric mineral dust. Dust particles are mobilized over the Gobi by high wind speeds and frontal lifting associated with cold low-pressure systems (Husar et al., 2001). This production occurs most often in spring, before the summer monsoon season commences (Prospero et al., 2002). Trans-Pacific transport of Asian dust can occur year-round, but also reaches a maximum in spring; dust has long been observed in this season over Korea and Japan, and has been detected in April and May in the North Pacific (Duce et al., 1980), Hawaii (Shaw, 1980), and over the western U.S. (Husar et al., 2001; Thulasiraman et al., 2002). Studies invoking a chemical signature for Asian dust have even been used to argue the presence of Asian dust as far east as the New England states (VanCuren and Cahill, 2002), at levels of 0.2 to 1.0 μg $m^{-3}$ averaged over 24 hours, and in the Greenland ice core (Biscaye et al., 1997). The height at which trans-Pacific transport of Asian dust occurs is uncertain; estimates place the dust cloud well above the marine boundary layer based

upon its relatively short (5-6 days) transport time across the North Pacific (Husar et al., 2001). Studies have found the dust lifted to a level between the 400 and 500 millibar levels (Merrill et al., 1989), whereas simulations suggest transport is maximized anywhere from the 800 (Ginoux et al., 2001) to 100 mb levels (Tegen and Fung, 1994). A climatological simulation for 1960-2003 found Asian dust transport across the Pacific to peak between 3 and 10 km in height, along a zonal axis at 40º N (Zhao et al., 2006). The zonal dust flux (μg $m^{-2}$ $s^{-1}$) between these levels for the 44-year simulation appears in Figure 1.5.

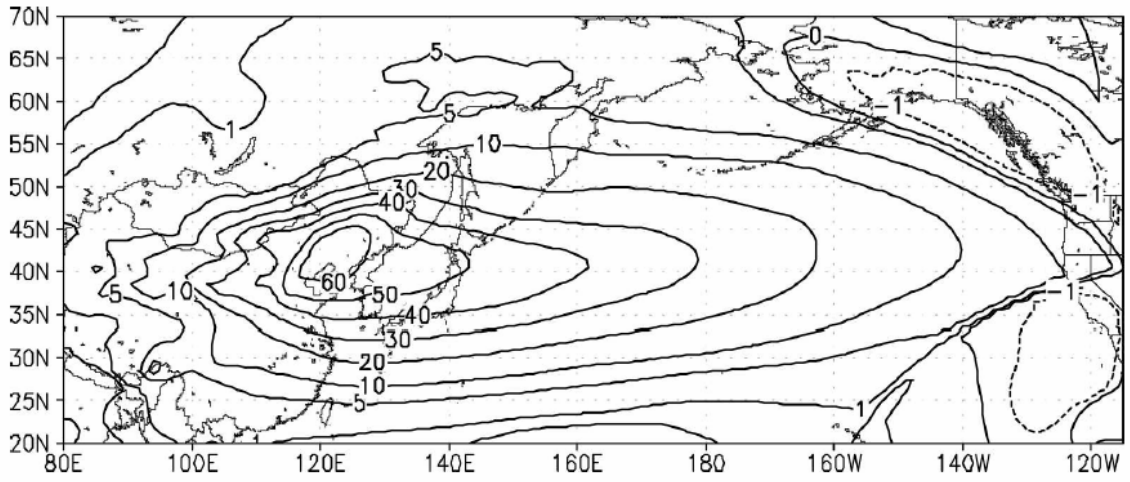


**Figure 1.5: Average zonal dust transport flux (μg $m^{-2}$ $s^{-1}$) between 3 and 10 km simulated for 1960 to 2003 (Zhao et al., 2006).**

### 1.1.2.2 North American Dust Sources

Although their contribution is small on a global scale (Prospero et al., 2002), a number of dust aerosol sources exist in North America, specifically in the western United States and northern Mexico. Prospero et al. (2002) argue that dust sources exist in basin regions between the Rocky and Sierra Nevada mountain ranges, north of the Mojave Desert and the Colorado Plateau. The area west and southwest of Great Salt Lake, Utah is one of significant dust activity, as are regions of the Salton Trough in southern

California/northern Mexico (Prospero et al., 2002). Owens lake, a lake east of the Sierra Nevada Mountains that was left barren due to water diversion in the 1930s, has been shown to be one of the largest sources of dust in North America (Reid et al., 1994). A map of North American soil dust sources identified by Prospero et al. (2002) is shown in Figure 1.6. Dust activity reaches a maximum in this region in May-June, when more sustained southwesterly surface flow sets in. The dust production spreads northward in June and July as this flow pattern persists (Prospero et al., 2002). A study of dust transport to the Grand Canyon from 1984 to 1989 confirmed this. Figure 1.7 shows that high measured coarse mass at Hopi Point, Arizona corresponded with air parcels having a significantly high confidence of a sustained residence time to the southwest (over southern California), whereas periods of low coarse mass showed a significantly high confidence of transport from the north or south (Vasconcelos et al., 1996).

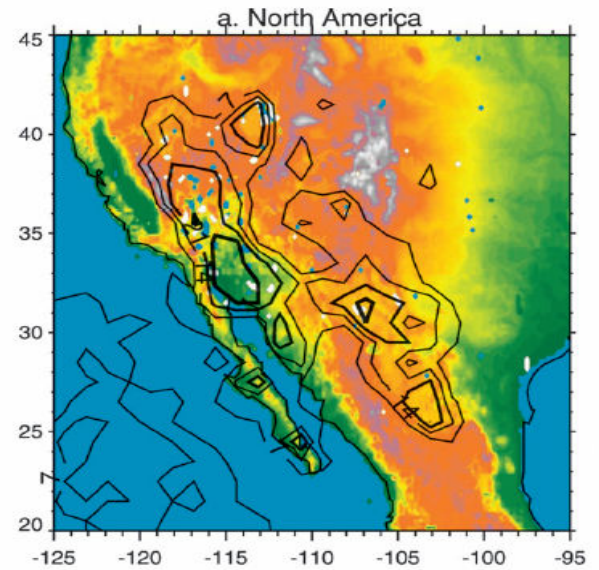


**Figure 1.6: North American dust sources indicated by TOMS Aerosol Index (AI), plotted as frequency of days per month when TOMS AI equals or exceeds 0.7 (Prospero et al., 2002). Warm colors refer to higher elevations, cool colors to lower elevations.**

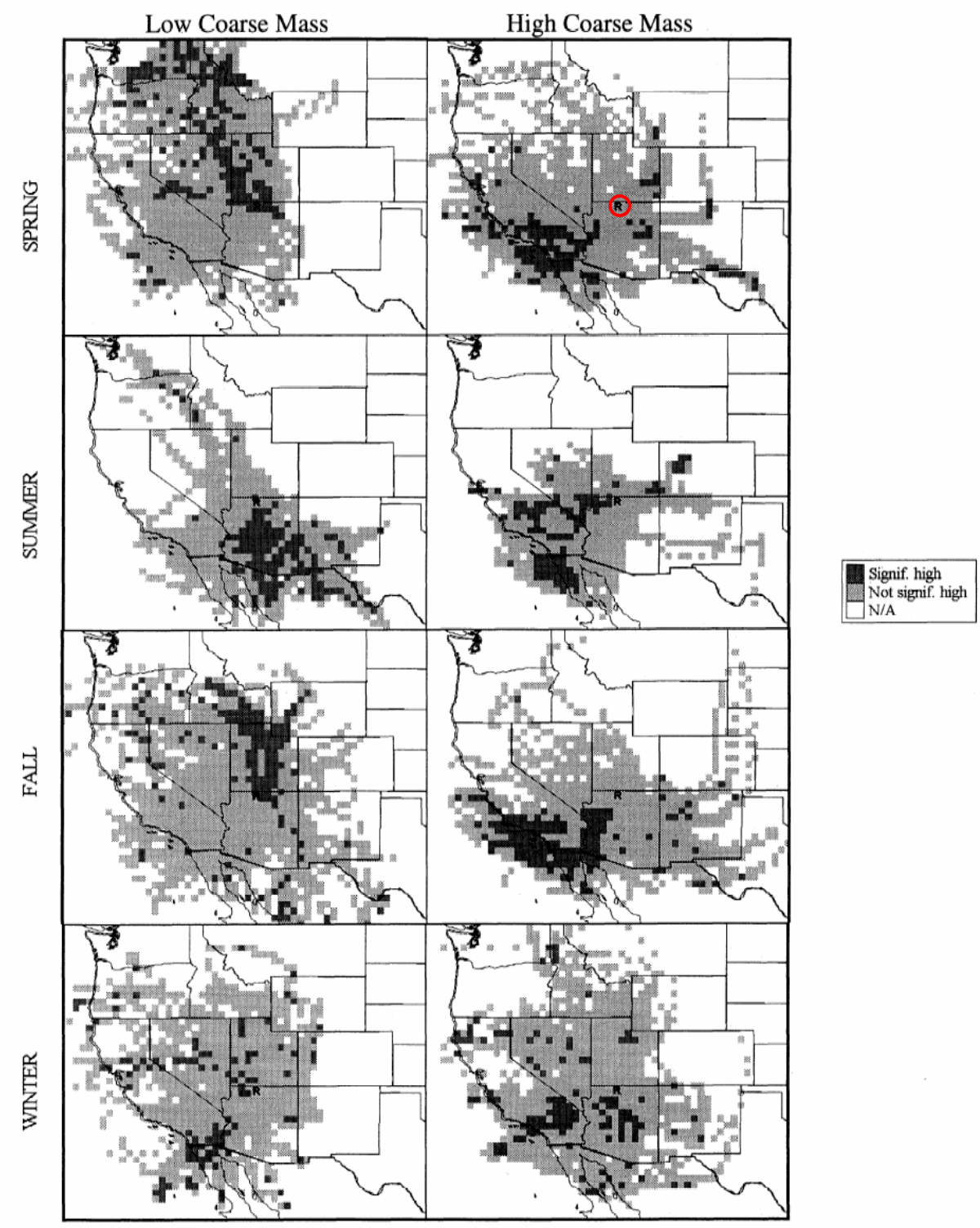


**Figure 1.7: Significance of conditional frequencies for parcels arriving at Hopi Point with low and high coarse mass concentrations. The receptor site is indicated by the "R" (Vasconcelos et al., 1996).**

## 1.2 Determination of Aerosol Properties

### 1.2.1 Optical Properties

The optical properties of aerosols can be examined remotely using satellites and ground-based sensors. A common aerosol product used by the remote sensing community to infer aerosol amount in the atmosphere is aerosol optical depth. Aerosol optical depth, $\tau_a$, is a unitless quantity defined by Equation (1.1)

$$\tau_a = \int_0^{z^*} b_{ext} \cdot dz \tag{1.1}$$

where $b_{ext}$ represents the aerosol extinction coefficient, $dz$ is the path length through the atmosphere, and $z^*$ is generally defined as the height of the top of the atmosphere. The extinction coefficient is a function of particle size, particle refractive index, $m$, and the wavelength of incident light, $\lambda$. For a population of different-sized particles of the same refractive index, $b_{ext}$ is given by Equation (1.2)

$$b_{ext}(\lambda) = \int_0^{D_p^{\max}} \frac{\pi D_p^{\,2}}{4} Q_{ext}(m,\alpha) n(D_p) dD_p \tag{1.2}$$

where $D_p^{max}$ is the upper limit diameter for the population, and $Q_{ext}$ is a dimensionless extinction efficiency, which is a function of refractive index and the size parameter, α ($\pi D_p/\lambda$). Soil dust aerosol exhibits the largest $b_{ext}$ of all aerosol species at visible wavelengths and, consequently, is associated with the largest shortwave optical depth values, according to satellite observations (Haywood et al., 2005).

The extent to which a particle extinguishes incident radiation is a function of that particle's ability to both scatter and absorb ($b_{ext} = b_{sca} + b_{abs}$). Since aerosol absorption could lead to local atmospheric heating, and aerosol optical depth is only a function of the

total extinction due to aerosols, it is useful to have an additional parameter by which to determine the amount of scattering relative to the amount of absorption due to aerosols. This is defined in terms of the single-scattering albedo, $\omega$, which, as defined by Equation (1.3), is a ratio of the scattering to extinction efficiencies

$$\omega(\lambda) = \frac{Q_{scat}}{Q_{ext}} \tag{1.3}$$

A single-scattering albedo of 1.0 corresponds to an aerosol that is purely scattering at a certain wavelength; a value less than 1.0 designates aerosols that absorb some portion of incident radiation. Single-scattering albedo values can depend strongly on the wavelength of incident radiation; values for dust aerosol contain further uncertainty since they depend on the mineral composition of the soil, which varies throughout the globe (Sokolik and Toon, 1999). Single-scattering albedo estimates for dust particles of 1 μm radius (Figure 1.8) range from purely scattering to weakly absorbing at visible wavelengths and moderately to strongly absorbing at UV and mid-IR wavelengths, depending on the aerosol mineral type (Weaver et al., 2002).

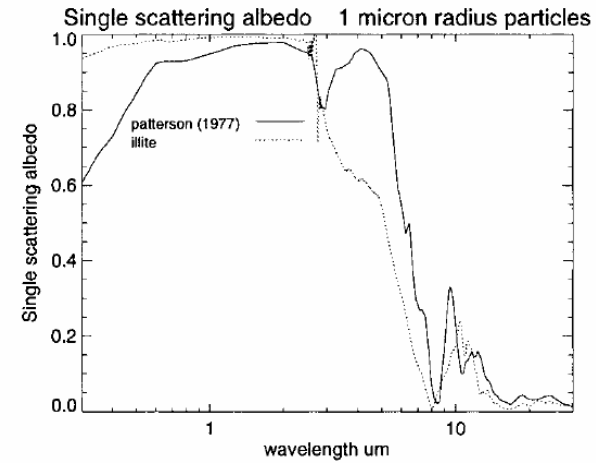


**Figure 1.8: Mie scattering calculations of the single-scattering albedo of 1 μm radius particles assuming an index of refraction from Patterson et al. (1977), as modified by Tegen and Lacis (1996); and assuming an index of refraction for pure illite (Weaver et al., 2002).**

As mentioned previously, TOMS AI is another quantity used to diagnose the presence and radiative effect of aerosols. It is represented by Equation (1.4)

$$AI = -100 \log_{10} \left[ \left( \frac{I_{340}}{I_{380}} \right)_{meas} - \left( \frac{I_{340}}{I_{380}} \right)_{calc} \right] \tag{1.4}$$

where $I_{meas}$ is the measured backscattered radiance at a given wavelength and $I_{calc}$ is the radiance computed (at wavelengths of 340 and 380 nm) assuming a purely gaseous atmosphere. Negative values of this parameter are associated with non-absorbing aerosols (sulfates and sea salt), whereas UV-absorbing aerosols such as dust and smoke yield positive AI values (Prospero et al., 2002). Frequency maps of high AI values for January and July (Figure 1.9) reveal the transport patterns in the Global Dust Belt discussed in earlier sections; however, the influence of biomass burning in equatorial Africa in July makes it difficult to separate the individual contribution of dust aerosol using AI values alone.

Another common aerosol parameter derived from satellite and ground-based retrievals is the Ångstrom exponent, α. The wavelength dependence of the aerosol extinction coefficient can be represented by Equation (1.5)

$$b_{ext} \approx \lambda^{-\alpha} \tag{1.5}$$

The Ångstrom exponent is computed using measured values of the extinction coefficient at different wavelengths, as in Equation (1.6)

$$\alpha = -\frac{d \log b_{ext}}{d \log \lambda} \cong -\frac{\log \left( \frac{b_{ext_1}}{b_{ext_2}} \right)}{\log \left( \frac{\lambda_1}{\lambda_2} \right)} \tag{1.6}$$

Given that the wavelength dependence of aerosol scattering and absorption varies for different size regimes, the Ångstrom exponent can be used to remotely infer aerosol size. In the Rayleigh regime ($D_p \leq 0.1$ μm), the Ångstrom exponent varies between 3 and 4; it ranges between 0 and 1 for supermicron particles. Values in the latter range usually indicate the presence of soil dust particles, given that such particles tend to dominate the coarse mode.

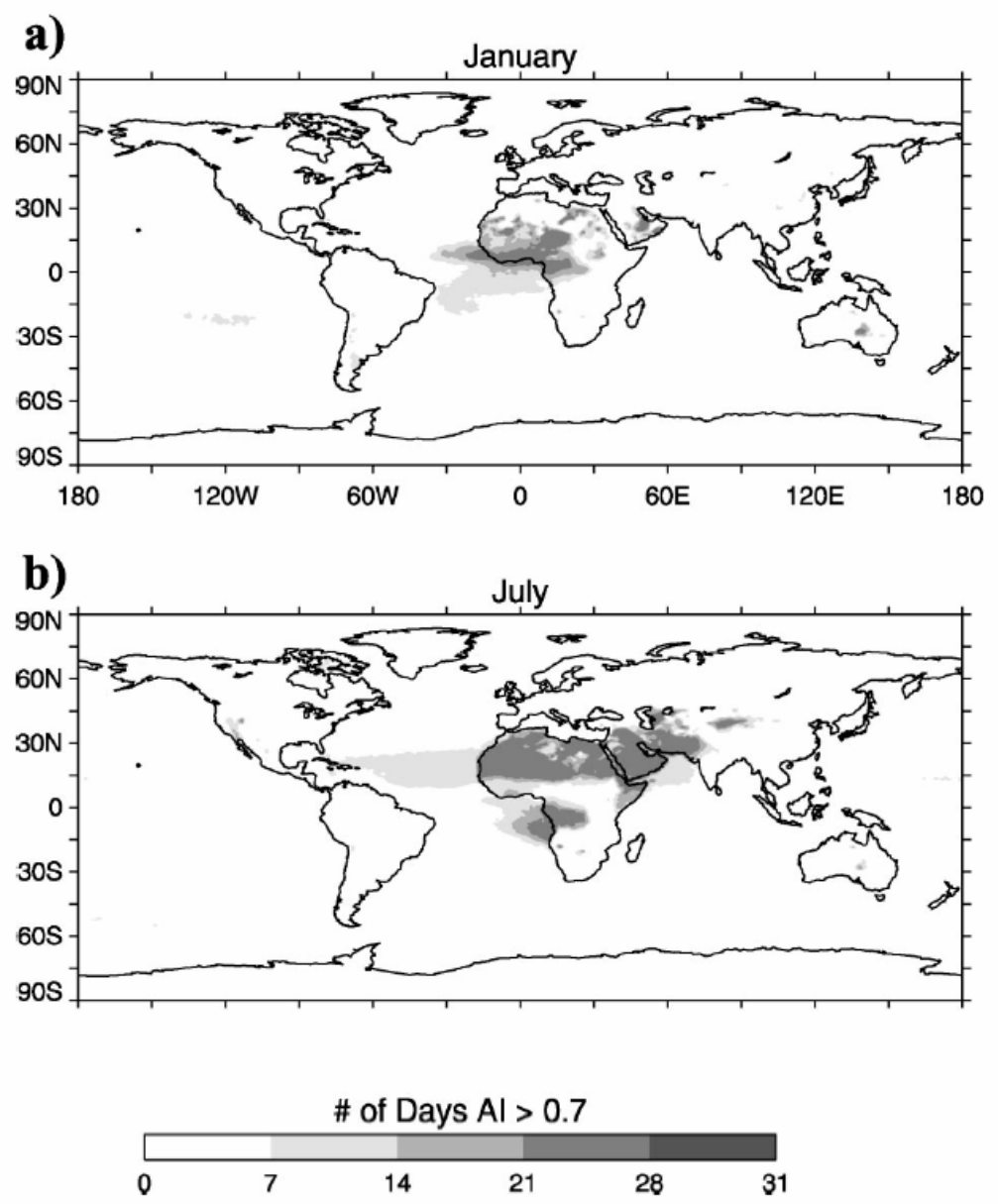


**Figure 1.9: Monthly occurrence of TOMS AI from 1980 to 1992. Units are in days per month where TOMS AI equals or exceeds 0.7 (Prospero et al., 2002).**

As previously mentioned, aerosol optical depth and the Ångstrom exponent can be retrieved using satellite-based instruments such as the Moderate Resolution Imaging Spectroradiometer (MODIS) and the Multi-angle Imaging Spectroradiometer (MISR). Aerosol measurement from space can be problematic over land, however, because the albedo of land surfaces is somewhat difficult to separate from the albedo of aerosols above the land surfaces. For dust aerosol, this is especially an issue, given that desert surfaces tend to be highly reflective. Ground-based instruments, such as the sunphotometers in the Aerosol Robotic Network (AERONET), can be useful in determining aerosol optical depth and Ångstrom exponent in light of this issue. Inversions of AERONET retrievals can also yield information about the column aerosol size distribution; the volume distribution in Figure 1.1 was determined using this method (Dubovik et al., 1999). Ground-based lidar instruments can even detect variability in the vertical distribution of aerosol reflectance—an important tool in diagnosing the long-range transport of elevated dust plumes.

### 1.2.2 Mass and Composition

Sampling of ambient air using cyclones or aerosol impactors is a common method used to determine the mass and composition of boundary layer aerosols. Certain measurement sites have maintained detailed chemical records for several years, providing valuable information on the temporal variability of local aerosol composition. Chemical records in the Virgin Islands, a location frequently impacted by dust from North Africa, for example, have been used to identify that Saharan dust is depleted of calcium. One Al-to-Ca ratio used to determine Saharan dust in the U.S. is 3.8, the 25$^{th}$ percentile of all Al-to-Ca ratios measured at Virgin Islands National Park when fine soil concentrations

exceeded 3 μg $m^{-3}$ (Perry et al., 1997). The presence of Asian dust in the U.S., on the other hand, has been associated with Al-to-Ca ratios below 2.6 (VanCuren and Cahill, 2002). Dust originating from dry lake beds, such as Owens Dry Lake in California, have been seen to contain salts that make them quite hygroscopic (Reid et al., 1994), enhancing their ability to degrade visibility; dust can also contain lead or vanadium from nearby industrial operations (Reid et al., 1994; Vasconcelos et al., 1996) or become coated with sulfates or remnants of biomass burning aerosols during transport (VanCuren, 2003). These unique properties of different dusts could be important tools in quantifying the local and global impacts of different soil dust source regions.

Aerosol sampling with instruments such as an optical particle counter can also help to characterize the aerosol size distribution. Knowledge of the size distribution is not only important in determining the radiative properties of soil dust, but also the relative fractions of clay and silt in the soil. Silt, which is comprised mainly of quartz, is defined by the U.S. Department of Agriculture as soil particles between 1 and 25 μm in radius; soil particles smaller than 1 μm in radius are defined as clay (Hillel, 1982). The two species differ in their aerodynamic behavior, lifetimes, and radiative effects; their relative fractions also vary with soil type. Silt particles can also be coated with smaller clay particles (Hillel, 1982), further complicating the source characterization of soil dust aerosol.

## 1.3 Problem Statement

Although we have the ability to make detailed measurements of both aerosol composition at the surface and optical properties from space and Earth's surface, integrating these measurements is difficult. Attempts have been made to correlate aerosol

optical depth with surface aerosol amount (Smirnov et al., 2000); however, this can only be successfully done with temporally-averaged data (generally monthly or seasonal means). The existence of elevated aerosol plumes does not always result in high aerosol concentrations near the surface (or vice-versa); thus, aerosol optical depth cannot really serve as a real-time diagnosis of conditions in the atmospheric boundary layer, where air quality concerns are most critical. Furthermore, the availability of data for one location from polar-orbiting satellites is limited to twice per day at most; some instruments, such as the Multiangle Imaging SpectroRadiometer (MISR), provide global coverage only every 9 days. Ground-based instruments can provide good temporal resolution, but are limited in their spatial extent by a lack of measurement sites in rural and oceanic regions of the globe. For these reasons, models are necessary to determine the impact of aerosol transport and production processes on visibility, air quality, and global climate.

An array of global aerosol transport models have been developed in the past several years to tackle the problem of determining global aerosol (or simply dust) distributions (Ginoux et al., 2001; Miller et al., 2004; Tegen and Fung, 1994; Zender et al., 2003). Many were designed to estimate global aerosol direct radiative forcing in order to constrain future climate change uncertainties in light of the predicted warming due to increased greenhouse gases; for this reason, they contain parameterizations that can be quite complex. Simulated dust in the GOCART model, for example, is segregated into seven size bins, with different proportions of clay and silt dust particles assigned to each bin (Ginoux et al., 2001). GOCART and other models also contain soil dust emission schemes that account for threshold wind velocity variations as functions of soil moisture, particle size, and soil type.

Such complexities result in models that are quite useful for reanalysis purposes, but they are also computationally expensive. Thus, they are not always practical tools for forecasting surface PM concentrations. The ability to generate such forecasts is of interest, however, given that the presence of soil dust and other aerosols can affect human health and visibility. Dust storms over the Arabian Peninsula frequently inhibit U.S. military operations, resulting in costly delays and even loss of life. The Navy Aerosol Analysis and Prediction System (NAAPS) is one global aerosol model that is used to forecast surface aerosol concentrations. In order for the model to efficiently produce real-time aerosol forecasts multiple times per day, it contains necessary simplifications to its source functions, transport, chemistry, and removal processes. In light of these simplifications, it is desirable to investigate whether NAAPS still contains enough detail to accurately represent surface aerosol amounts and long-range transport processes. To date, however, few systematic analyses of NAAPS aerosol mass predictions have been carried out using surface-based chemical measurements. Furthermore, optical depths as determined from ground-based sunphotometers are the only data that have been used to evaluate the model's performance over the U.S.

This study makes use of data from the Interagency Monitoring of Protected Visual Environments (IMPROVE) network of monitoring stations to evaluate NAAPS predicted surface concentrations in the continental U.S. It also examines the behavior of local and long-range transport of dust aerosol to the U.S. and the subsequent implications of such processes. We choose a factor of two agreement between modeled and measured data to be a successful simulation. NAAPS predictions of soil dust that are due to large-scale sources and long-range transport are expected to be within a factor of two of the

IMPROVE measurements more frequently than those of dust that is due to primarily North American sources for several reasons. First, there has been more validation of mass concentrations and optical depths in dust-producing regions outside of North America. Secondly, the effects of complex sub-grid scale topography will be less of an issue in large-scale source regions which span several model grid boxes. Also, NAAPS dust flux parameterization was derived for dust emitted from bare deserts, whereas most North American dust source regions are semi-desert surfaces (Loveland et al., 2000). The choice of IMPROVE measurements as comparison variables also may or may not be good metrics for actual soil dust concentration depending upon the station location and the subsequent influence of non-soil aerosols on the coarse fraction mass. Because there is limited information on the chemical speciation of aerosols collected in the IMPROVE network, we hypothesize that there may be difficulties in unambiguously determining the fraction of particulate matter attributable to dust particles.

# 2 Datasets and Methodology

## 2.1 Overview of NAAPS

The Navy Aerosol Analysis and Prediction System (NAAPS) was developed at the Naval Research Laboratory in Monterey, California as a multi-component three-dimensional Eulerian model to be used as a global aerosol forecasting tool for the U.S. Navy. The model currently contains four prognostic aerosol/trace gas species: gaseous $SO_2$, particulate sulfate, soil dust, and smoke. All four species are treated as passive tracers (i.e. they do not interact with the model fields or with each other), and are tracked by mass alone. Driven by meteorological analyses and forecasts from the Navy Operational Global Atmospheric Prediction System (NOGAPS), NAAPS produces 120-hour forecasts of its component aerosol species every six hours on a 1º x 1º horizontal grid and at 25 vertical hybrid σ-levels (18 before September 2002). Real-time global surface concentration and aerosol optical depth forecasts for the three particulate species in NAAPS are available at http://www.nrlmry.navy.mil/aerosol/.

### 2.1.1 The Navy Operational Global Atmospheric Prediction System (NOGAPS)

Six-day global operational forecasts of surface and atmospheric conditions are produced by NOGAPS; these forecasts provide the forcing in NAAPS. The current version of NOGAPS has a 0.5º x 0.5º resolution and 30 vertical hybrid σ-levels (24 prior to 2002). Hybrid σ-coordinates are an energy conserving vertical coordinate; NOGAPS

places layers between the surface and 1 mb level in order to resolve boundary layer processes in addition to the location of the stratosphere. The pressure on any σ-level, $p_i$, can be computed using Equation (2.1)

$$p_i = 1.0 + \sigma_i \cdot p_s \tag{2.1}$$

where $p_s$ denotes the surface pressure and $\sigma_i$ is the corresponding σ-value (ranging from 1.0 at the surface to zero at the model top) for that level.

In addition to wind, temperature, cloud, and precipitation fields, one NOGAPS parameter that is used in the generation of NAAPS forecasts is ground wetness. The ground wetness, $w_s$, is defined as the amount of water in the top ground level divided by the saturated water amount, ranging from 0 for a completely dry surface to 1 for a completely saturated surface (Hogan and Rosmond, 1991). Climatological values are used for this parameter, and are simply interpolated to the initial forecast day. The ground wetness is held constant in NOGAPS forecasts.

### 2.1.2 Mineral Dust Aerosol in NAAPS

The following description of mineral dust aerosol in NAAPS is taken from an online description of NAAPS (www.nrlmry.navy.mil/aerosol/Docs/globaer_model.html). Global sources of atmospheric mineral dust are defined in NAAPS by the USGS Land Cover Characteristics Database. The database was created with the use of Advanced Very High Resolution Radiometer (AVHRR) data, and has a resolution of 1 km. Details on the construction of this database can be found in Loveland et al. (2000). Of the 92 land-use types characterized in the database, eight are considered to be dust-producing: low sparse grassland, bare desert, sand desert, semi-desert shrubs, semi-desert sage, polar and alpine desert, salt playas, and sparse dunes and ridges. In order to incorporate these source

regions into NAAPS, the Land Cover Characteristics Database was first aggregated to a resolution of 0.1º, from which the dominant land-use type for each 1º x 1º box was determined. For grid boxes containing dust-producing land types, the fraction of the box covered by the dominant land surface type was converted to an erodible fraction (0-1.0). Additionally, low sparse grasslands were included as a dust source only in China and Mongolia (based upon observational evidence of their behavior in other regions of the world), and dust source regions located north of 60º N were excluded.

An analysis of TOMS AI data was also included to define dust source regions in NAAPS. Using the method of Prospero et al. (2002) in which the frequency of high TOMS AI values is converted to an erodible fraction, further dust sources were identified in North Africa, Australia, and the Arabian peninsula. Due to a lack of information about the distribution of land-use type in these regions, the TOMS-identified dust sources have all been defined as bare desert in the model. Global maps of the locations of the dominant dust-producing land types and their corresponding erodible fractions in NAAPS are shown in Figure 2.1 and Figure 2.2, respectively.

Forecasted friction velocities are utilized to predict dust mobilization in NAAPS. Friction velocity, $u_*$, is related to the wind speed, $U$, at some reference height, $r$, by Equation (2.2)

$$u_* = (C_D U_r^{\,2})^{1/2} \tag{2.2}$$

where $C_D$ denotes the drag coefficient. Dust is emitted from the surface whenever the friction velocity exceeds a threshold value and the surface moisture fraction is below a critical value. The critical surface moisture fraction is 0.3, and the friction velocity threshold is currently set to 60 cm $s^{-1}$ everywhere in the model domain. This threshold

value is based upon a study of mobilization and transport of Saharan dust (Westphal et al., 1988), and thus may not be entirely appropriate for all dust-producing areas of the world. Plans exist to vary the threshold friction velocity value in NAAPS as a function of land-use type.

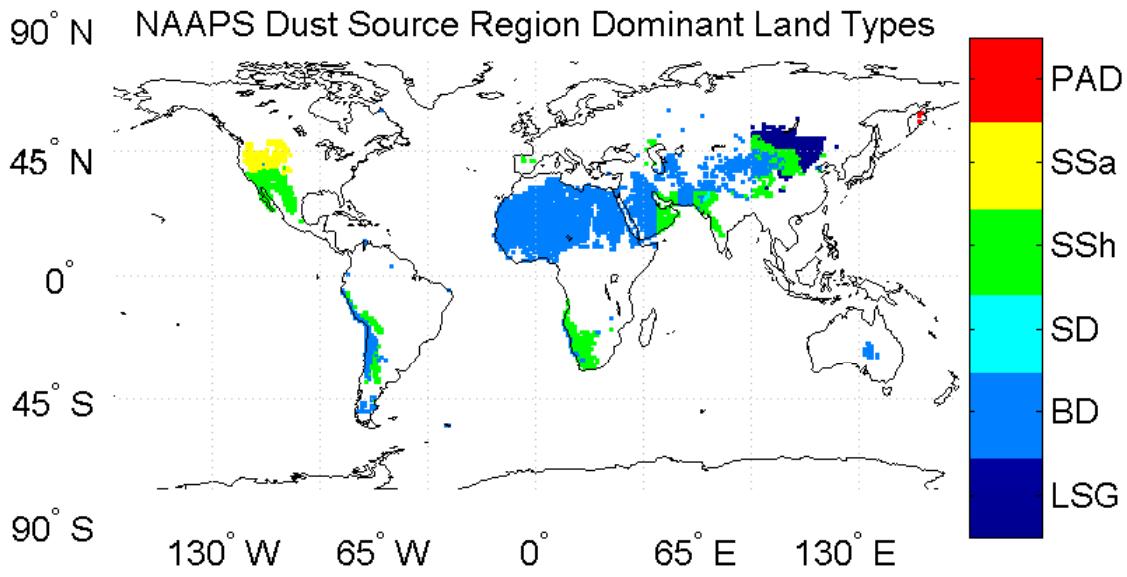


**Figure 2.1: Dominant land types for NAAPS dust-producing regions of the world: polar alpine deserts (PAD), semi-desert sage (SSa), semi-desert shrubs (SSh), sand desert (SD), bare desert (BD), and low sparse grassland (LSG).**

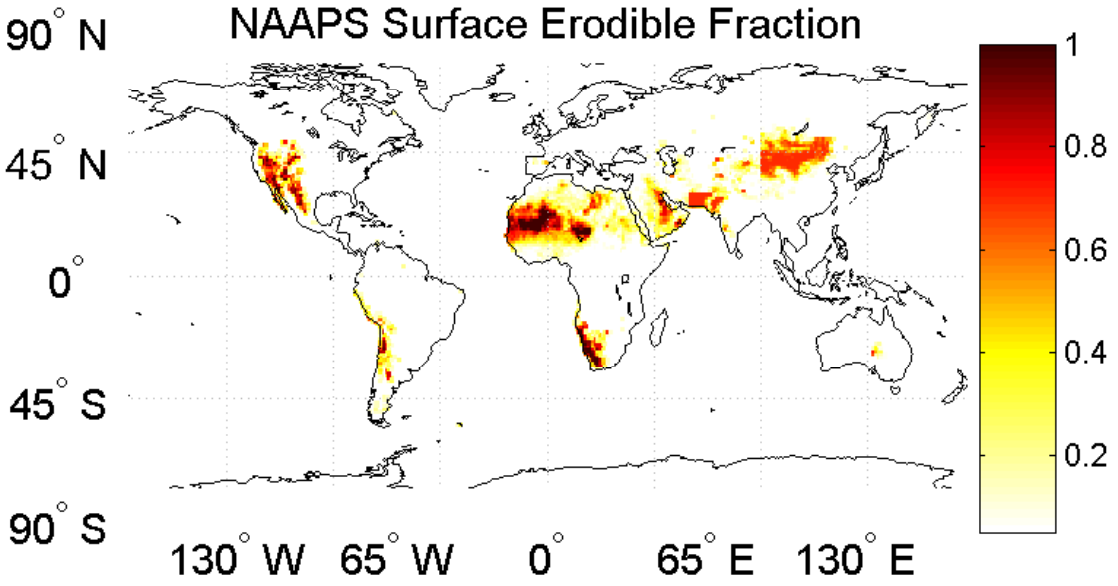


**Figure 2.2: Surface erodible fraction of NAAPS 1° x 1° model grid boxes.**

When the emission criteria are met, a dust flux is released into the lowest two layers of the model. The flux (g $cm^{-2}$ $s^{-1}$) was taken from Westphal et al. (1988), which is estimated by Equation (2.3) for particles between 0.2 and 160 μm in diameter

$$F = 2.9x10^{-14} u_*^{4} \tag{2.3}$$

In NAAPS, $F$ is scaled to represent the mass attributable to dust particles smaller than 10 μm in diameter, at a mean size of ~2 μm in diameter.

### 2.1.3 Diffusion, Advection and Removal in NAAPS

Advection of the aerosol species in NAAPS is carried out by the NOGAPS-generated wind field using a semi-Lagrangian algorithm. Diffusion is computed using a finite element method. Horizontal diffusion is assumed constant, whereas vertical diffusion is computed based on $K_z$ profiles using Monin-Obukhov similarity theory in the surface layer. The profile is extrapolated to extend through the entire boundary layer in order to ensure that $K_z$ decreases in the upper portion of the boundary layer (Christensen, 1997).

All aerosol species in NAAPS are subjected to dry and wet removal processes. Dry deposition occurs at the lowest model level and is based on the deposition velocity for sulfate aerosols, which is defined differently over land and water. Over open water, the dry deposition for sulfate particles of ~ 2 μm diameter is given by Equation (2.4)

$$v_d(2m) = 1.3x10^{-3} u_{10} \tag{2.4}$$

where $2m$ refers to the height of the lowest model level, and $u_{10}$ refers to the wind speed at a height of 10 meters (Christensen, 1997). Dry deposition of sulfate particles is less effective over land, and is dependent upon the Monin-Obukhov length, $L$, as shown in Equation (2.5)

$$v_d(2m) = \begin{cases} \dfrac{u_*}{a}\left(1+\left(\dfrac{-300}{L}\right)^{2/3}\right) & \text{for } L < 0 \\ \dfrac{u_*}{a} & \text{for } L > 0 \end{cases} \tag{2.5}$$

where $a$ is equal to 100 for forests with leaves, and 500 for all other surface types (Christensen, 1997). Gravitational settling is not parameterized as a removal process in NAAPS, which may or may not be reasonable depending upon the mean dust aerosol size, given that gravitational settling is an efficient removal process for large dust particles (Ginoux et al., 2001).

Wet deposition is driven by NOGAPS precipitation and cloud fields at a given σ-level using the scavenging ratio formulation for sulfate particles in Equation (2.6)

$$W(\sigma) = \begin{cases} \dfrac{\Lambda_{bc}}{H}\dfrac{P_a(\sigma)}{\rho_w} & \text{below-cloud scavenging} \\ \dfrac{\Lambda_c}{H}\dfrac{P(\sigma)}{\rho_w} & \text{in-cloud scavenging} \end{cases} \tag{2.6}$$

where $\Lambda_{bc}$ is the below-cloud scavenging ratio, $P_a(\sigma)$ is the total precipitation at the σ-level, $H$ is an effective thickness for scavenging (1000 m), $\Lambda_c$ is the in-cloud scavenging ratio, $P(\sigma)$ is the precipitation inside the cloud layer, and $\rho_w$ is the density of water. The in-cloud scavenging ratio is seven times larger than the below-cloud scavenging ratio for sulfate particles (Christensen, 1997).

### 2.1.4 Validation of NAAPS Forecasts

Since the widest available tool for estimating total aerosol amount is aerosol optical depth from satellites and ground-based sensors, NAAPS forecasts are converted to aerosol optical depth (at a wavelength of 550 nm) for validation purposes. This is done

for each of the three aerosol species using the following mass extinction efficiencies: 0.56 $m^2 g^{-1}$ for dust; 7.1 $m^2 g^{-1}$ for smoke; and 4.5, 5.1, 7.2, 15.0, and 31.6 $m^2 g^{-1}$ for sulfate at relative humidities of 30, 50, 70, 90, and 98%, respectively (NOGAPS relative humidity forecasts are utilized for sulfate aerosol optical depth estimation). One-to-one pixel comparisons between NAAPS predicted aerosol optical depth and aerosol optical depth values measured by MODIS and NOAA/NESDIS are performed daily. Timelines are also constructed to compare the magnitudes and temporal variability of NAAPS and ground-based AERONET aerosol optical depth and Angstrom exponent retrievals. An example of a NAAPS/AERONET comparison timeline for a Mediterranean site is shown in Figure 2.3. NAAPS predicted optical depths are often on the order of those determined from AERONET, as was the case at the site shown in Figure 2.3 for most of the two week period.

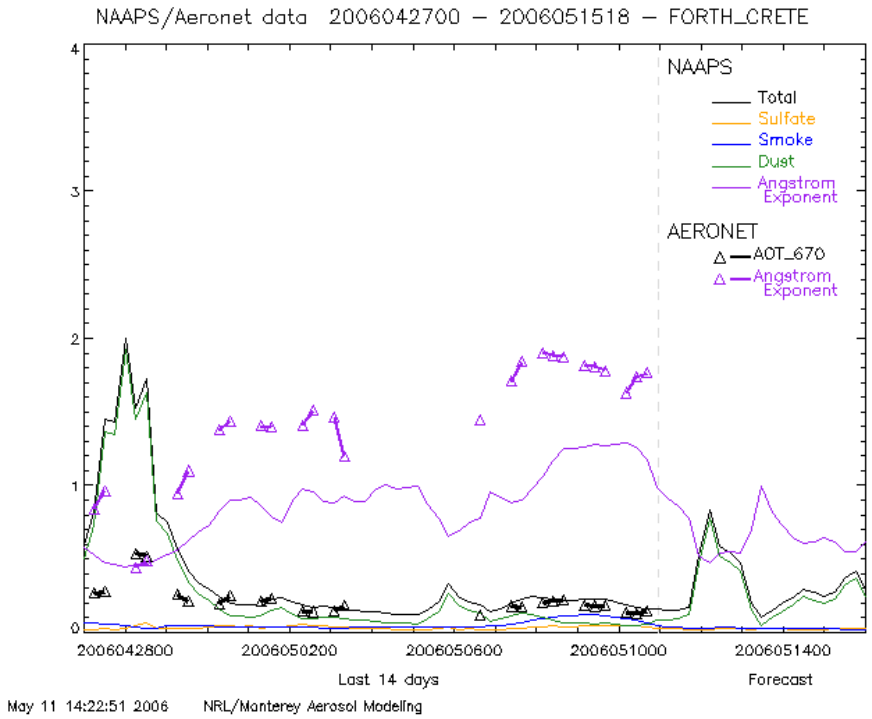


**Figure 2.3: AERONET/NAAPS timeline for a Mediterranean AERONET site (Source: http://www.nrlmry.navy.mil/aerosol/).**

Synoptic reports of visibility and the presence of haze or blowing sand are also compared against NAAPS predictions. However, although such reports can verify the presence of aerosol in the vicinity of an observing station (presumably in high enough quantities to affect visibility conditions), they do not facilitate a quantitative evaluation of NAAPS forecasts near the surface, where air quality concerns are most critical. Furthermore, AERONET retrievals are the only data that have been used to date to evaluate the performance of NAAPS over the continental U.S.

## 2.2 The IMPROVE Network

Measurements of aerosol composition from the Interagency Monitoring of Protected Visual Environments (IMPROVE) network were utilized in this study. An overview of the network initiation, measurement, and data reporting methods is provided in the following sections.

### 2.2.1 Background on Visibility Regulation

In response to the amended Clean Air Act of 1977, which mandated the prevention of future and the improvement of existing visibility degradation in federal Class I areas,[1] the IMPROVE network was initiated in the spring of 1988 by the National Park Service (NPS), the Fish and Wildlife Service (FWS), the Bureau of Land Management (BLM), the Forest Service (FS), and the Environmental Protection Agency (EPA). The initial network contained 30 monitoring sites, located mostly in the western United States. The sites were equipped with instruments to measure total $PM_{10}$

[1] Federal Class I areas include national parks greater than 6,000 acres, wilderness areas and national memorial parks greater than 5,000 acres, and international parks that existed as of 1977 (IMPROVE Regional Haze Rule overview (http://vista.cira.colostate.edu/improve/Overview/Overview.htm)).

concentration (particles with aerodynamic diameters less than 10 μm) and $PM_{2.5}$ (particles with aerodynamic diameters below 2.5 μm, also referred to as "fine" particles in the network) concentration and composition; 20 of the 30 sites also operated nephelometers to measure light extinction due to particles (Malm et al., 1994).

With data from the network, the EPA developed the Regional Haze Rule, which requires a return to natural visibility conditions in all of the nation's 156 national parks by the year 2064. Since the 1999 issue of the rule, the IMPROVE network has expanded to include 110 monitoring sites in order to further meet the rule's goals of establishing background visibility, identifying chemical constituents and emissions that lead to regional haze, and tracking visibility improvement in U.S. national parks (Malm et al., 1994). A map of the current IMPROVE network site locations is shown in Figure 2.4.

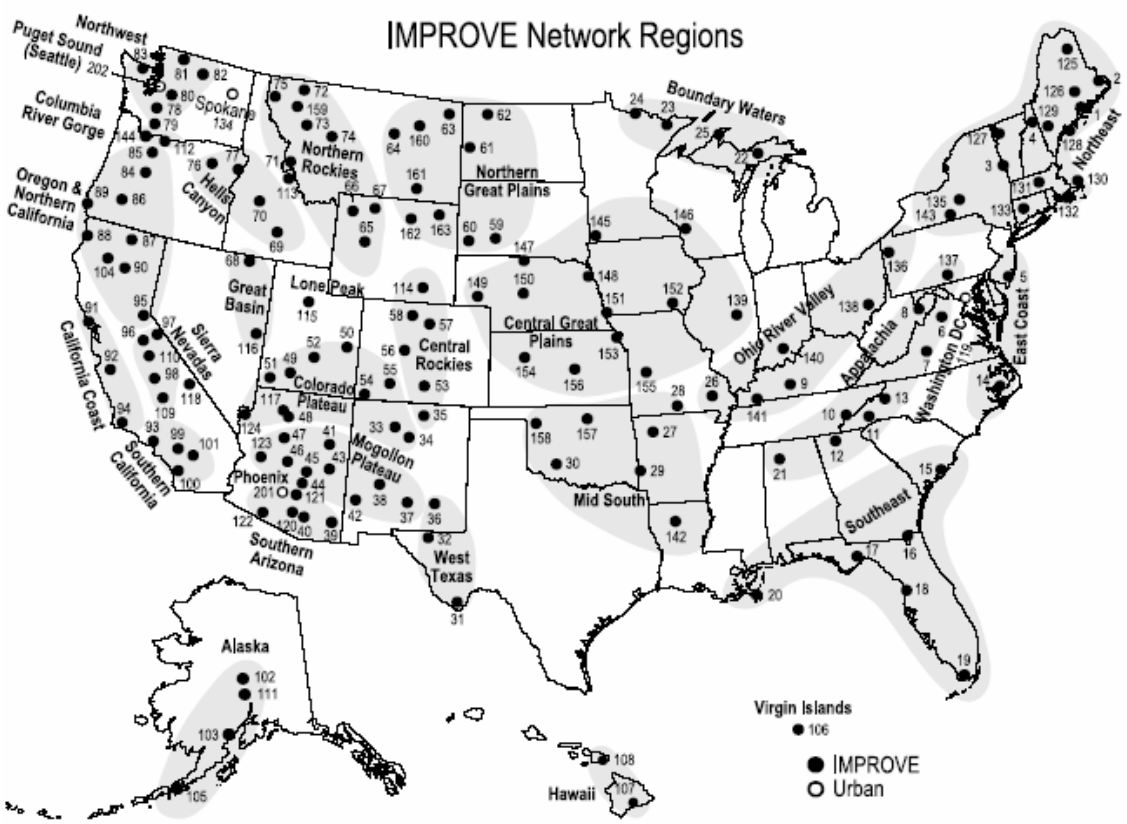


**Figure 2.4: IMPROVE monitoring sites. Shading indicates grouping of measurement regions (from Malm et al., 2004).**

### 2.2.2 IMPROVE Sample Collection

The standard IMPROVE sampler contains four modules as summarized in Table 2.1: a Teflon filter to collect $PM_{2.5}$, a nylon filter with attached denuder upstream of the filter to collect acidic gases (primarly nitrate species) to reduce artifacts, tandem quartz filters to measure fine carbonaceous aerosol and perform artifact correction, and a second Teflon filter to collect the total $PM_{10}$ mass present in the atmosphere. Each module has a separate inlet, sizing device, flow controller, and pump (California-Davis, 1995). Some IMPROVE sites are equipped only with a Module A Teflon filter; whereas some contain a fifth module to measure $SO_2$ amounts.

| Module | Particle Size | Filter Type | Analysis | Variables |
|---|---|---|---|---|
| A | Fine | Teflon | -Gravimetric<br>-PIXE/PESA<br>-XRF<br>-Absorption | -Fine mass<br>-H, Na - Pb<br>-$b_{abs}$ |
| B | Fine | Nylon | Ion Chromatography | -Nitrate ion<br>-Sulfate ion<br>-Chloride ion |
| C | Fine | Quartz | TOR Combustion | Carbon at eight temp fractions |
| D | $PM_{10}$ | Teflon | Gravimetric | $PM_{10}$ mass |
| A2 or D2 | Gas | Impregnated | Ion Chromatography | Sulfur dioxide |

**Table 2.1: Measurements by module of IMPROVE samplers (from California-Davis, 1995).**

Samples are collected at each IMPROVE site every three days from midnight to midnight local time. The samples are removed weekly and sent to the University of California-Davis for analysis. The $PM_{2.5}$ is analyzed for elemental composition (H, Na, Mg, Al, Si, P, S, Cl, K, Ca, Ti, V, Cr, Mn, Fe, Co, Ni, Cu, Zn, As, Se, Br, Rb, Sr, Zr, Mo, Pb) using Particle Induced X-ray Emission (PIXE), X-ray Fluorescence (XRF), and Proton Elastic Scattering Analysis (PESA). Nitrate, sulfate, and chloride ion amounts are determined from the nylon filter using ion chromatography; the quartz filter is analyzed

for carbon content using the Thermal Optical Reflectance (TOR) combustion method. The $PM_{10}$, however, is analyzed only for gravimetric mass (California-Davis, 1995). Concentrations, *c*, of measured species are determined with the use of Equation (2.7)

$$c = \frac{A - B}{V} \tag{2.7}$$

where *A* is the measured mass of the constituent, *B* is the artifact mass determined from field blanks or secondary filters, and *V* is the volume of air sampled as determined from the average flow rate and the sampling time (California-Davis, 1995).

IMPROVE data are flagged if they fail to meet certain standards of quality control. For example, data are flagged if the sample flow rate has changed over the course of the sampling period, since the flow rate determines the particle size cut point of the sampler. Flags also exist for data that are missing due to a clogged filter, possible contamination during sampling or analysis, or sampling equipment failure. Any data that were flagged due to possible QC issues were thrown out prior to analysis in this study, with the exception of those flagged due to moderate changes (≤ 15%) in flow rate during the sampling period. Such changes result in a cyclone cut point that is within 2 to 3 μm. Furthermore, any measurement that was below detection limit was set to zero.

### 2.2.3 IMPROVE Soil Parameter

Since only the IMPROVE $PM_{2.5}$ filters are analyzed for chemical composition, IMPROVE sites only report soil dust aerosol amounts that appear in the fine mode. The fine soil concentration (μg $m^{-3}$) is reconstructed from the masses of soil-derived elements (Al, Si, Ca, Fe, K, and Ti) and their normal oxides ($Al_2O_3$, $SiO_2$, CaO, $K_2O$, FeO, $Fe_2O_3$, $TiO_2$) using Equation (2.8)

$$[\text{Soil}] = 2.20[\text{Al}] + 2.49[\text{Si}] + 1.63[\text{Ca}] + 2.42[\text{Fe}] + 1.94[\text{Ti}] \quad (2.8)$$

Equation (2.8) is based upon the assumptions that FeO and $Fe_2O_3$ are equally abundant in the soil, and that the soil mass can be determined by summing the masses of the constituent oxides. A correction factor of 1.6 is included in each of the coefficients to account for the presence of other species in the soil such as MgO, $Na_2O$, water, and carbonate (Malm et al., 1994). Also, because fine potassium is found in smoke as well as dust, this element is replaced in Equation (2.8) by iron, based on a K/Fe ratio of 0.6 measured on coarse filters from 1982 to 1986 (California-Davis, 1995).

The mass concentration of the coarse aerosol fraction is estimated in the IMPROVE samples by subtracting the gravimetric fine mass from the total $PM_{10}$ aerosol mass, [$PM_{10}$-$PM_{2.5}$]. This quantity is assumed to contain only insoluble soil particles (California-Davis, 1995). Thus, if we take this and the assumptions used in calculating fine soil to be true, we can define the total $PM_{10}$ soil dust aerosol measured by IMPROVE ($D_p < 10$ μm) as the sum of the coarse fraction and fine soil masses, [$PM_{10}$-$PM_{2.5}$]+[Soil], a parameter that should be analogous to the soil dust simulated in NAAPS. Issues related to this definition and corresponding assumptions will be discussed alongside the results.

## 2.3 Study Methodology

### 2.3.1 Model Simulations

The NAAPS simulations for this study were run remotely at the Naval Research Laboratory by Marcin Witek as re-runs (i.e. not in forecast mode) from 2001-2004, with December 2000 serving as a spin-up time for the modeled aerosol to reach a steady state.

Archived initialized NOGAPS data fields provided meteorological input every six hours during the simulation. In order to separately examine the behavior of long-range and local dust transport to the continental U.S. in NAAPS, two simulations were performed and differenced: one in which all of the model's dust sources were kept active, and one in which North American dust sources were suppressed. The latter simulation was achieved by setting the threshold friction velocity to an infinite value over the North American domain. The model was kept as close to its operational state as possible for both re-runs, with the exception of the inclusion of a new sea salt parameterization. The integration time step was set to 30 minutes for vertical diffusion, and one hour for all other model processes.

### 2.3.2 Spatial and Time Averaging

Forecasted aerosol amounts are output by NAAPS as mass mixing ratios. Thus, in order to facilitate comparisons with the IMPROVE measurements, the output data were converted to concentration units ($\mu g\ m^{-3}$) for a layer, *i*, using Equation (2.9)

$$\left[\frac{\mu g}{m^3}\right]_i = x_i \cdot \rho_i \cdot 10^9 \tag{2.9}$$

where $x$ is the aerosol mass mixing ratio and $\rho$ denotes the air density at the layer midpoint in units of $kg\ m^{-3}$. The scaling factor of $10^9$ was included for unit conversion. The layer air density was estimated using the relation in Equation (2.10)

$$\rho_i = 100\frac{p_i}{RT_i} \tag{2.10}$$

where $p$ and $T$ refer to the average (linearly-weighted) pressure and temperature between two layers.

It should be noted that negative concentrations sometimes occur in NAAPS because the model's advection scheme is not positive-definite. Negative dust mass tends to be generated in the vicinity of source regions, where sharp vertical and horizontal mass gradients exist. These amounts are generally small (0-1 $\mu g\ m^{-3}$), however, and do not constitute a large percentage of the total NAAPS soil dust predictions for 2001-2004. A filter was created to set any negative concentrations to zero prior to data analysis.

In order to account for potential small discrepancies in the spatial distribution of NAAPS versus real-world soil dust that might be due to the model resolution and topographical smoothing, the computed concentrations were averaged over 2º x 2º boxes with midpoints chosen to correspond most closely to the locations of each of 28 IMPROVE monitoring sites throughout the U.S. Monitoring site names, coordinates, and elevations are listed in Table 2.2; Figure 2.5 contains a corresponding map of their locations. IMPROVE measured concentrations are reported as 24-hour averages (midnight-to-midnight local time), so the NAAPS data were also averaged over 24-hour time periods. Because NAAPS only generates forecasts at 00, 06, 12, and 18 UTC, the model data were averaged from 06-06 UTC. However, this time period only corresponds to the IMPROVE averaging period in the Central Time Zone of the U.S., meaning the NAAPS averages do not exactly represent the same time period as the IMPROVE average concentrations at sites located in other time zones of the U.S. Comparisons of the spatially- and temporally-averaged NAAPS simulated soil dust amounts to IMPROVE soil parameters are contained in the following chapter, in addition to summary statistics and comparisons of NAAPS global soil dust production.

| Site Code | Site Name | Latitude | Longitude | Elevation (m) |
|---|---|---|---|---|
| BADL | Badlands National Park, South Dakota | 43.74 | -101.94 | 736 |
| BAND | Bandelier National Monument, New Mexico | 35.78 | -106.27 | 1988 |
| BRET | Breton, Louisiana | 29.12 | -89.21 | 2 |
| BRIG | Brigantine National Wildlife Reserve, New Jersey | 39.47 | -74.45 | 5 |
| DEVA | Death Valley National Park, California | 36.51 | -116.85 | 125 |
| EVER | Everglades National Park, Florida | 25.39 | -80.68 | 3 |
| GUMO | Guadelupe Mountains National Park, Texas | 31.83 | -104.81 | 1674 |
| ISLE | Isle Royale National Park, Michigan | 47.46 | -88.15 | 186 |
| KALM | Kalmiopsis, Oregon | 42.55 | -124.06 | 90 |
| LABE | Lava Beds National Monument, California | 41.71 | -121.51 | 1469 |
| LOST | Lostwood, North Dakota | 48.64 | -102.40 | 692 |
| LYBR | Lye Brook Wilderness, Vermont | 43.15 | -73.13 | 1006 |
| MELA | Medicine Lake, Montana | 48.49 | -104.48 | 605 |
| MEVE | Mesa Verde National Park, Colorado | 37.20 | -108.49 | 2177 |
| MING | Mingo, Missouri | 36.97 | -90.14 | 112 |
| MONT | Monture, Montana | 47.12 | -113.15 | 1293 |
| MOOS | Moosehorn National Wildlife Reserve, Maine | 45.13 | -67.27 | 94 |
| MORA | Mount Rainier National Park, Washington | 46.76 | -122.12 | 427 |
| OKEF | Okefenokee National Wildlife Reserve, Georgia | 30.74 | -82.13 | 49 |
| ROMO | Rocky Mountain National Park, Colorado | 40.28 | -105.55 | 2755 |
| SAWT | Sawtooth National Forest, Idaho | 44.17 | -114.03 | 1980 |
| SEQU | Sequoia National Park, California | 36.49 | -118.83 | 535 |
| SYCA | Sycamore Canyon, Arizona | 35.14 | -111.97 | 2040 |
| THRO | Theodore Roosevelt, North Dakota | 46.89 | -103.38 | 853 |
| UPBU | Upper Buffalo Wilderness, Arkansas | 35.83 | -93.20 | 723 |
| VOYA | Voyageurs National Park, Minnesota | 48.41 | -92.83 | 429 |
| WASH | Washington, D.C. | 38.88 | -77.03 | 16 |
| YELL | Yellowstone National Park, Wyoming | 44.57 | -110.40 | 2425 |

**Table 2.2: Code names, location and elevation information for the 28 IMPROVE sampling sites considered in this study.**

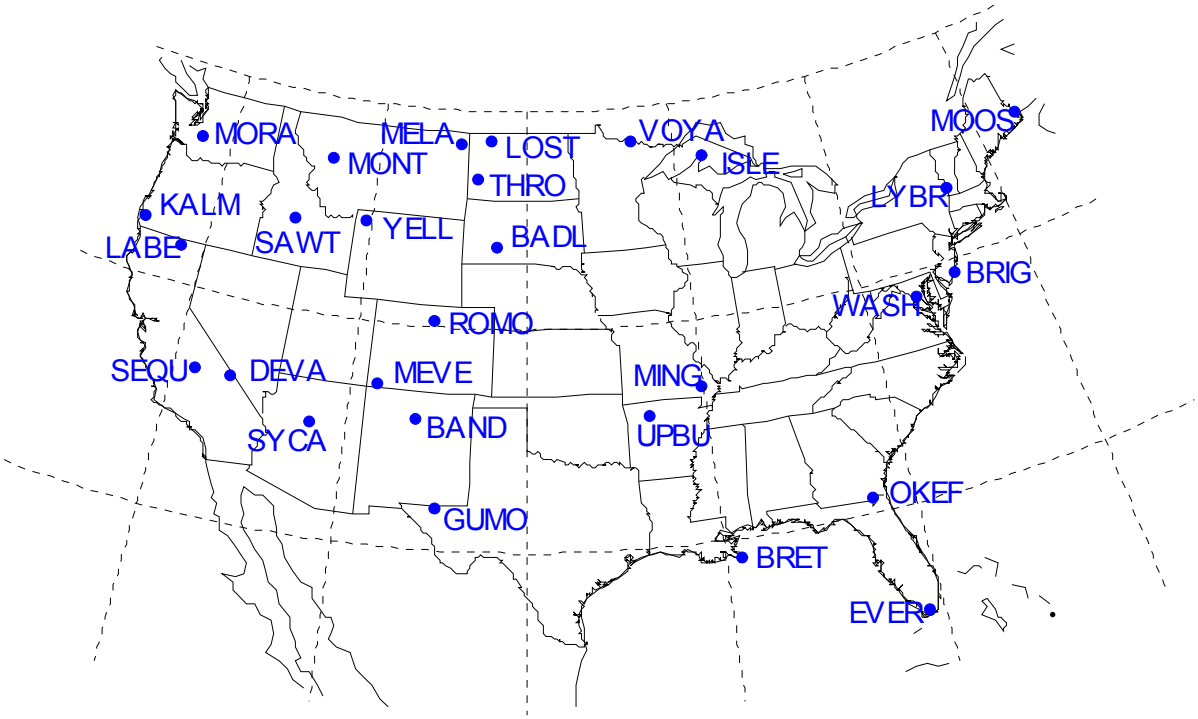


**Figure 2.5: Map of IMPROVE sites examined in this study.**

# 3 Soil Dust Aerosol Results

## 3.1 Global Overview

The total soil dust mass emitted into the atmosphere can vary strongly from year-to-year, as it is highly dependent upon both surface and meteorological conditions (in addition to the range of particle sizes being considered). Thus, estimates of annual soil dust emission span a wide range of values. A summary of annual soil dust emission in several models is given in Table 3.1. For the years 2001 to 2004, NAAPS predicted an average global dust emission of 1306 Tg $yr^{-1}$ with all sources active, an amount that falls within the range of 1019 to 1814 Tg $yr^{-1}$ produced by the five models listed for comparison.

| Model | Emission (Tg $yr^{-1}$) |
|---|---|
| NAAPS | 1306 |
| Miller et al. (2004) | 1019 |
| Ginoux et al. (2001) | 1814 |
| Tegen et al. (2002) | 1100 |
| Luo et al. (2003) | 1654 |
| Zender et al. (2003) | 1490 |

**Table 3.1: Annual soil dust emission for six global models (adapted from Miller et al., 2004).**

NAAPS soil dust can be attributed to source regions in North America, South America, Australia, Eastern Asia, South Africa, and North Africa and the Arabian Peninsula. The average annual contributions of each of these source regions in NAAPS are listed in Table 3.2. A map of NAAPS annual emission amounts for 2001 to 2004 containing the boundaries which define the regions listed in Table 3.2 is shown in Figure

3.1. As expected, North African and Arabian dust source regions produced the overwhelmingly largest fraction of soil dust in NAAPS from 2001-2004, ranging from ~71 to over 75% of the total soil dust produced in the model. The largest emissions from this region occurred in northwestern Africa and central North Africa, where dust storms are frequently generated throughout the year over the Bodele Depression (Prospero et al., 2002). East Asian sources emit the second largest amount of soil dust for the study period, the strongest of which is in the vicinity of the Gobi desert. The contribution from these sources ranged from ~17 to just under 19% of NAAPS total soil dust production year-to-year. Additionally, although they are not located in the Northern Hemisphere dust belt, both South Africa and Australia contained fairly strong dust emission "hot spots" on an annual basis in NAAPS. Australian dust made up only a small fraction of total dust emissions, however, which is consistent with the observation that, despite being over 1/3 desert, very little soil dust mobilization occurs over the continent (Prospero et al., 2002). North and South America were also weak dust emitters on a global scale, as we would expect. Less than 2% of soil dust in NAAPS could be attributed in any one year to North American sources.

| Region | 2001 (Tg) | 2002 (Tg) | 2003 (Tg) | 2004 (Tg) |
|---|---|---|---|---|
| North America | 16.7 | 14.7 | 22.5 | 20.3 |
| South America | 13.6 | 14.7 | 19.5 | 10.9 |
| North Africa/ Arabian Peninsula | 952.5 | 1003.9 | 967.5 | 915.8 |
| Southern Africa | 64.4 | 55.5 | 69.5 | 38.2 |
| East Asia | 232.5 | 226.2 | 254.5 | 206.2 |
| Australia | 17.9 | 28.4 | 30.3 | 25.6 |
| Globe | 1297.8 | 1343.5 | 1363.9 | 1217.0 |

**Table 3.2: Source contributions by year to total global soil dust emission in NAAPS.**

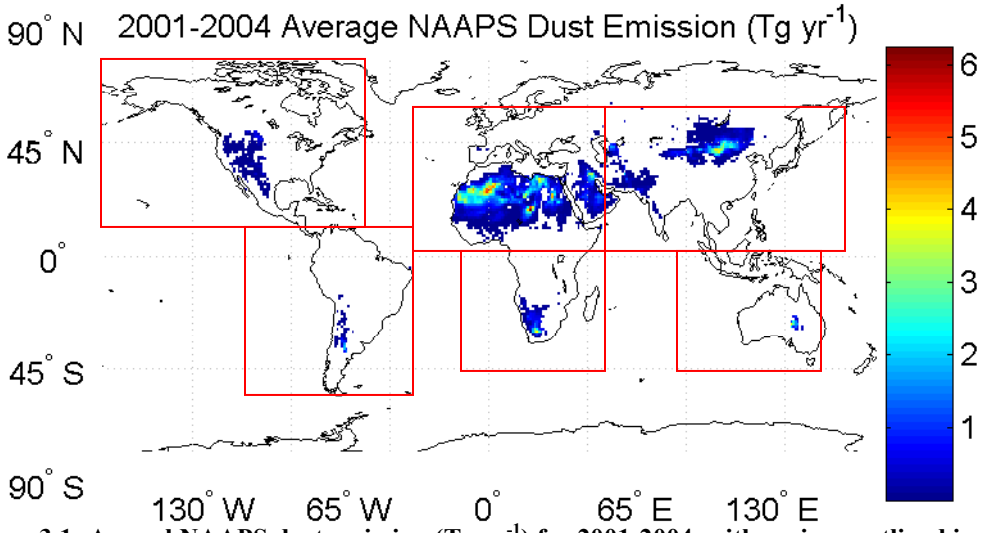


**Figure 3.1: Annual NAAPS dust emission (Tg yr$^{-1}$) for 2001-2004, with regions outlined in red as they were defined for this study.**

Even though the majority of soil dust production on an annual basis is confined to a few key sources, as discussed previously, we know that these sources have a large-scale impact. The "Global Dust Belt" is clearly visible in NAAPS dry deposition and rainout distributions, as shown in Figure 3.2 and Figure 3.3, respectively. The westward propagation of Saharan dust and the eastward propagation of Asian and Arabian dust becomes readily apparent in these distributions. How these transport processes play out over North America will be discussed in the following section.

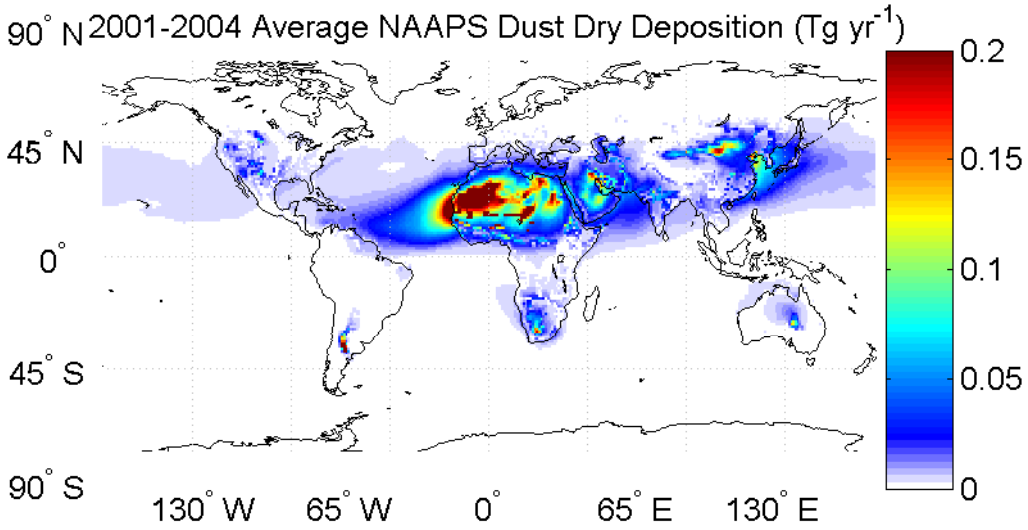


**Figure 3.2: Annual NAAPS dust dry deposition (Tg yr$^{-1}$) for 2001-2004.**

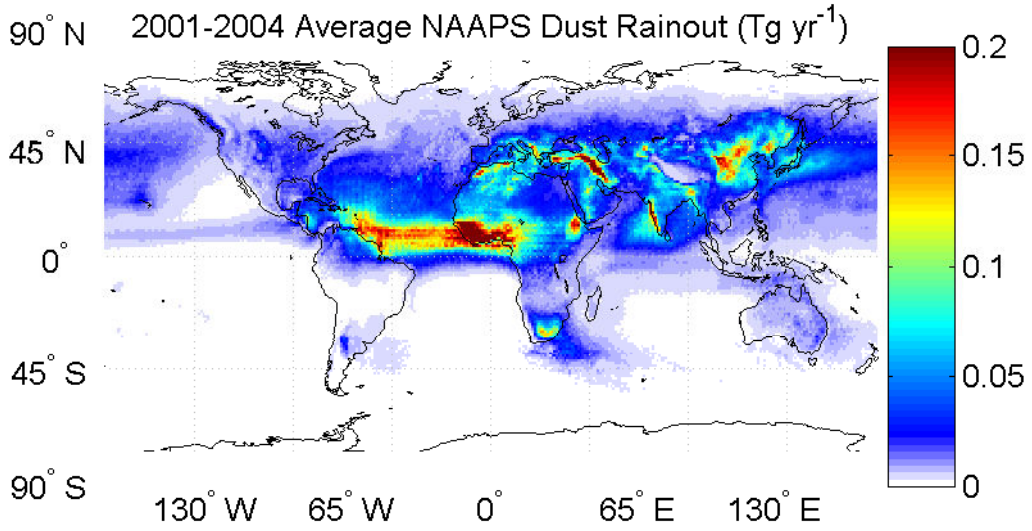


**Figure 3.3: Annual NAAPS rainout (Tg yr$^{-1}$) for 2001-2004.**

## 3.2 Soil Dust over North America

### 3.2.1 NAAPS Seasonal Averages

Seasonal averages of NAAPS surface dust amounts over North America for 2001 to 2004 for the simulation including all model dust sources are displayed in Figure 3.4. Although their intensity and spatial extents vary from season to season, two consistent regions of simulated North American dust activity can be seen throughout the year: an area of eastern Montana, and another along the Texas/New Mexico border. Maximum surface concentrations extend from the northern Great Plains of eastern Montana, eastern Wyoming and western South Dakota, moving southward into the central U.S. during the fall and winter months. NAAPS predicts high surface concentrations of soil dust over New Mexico in the spring and fall; elevated surface dust amounts are also predicted over southeastern Colorado during the summer, fall, and winter months.

In addition to the large seasonal surface dust concentration maxima over the North American continent during the study period, higher dust concentrations also

2001-2004 DJF Average NAAPS Surface Dust Concentration ($\mu g/m^3$)

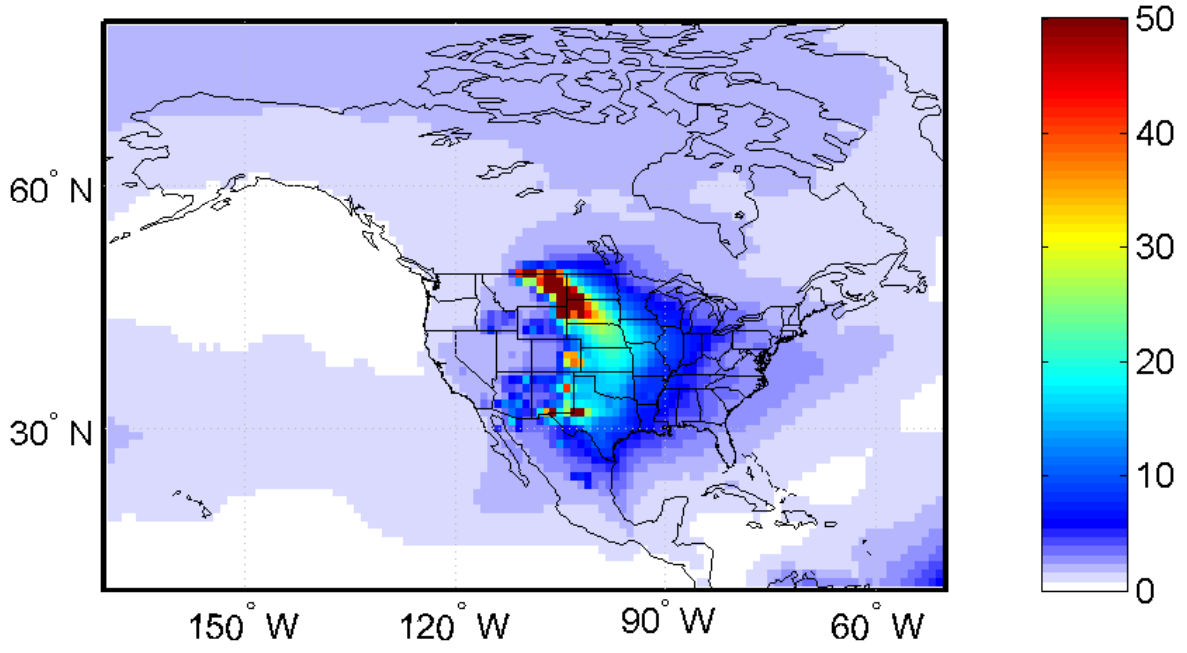


2001-2004 MAM Average NAAPS Surface Dust Concentration ($\mu g/m^3$)

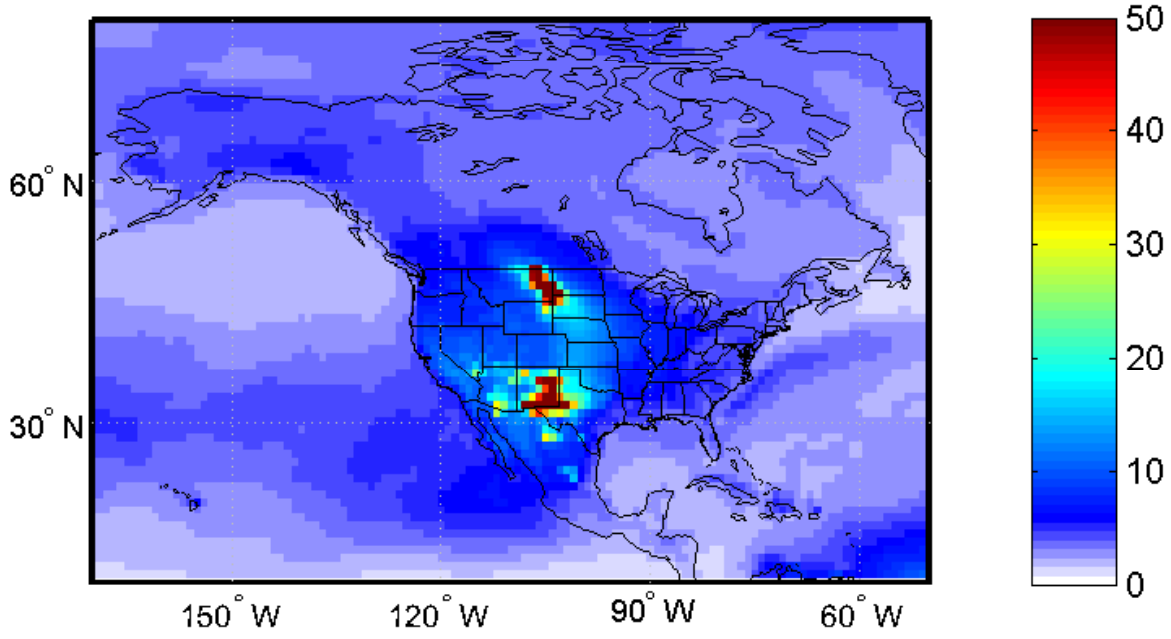

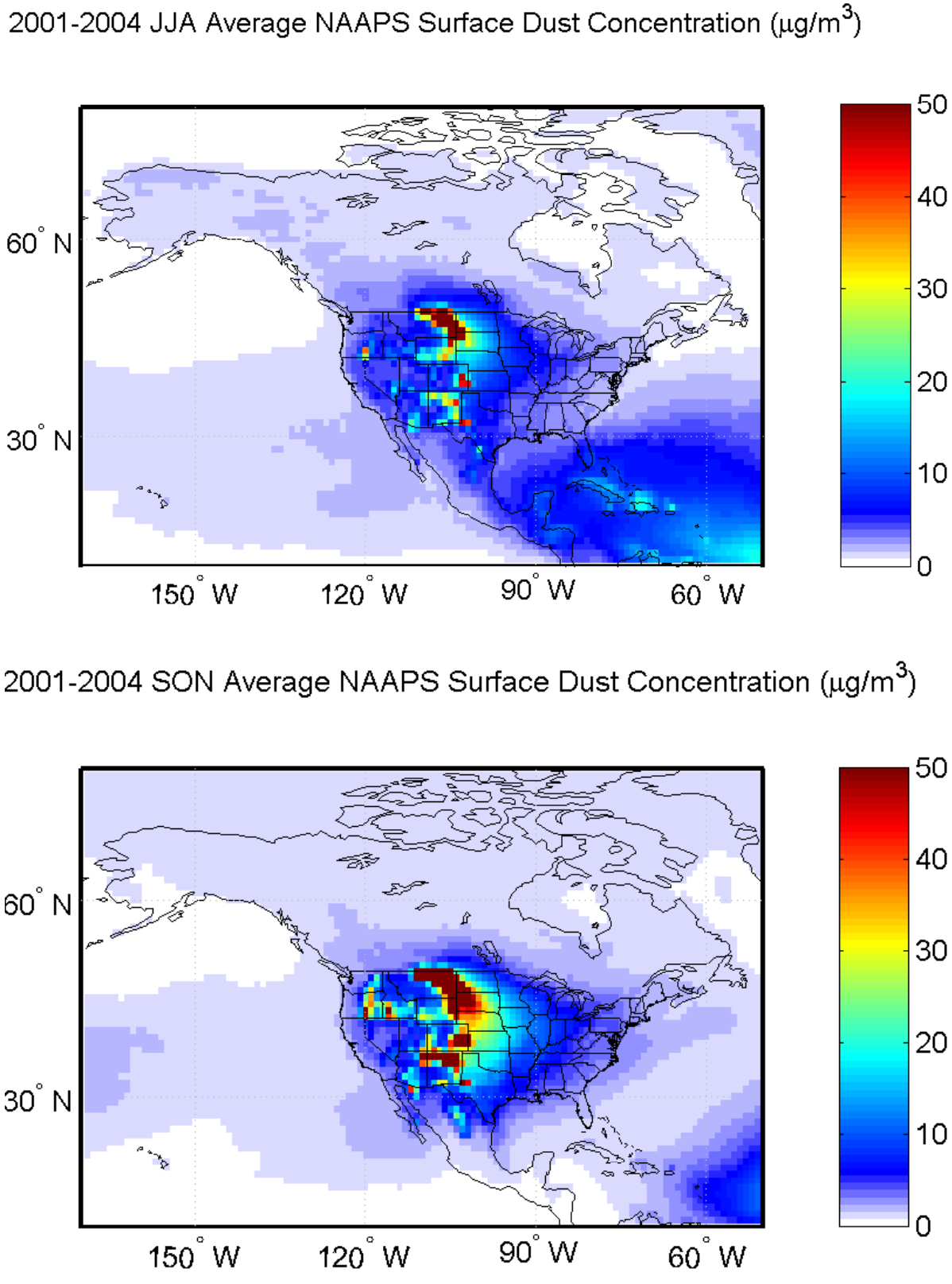


**Figure 3.4: 2001-2004 seasonal NAAPS surface dust concentration (µg $m^{-3}$).**

appear over oceanic regions. The area extending zonally along 30º N in the East Pacific exhibits higher dust concentrations seasonally than are predicted to the north and south; this band contains the most dust aerosol in spring, when, as previously discussed, Asian dust incursions over North America reach a peak in frequency and magnitude. A further dust maximum exists over the Caribbean, reaching its largest magnitude in the summer months, when Saharan dust transport to the eastern U.S. is most common. In general, however, these maxima over oceanic regions contain less mass than adjacent regions over land surfaces in the model; a more efficient soil dust scavenging ratio parameterized over open ocean (2:1 versus over land surfaces) and elevated terrain are the main reasons for this behavior (Christensen, 1997).

These features can be seen in greater detail in the average seasonal surface concentrations from the simulation in which North American dust sources were suppressed (Figure 3.5). The band of soil dust along 30º N in the East Pacific is visible in all seasons, reaching a maximum in magnitude and spatial extent in the spring. Furthermore, the surface concentrations of non-North American dust are smaller in magnitude than those due to North American sources, as one would expect, because larger soil dust particles generally have a lifetime shorter than the timescale of trans-oceanic transport. However, we can see that NAAPS predicts a very widespread influence of non-North American dust sources over North America in the spring throughout the western half of the United States and southern Canada. Since Asian soil dust is often observed over this region in spring, we can infer with some confidence that the bulk of springtime non-North American dust predicted by NAAPS over North America originated in East Asia.

2001-2004 DJF Average NAAPS Non-North American Surface Dust Concentration (μg/m$^3$)

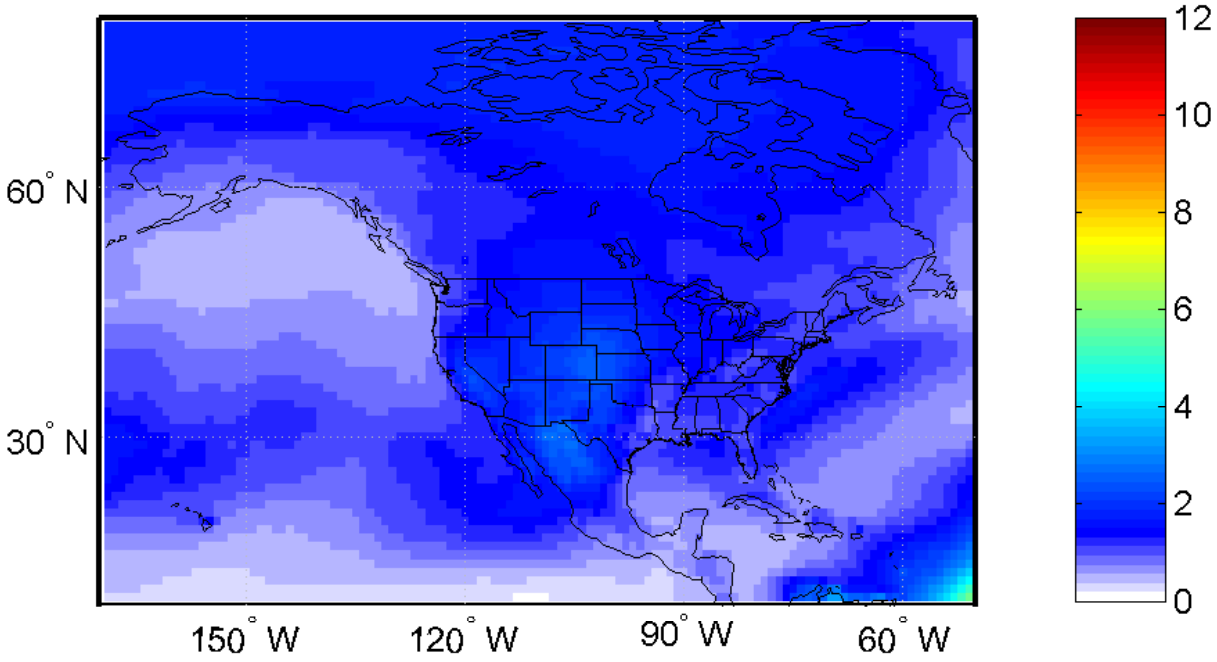


2001-2004 MAM Average NAAPS Non-North American Surface Dust Concentration (μg/m$^3$)

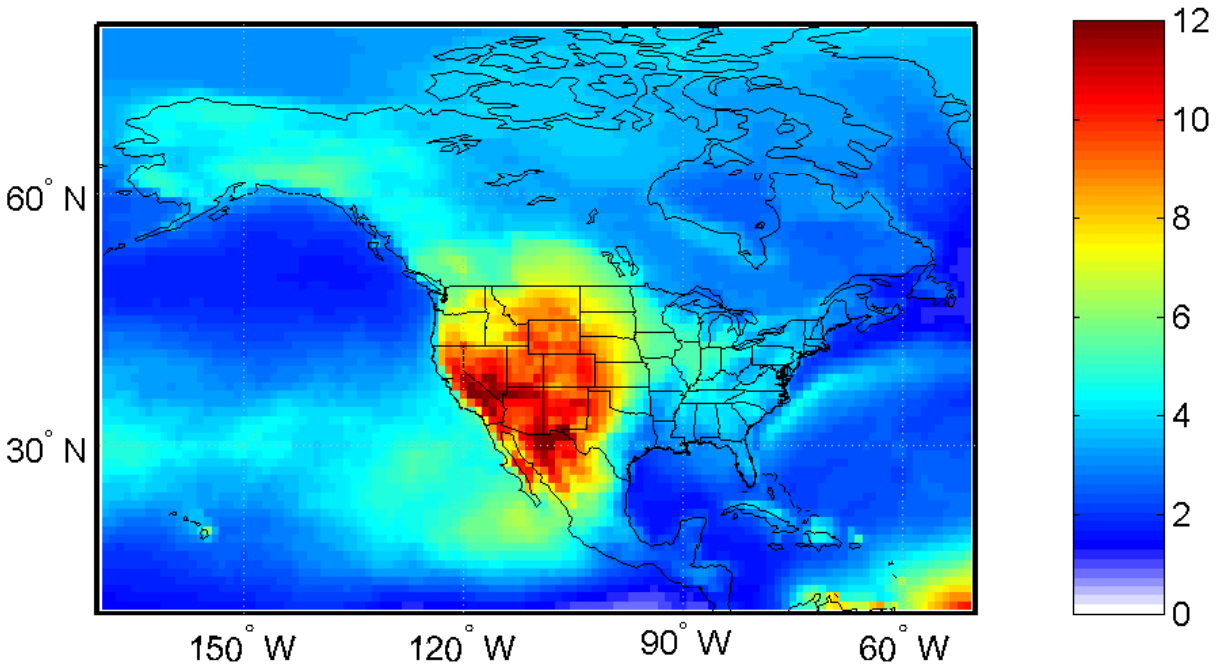

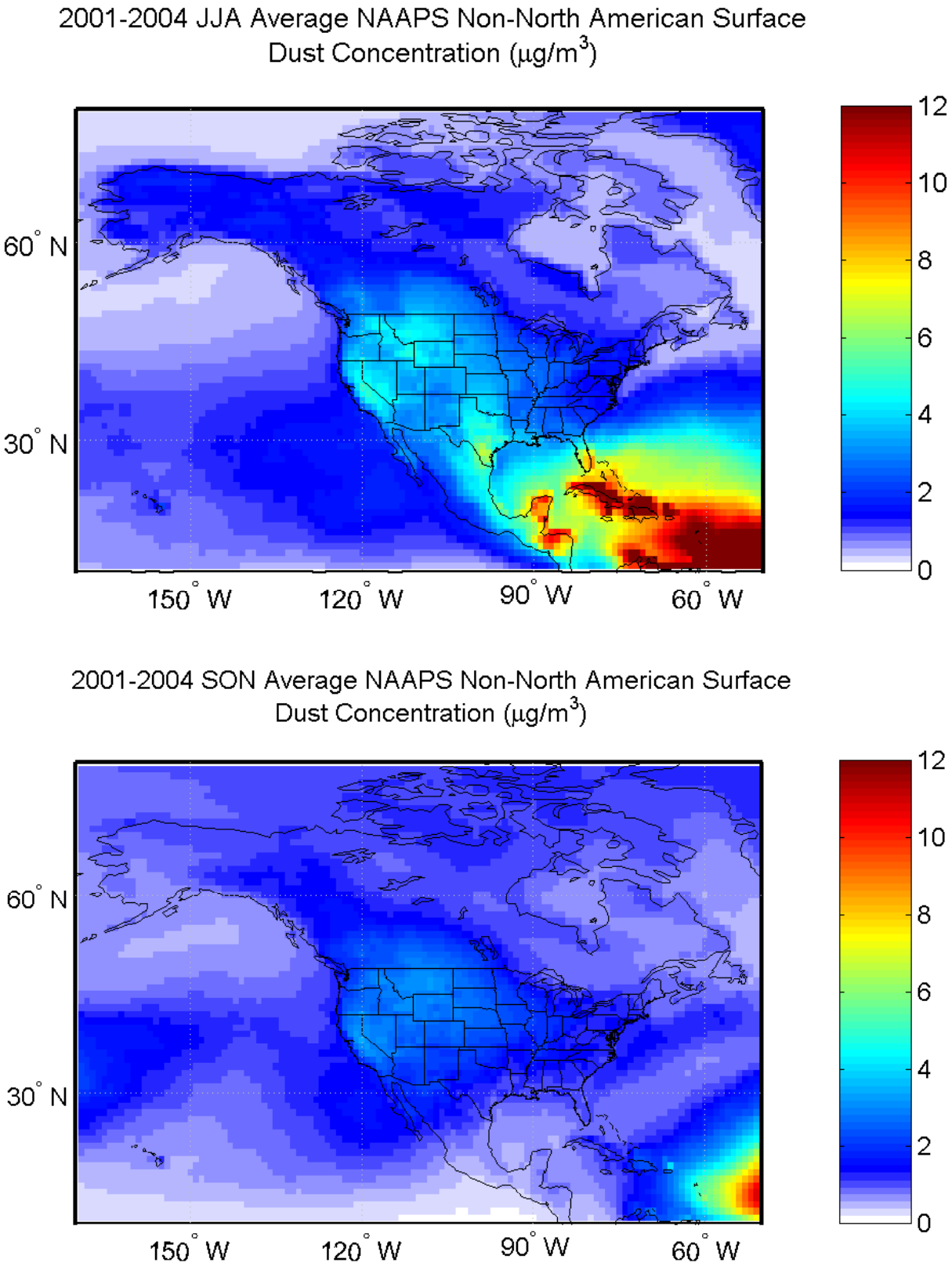


**Figure 3.5: 2001-2004 seasonal Non-North American NAAPS surface dust concentration (µg $m^{-3}$).**

A second peak of non-North American dust is predicted over the Caribbean and the North Atlantic in spring, summer, and autumn of 2001 to 2004. The highest surface concentrations in this region occur in summer, the period of most frequent North African dust transport to North America. If we compare the spring and summer non-North American dust distributions as predicted by NAAPS, however, we can see that there is less non-North American dust simulated over North American land surfaces in the summer months than in spring. Thus, it seems that NAAPS predicts a more widespread influence of Asian dust sources than Saharan dust sources over the continental U.S. Reasons for this will be explored below.

### 3.2.2 Seasonal Transport and Meteorology

As previously stated, the presence of dust plumes aloft does not always coincide with regions of high surface dust concentrations and vice versa. This is demonstrated in Figure 3.6, which contains the average seasonal total column mass of soil dust predicted by NAAPS over North America for 2001-2004 from the simulation with all sources active. A few features are of note. First, NAAPS predicts relatively low total column dust loadings over North America in winter and fall, when both Asian and Saharan dust transport to the U.S. is less pronounced. It predicts localized total column dust maxima during all seasons over the High Plains of the U.S., where the most frequent dust production in North America occurs in the model. NAAPS predicts these North American sources to have a regional influence at most, since the surface concentration maxima in Figure 3.4 have roughly the same spatial extent as the total column maxima in the vicinity of these source regions.

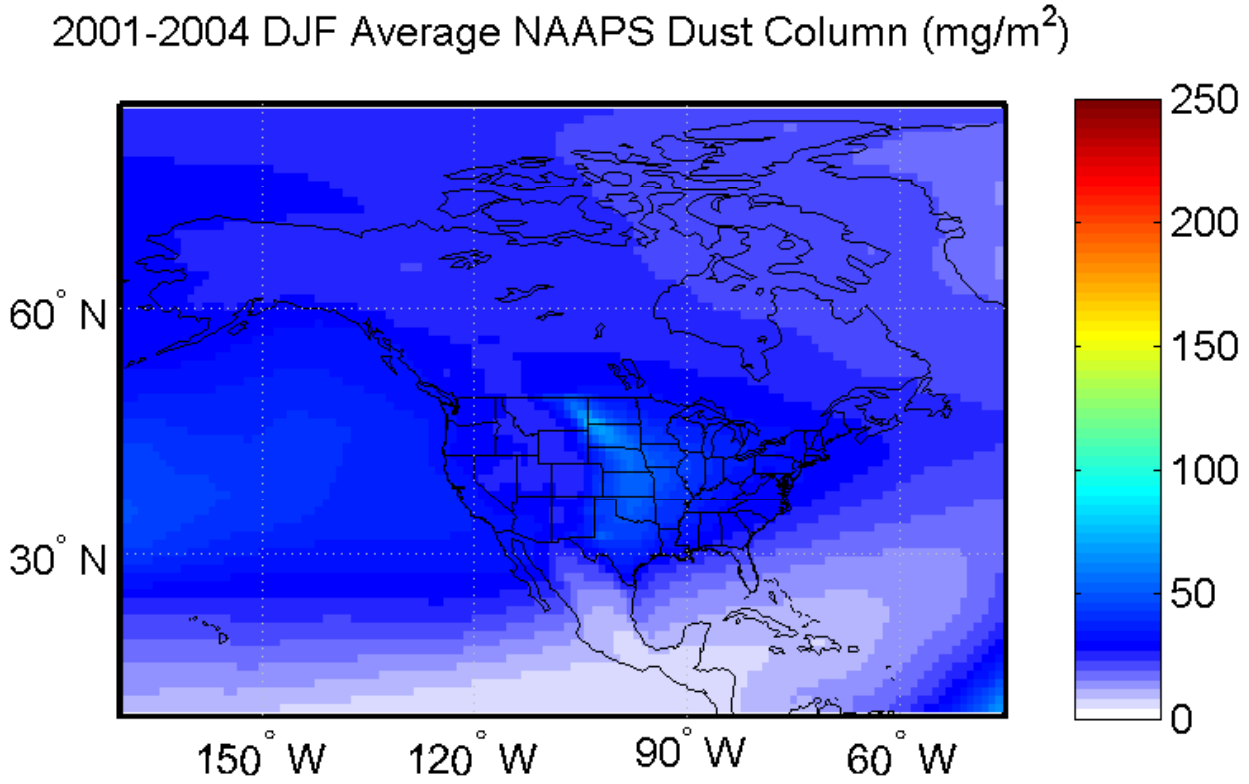
2001-2004 DJF Average NAAPS Dust Column (mg/m2)
60° N
30° N
150° W
120° W
90° W
60° W
250
200
150
100
50
0

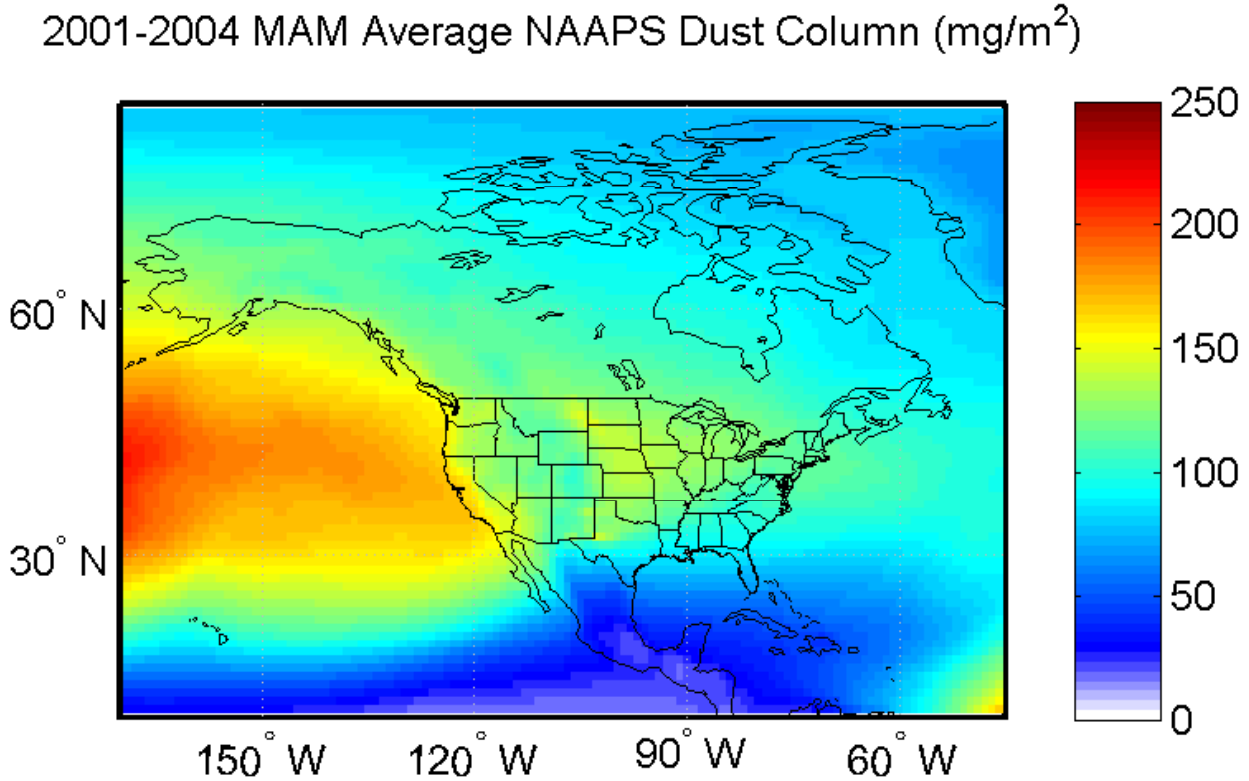
2001-2004 MAM Average NAAPS Dust Column (mg/m2)
60° N
30° N
150° W
120° W
90° W
60° W
250
200
150
100
50
0

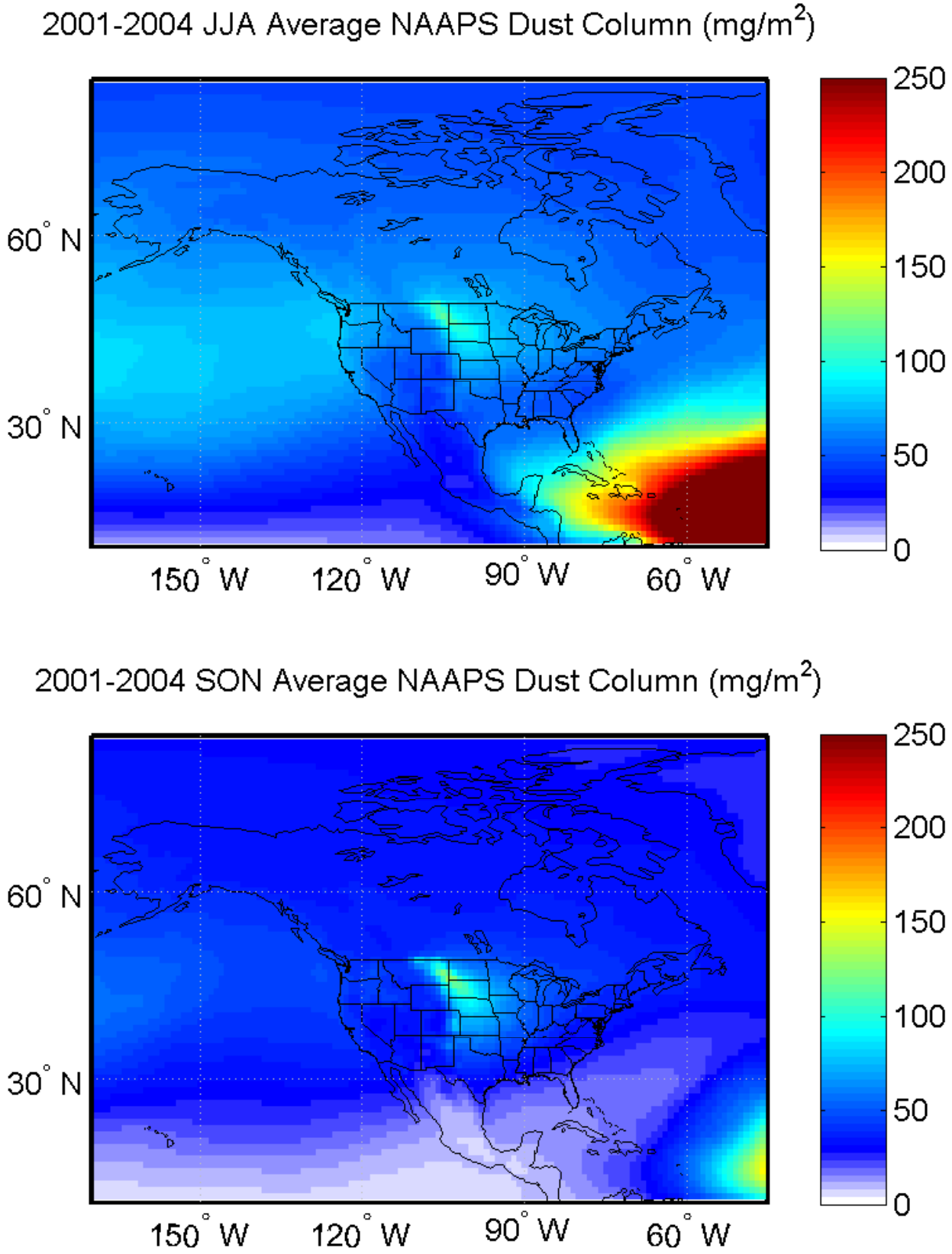


**Figure 3.6: 2001-2004 average seasonal NAAPS dust column (mg $m^{-2}$).**

A second feature of interest in Figure 3.6 is the zonal maximum of column dust loading over the eastern Pacific between ~30º and 50º N in springtime. This feature is consistent with the climatological maximum band of spring trans-Pacific Asian dust transport from 1960-2003 simulated by Zhao et al. (2006). Unlike over the continental U.S., the heaviest total column dust loadings over the Pacific predicted by NAAPS in spring do not correspond with the highest surface concentrations of non-North American dust during the season (Figure 3.5). The band of maximum surface concentrations over the ocean is located along 30º N, south of the line of bulk Asian dust transport predicted by NAAPS.

This is consistent with the numerous hypotheses (Ginoux et al., 2001; VanCuren and Cahill, 2002; Zhao et al., 2006) that trans-Pacific Asian dust transport is elevated above the marine boundary layer. A look at the meteorology for the time period reveals why this is so. The mean 500 millibar height pattern (Figure 3.7) for spring 2001-2004 indicates primarily zonal flow aloft, leading to the zonally-symmetric column dust loading that NAAPS produces over the Pacific. Thus, if the dust is suspended in this zonal flow aloft, it would only reach the Earth's surface in the presence of descending air masses or at sites that extend into the free troposphere. The issue of elevation will be discussed in later sections, but the former argument is illustrated by the composite mean sea level pressure charts in Figure 3.8. In spring, the subtropical high pressure system over the East Pacific intensifies and shifts to the north. As air undergoes a clockwise circulation around the system, it descends, reaching the surface in the eastern and southern regions of the system (Danielsen, 1980). This location correlates well with the

2001–2004 DJF 500 mb height (m) Composite Mean

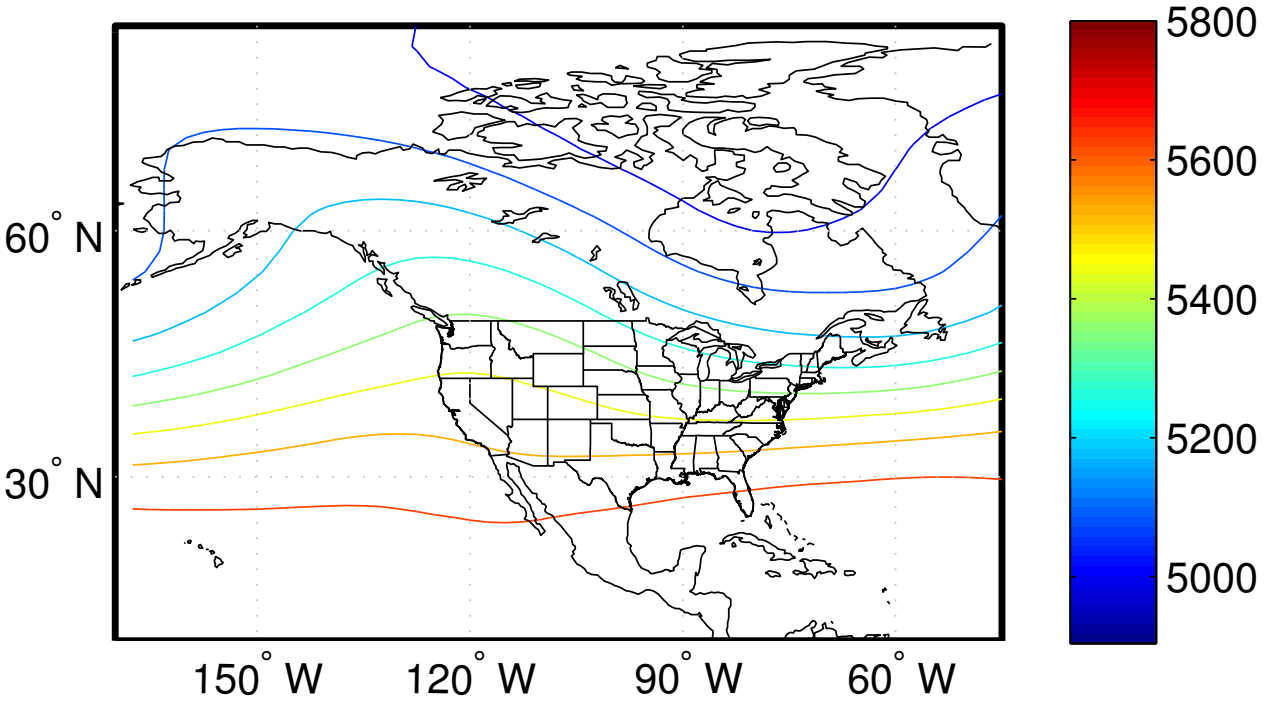


2001–2004 MAM 500 mb height (m) Composite Mean

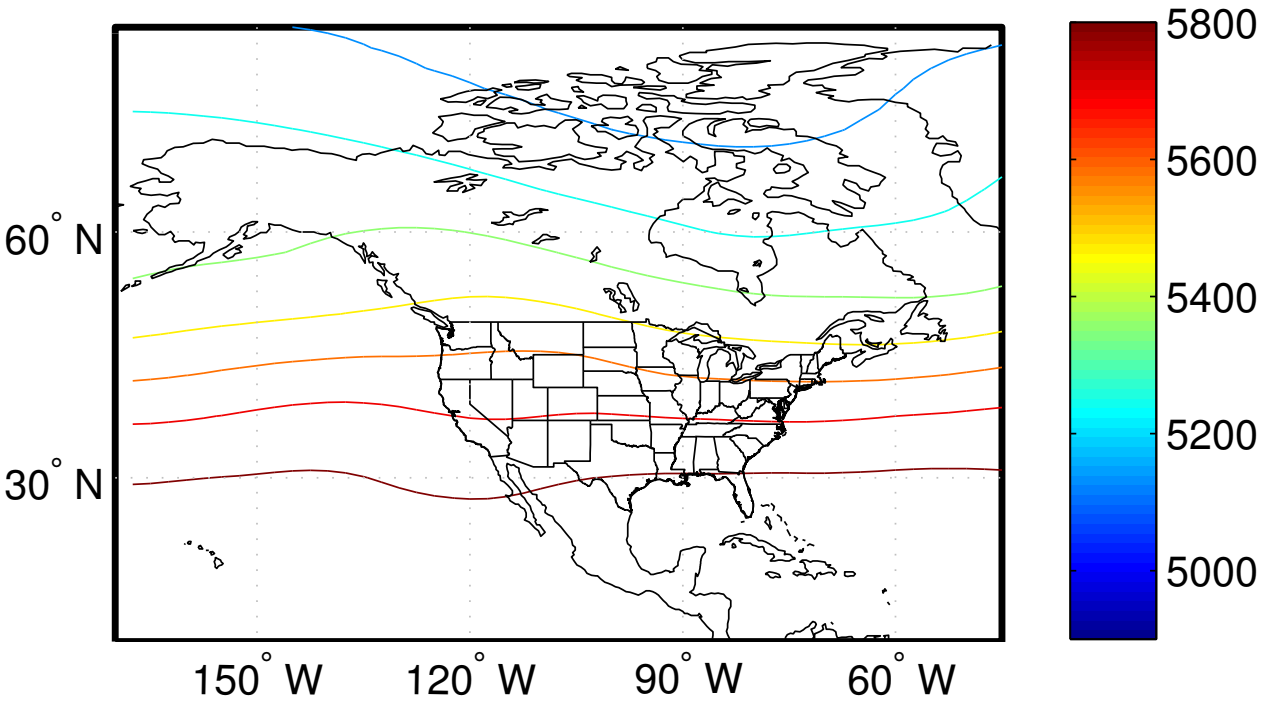

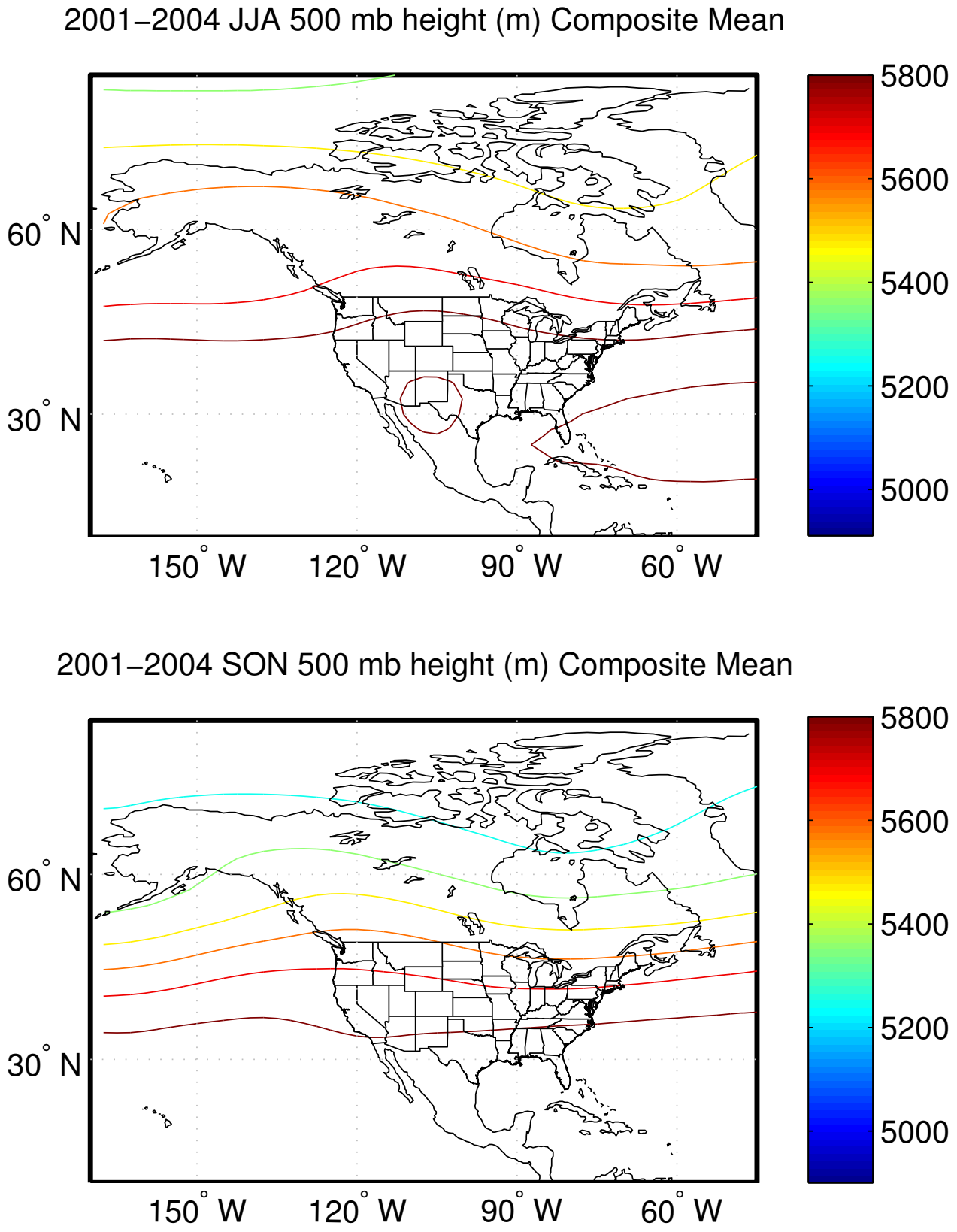


**Figure 3.7: 2001-2004 500 mb height (m) composite means (source: NOAA CDC Reanalysis Data).**

2001–2004 DJF Sea Level Pressure (mb) Composite Mean

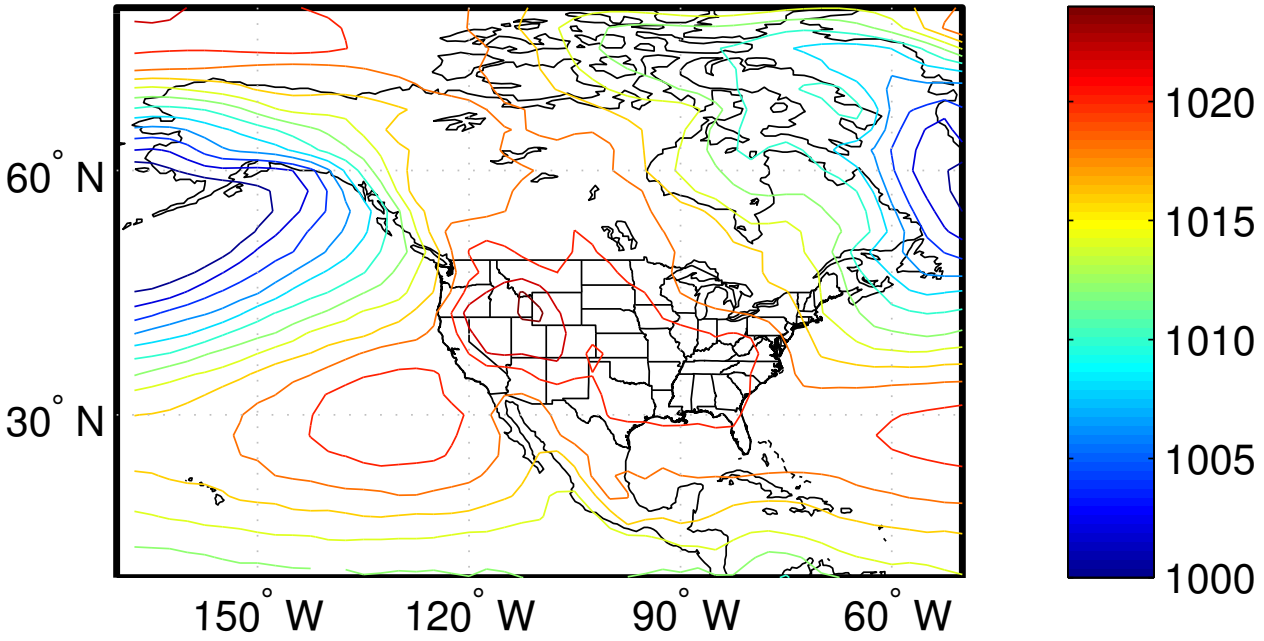


2001–2004 MAM Sea Level Pressure (mb) Composite Mean

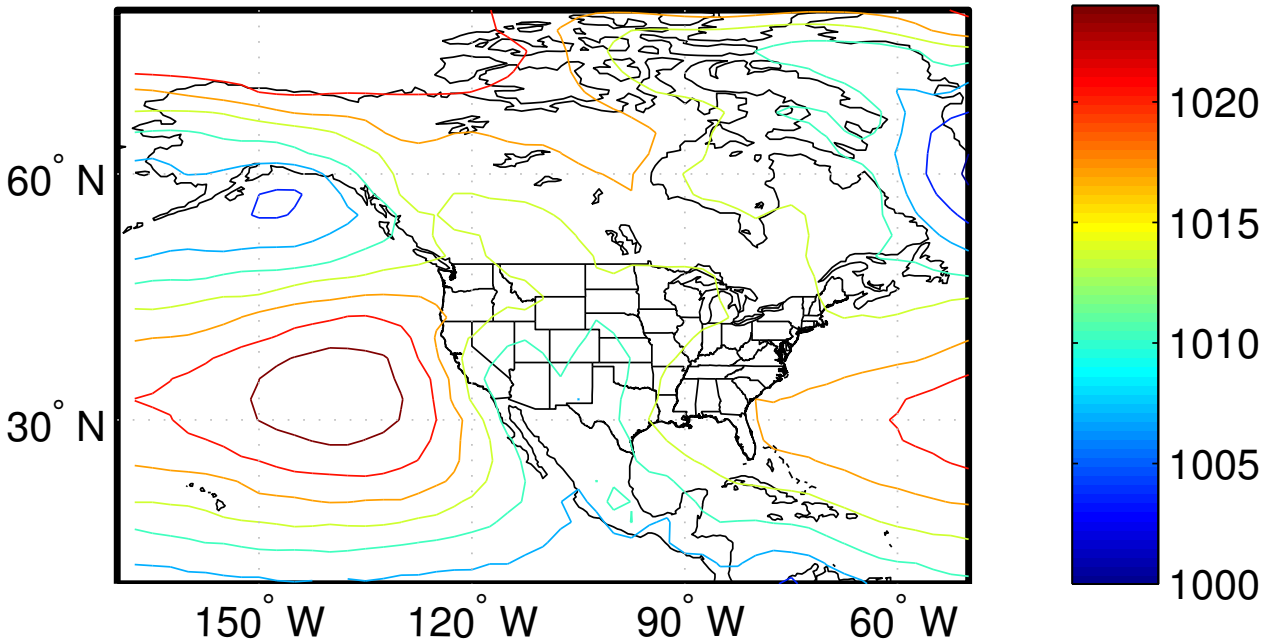

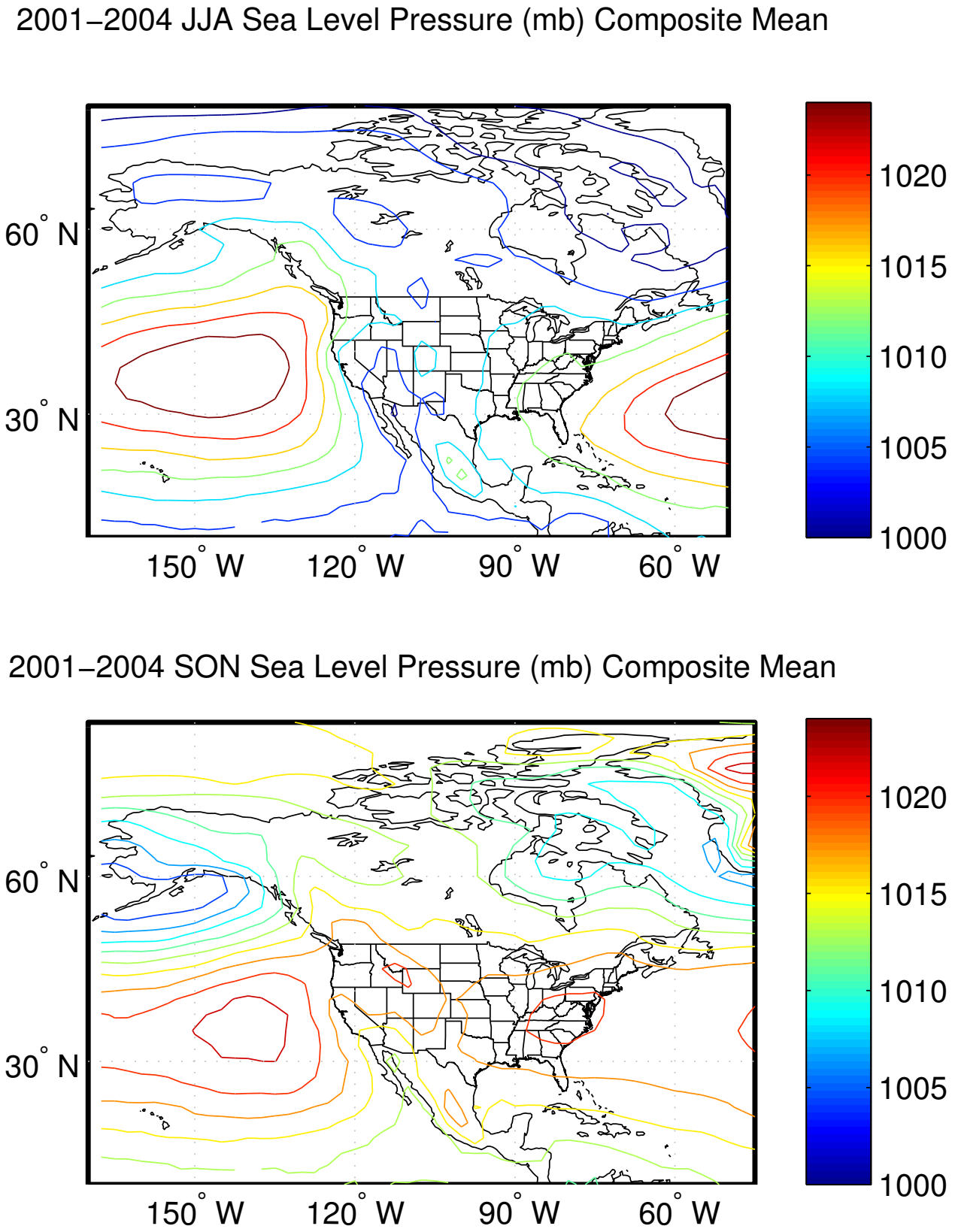


**Figure 3.8: 2001-2004 sea level pressure (mb) composite means (source: NOAA CDC Reanalysis Data).**

maximum of predicted non-North American surface dust concentrations over the Pacific. Furthermore, surface concentrations of non-North American dust in NAAPS are at a minimum near the center and to the south of the Aleutian low, where surface convergence would inhibit elevated dust plumes from descending into the marine boundary layer.

In the summer months, however, NAAPS predicts the largest surface concentrations over North America in the same region as the heaviest total column dust loadings: just south of 30º N over the Caribbean. During the spring and summer months, the semi-permanent Bermuda high shifts northward and intensifies (Figure 3.8). The system is still resolved in the height pattern at the 500 millibar level, shown in Figure 3.7, indicating the deep structure of the system. The vertical structure of the Bermuda high can explain the observed mid-level westward transport of Saharan dust (Karyampudi et al., 1999); the deep region of tropical easterlies along the southern branch of the system carries Saharan dust westward across the Atlantic (Perry et al., 1997). The maximum summer concentrations of non-North American dust predicted by NAAPS correspond well with the location of the southern branch of the Bermuda high for 2001-2004.

In addition to transport patterns, we can also use precipitation patterns to explain the spatial distribution of predicted surface dust concentrations, and why it might appear different than that of total column dust mass. High surface concentrations of dust cannot exist in regions where dust particles are scavenged by rainfall, whether or not the model predicts a consistently large total dust column in the region. Such is definitely the case over the Pacific in spring; the largest surface concentrations of non-North American dust over the ocean appear in the region where the average annual rainout in NAAPS is at a

minimum (Figure 3.3). Over the Atlantic, however, maximum surface dust concentrations occur in regions where average annual dust rainout is also very high; this behavior is attributable to the fact that the northward shift of the Bermuda high is accompanied by the northward shift of the ITCZ during the summer months. Thus, maximum over-ocean precipitation rates are realized at the same time that total column dust loadings are maximized over the Caribbean. Because the mid-level transport of Saharan dust would permit larger particles to be transported than those from Asian sources, more total mass is transported westward in North African dust plumes. The end result is surface concentrations which are less dependent on wet dust scavenging rates.

### 3.2.3 IMPROVE Seasonal Averages

Seasonal averages of IMPROVE [$PM_{10}$-$PM_{2.5}$]+[Soil] measured from 2001-2004 at the 28 sites investigated in this study appear in Figure 3.9. Concentrations of this parameter are quite low at all sites in the winter months, with the exception of Guadelupe Mountains National Park, Texas. In spring this site still yields the highest average mass concentration; increased levels also appear at the two southern California sites and in New Jersey, as well as sites in the northern Great Plains and the Mississippi valley. In summer, these same sites have even higher [$PM_{10}$-$PM_{2.5}$]+[Soil], with maximum concentrations occurring in the southwestern-most sites in the U.S. (an absolute maximum occurs at Sequoia National Park in California), Upper Buffalo Wilderness, Arkansas and Everglades in Florida. The same spatial pattern appears in the average of measurements taken in fall (at lower total magnitudes), although concentrations are lower at Everglades. Sites in the upper New England states, the Great Lakes region, and the Pacific Northwest exhibit low [$PM_{10}$-$PM_{2.5}$]+[Soil] concentrations throughout the year.

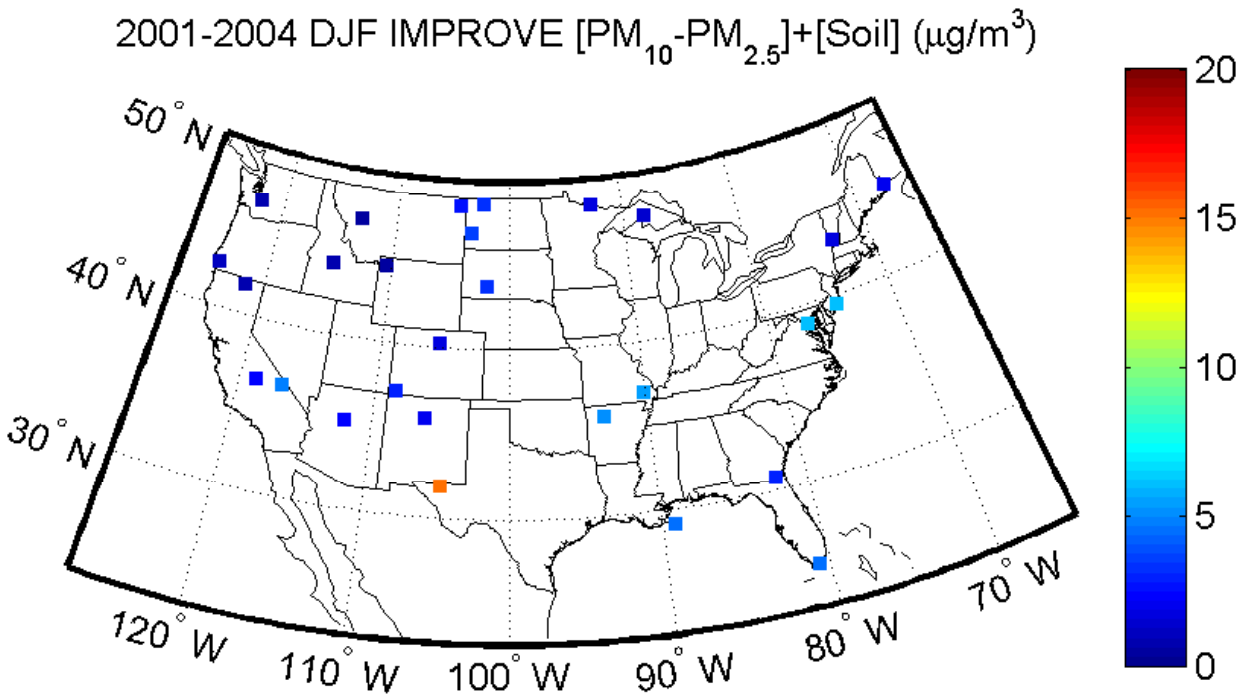
2001-2004 DJF IMPROVE [PM10-PM2.5]+[Soil] (µg/m3)
50° N
40° N
30° N
120° W
110° W
100° W
90° W
80° W
70° W
20
15
10
5
0

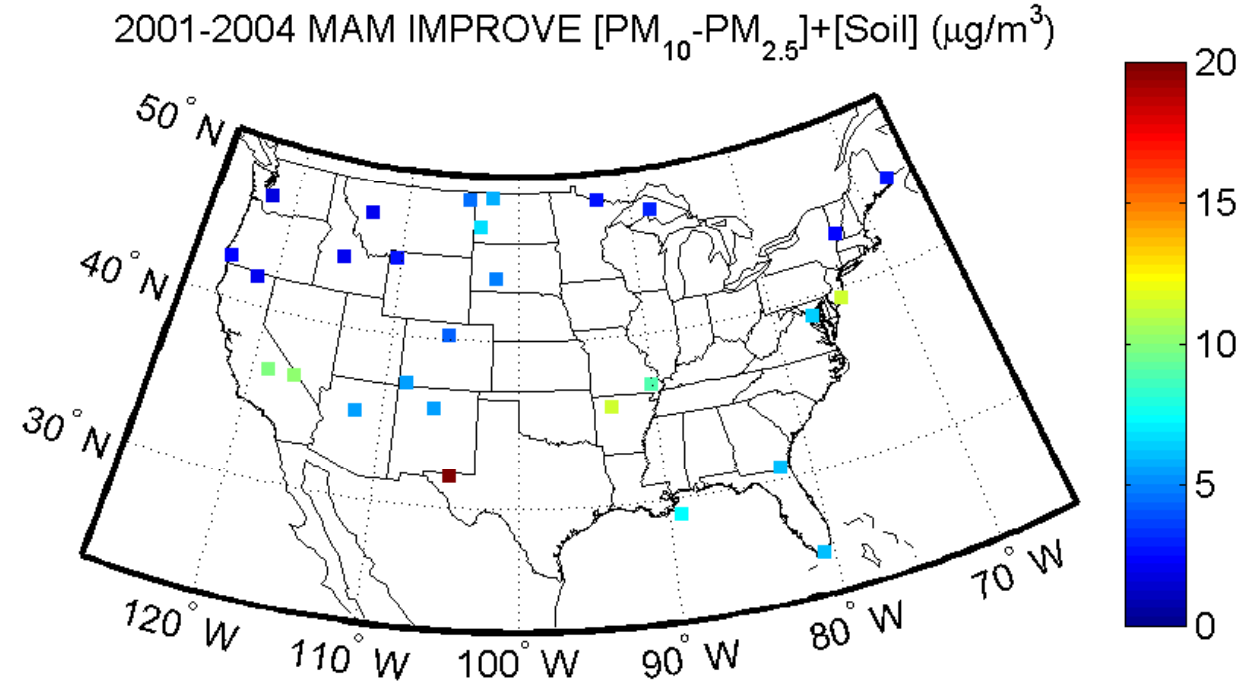
2001-2004 MAM IMPROVE [PM10-PM2.5]+[Soil] (µg/m3)
50° N
40° N
30° N
120° W
110° W
100° W
90° W
80° W
70° W
20
15
10
5
0

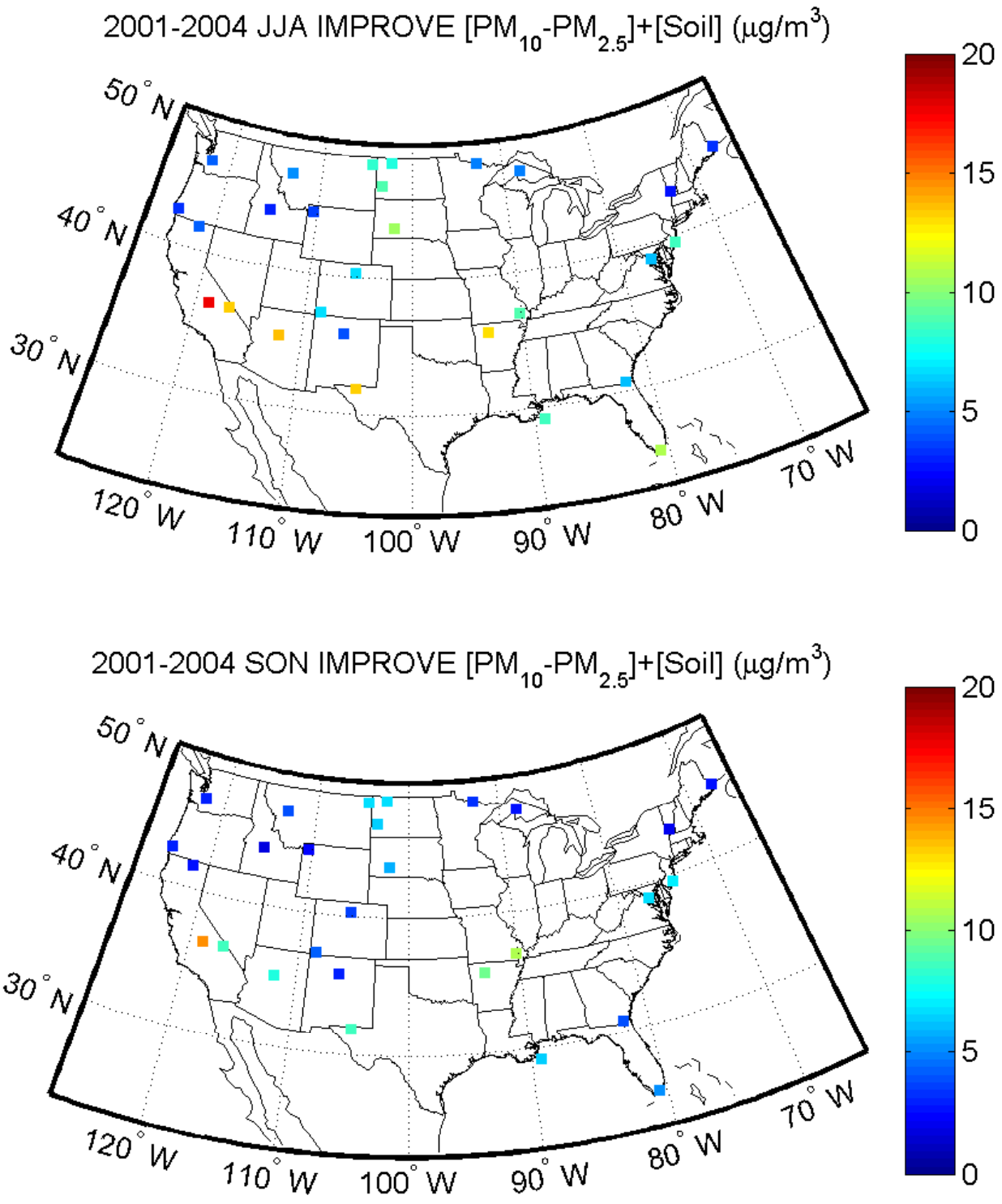


**Figure 3.9: 2001-2004 seasonal IMPROVE [$PM_{10}$-$PM_{2.5}$]+[Soil] concentrations (µg $m^{-3}$).**

Although the IMPROVE measurements are somewhat limited in their spatial and temporal coverage as compared to the global NAAPS output, we can nonetheless see some general similarities in the seasonal means of the two datasets. High mass concentrations are present in the upper Great Plains and the desert Southwest in both NAAPS and IMPROVE, although NAAPS predicts soil dust amounts that are, on average, larger in magnitude than the mass in the IMPROVE dataset. NAAPS predicts high non-North American surface dust concentrations in the western/southwestern U.S. and in Florida and southern Texas, which is consistent with the locations of some sites that have consistently higher values of $[PM_{10}\text{-}PM_{2.5}]$+[Soil]. A more detailed comparison of the two datasets is contained in the following sections.

## 3.3 Comparisons of NAAPS Surface Soil Dust Concentrations to IMPROVE *In Situ* Data

### 3.3.1 Local Production versus Long-range Transport

From the seasonal averages of NAAPS dust aerosol we can see that the model clearly predicts long-range soil dust transport to the U.S. in significant amounts at certain times of the year. The validity of these predictions, in addition to how they compare to the modeled impact of local dust sources, can be discerned most clearly by examining NAAPS and IMPROVE data at specific sites in the U.S.

#### 3.3.1.1 Kalmiopsis, Oregon

Kalmiopsis is an IMPROVE station near the west coast of Oregon, located at an elevation of 90 meters. The site's location is quite ideal for examining the behavior of long-range transport from Asia in NAAPS; since we would expect the site to receive

mostly marine air masses from the west, the potential influence of continental U.S. and North African dust sources is minimal. Timelines of NAAPS daily average predictions and IMPROVE measurements at Kalmiopsis for 2001-2004 are shown in Figure 3.10. In these plots, the blue line corresponds to the NAAPS re-run in which all dust sources were active, the red line represents the NAAPS re-run with North American sources suppressed, and the green line corresponds to the IMPROVE measurements. Whenever a blue line appears above the red line in the following timelines, the model predicts the presence of North American dust. Thus, at times when only a red line is visible, the model predicts dust of only non-North American origin.

NAAPS predicts no influence of North American dust sources at this location, with the exception of a few instances in October-November in 2002, 2003, and 2004. Furthermore, the model predicts generally low total concentrations of soil dust at Kalmiopsis. Average NAAPS simulated amounts of total soil dust and non-North American soil dust for 2001 to 2004 are listed by season in Table 3.3. The bulk of the dust mass predicted at Kalmiopsis appears in spring, early summer, or late fall. A period of episodic non-North American dust incursions over Kalmiopsis from March-June is predicted each year in the four-year NAAPS simulation. Given that this is the period of peak Asian dust transport to the U.S., and the site is located in an area that would be influenced by Asian air masses, we conclude that the model predicts the presence of Asian dust each spring at Kalmiopsis, with some annual variation. The large peak in NAAPS soil dust on 14 April 2001 is consistent with observations of an Asian dust-laden plume over the western U.S. using sunphotometry (Thulasiraman et al., 2002). The second set of soil dust peaks predicted by the model in October and November 2002

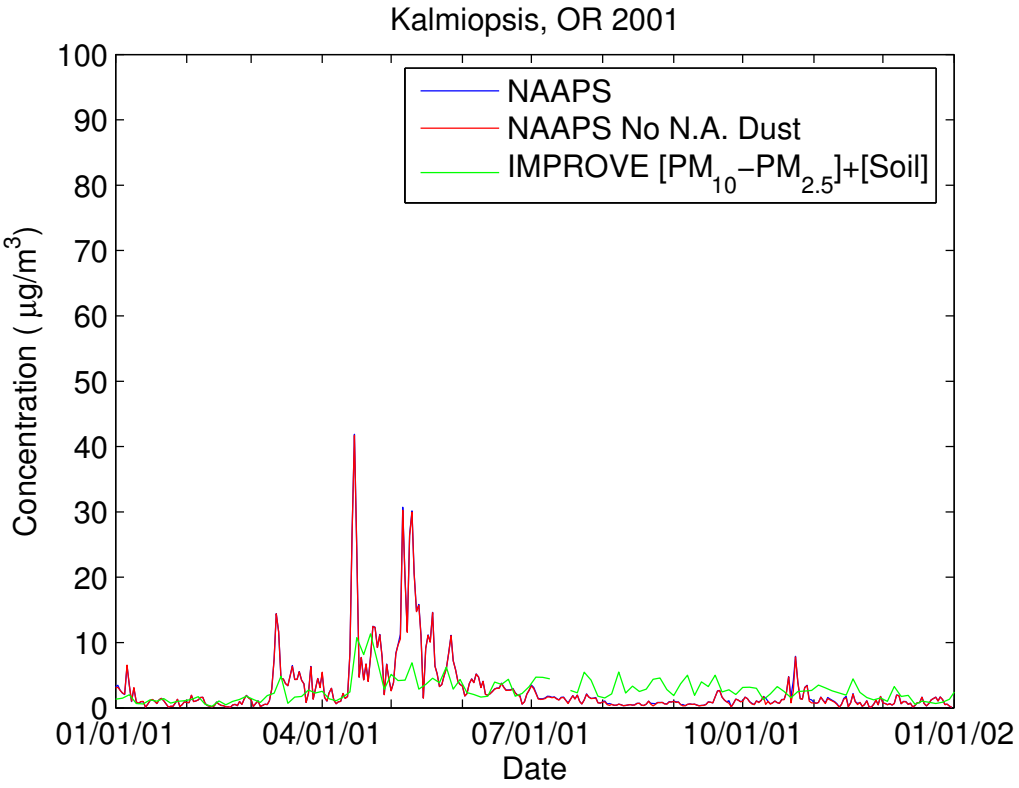
Kalmiopsis, OR 2001
NAAPS
NAAPS No N.A. Dust
IMPROVE [PM10−PM2.5]+[Soil]
Concentration ( µg/m3)
0
10
20
30
40
50
60
70
80
90
100
01/01/01
04/01/01
07/01/01
10/01/01
01/01/02
Date

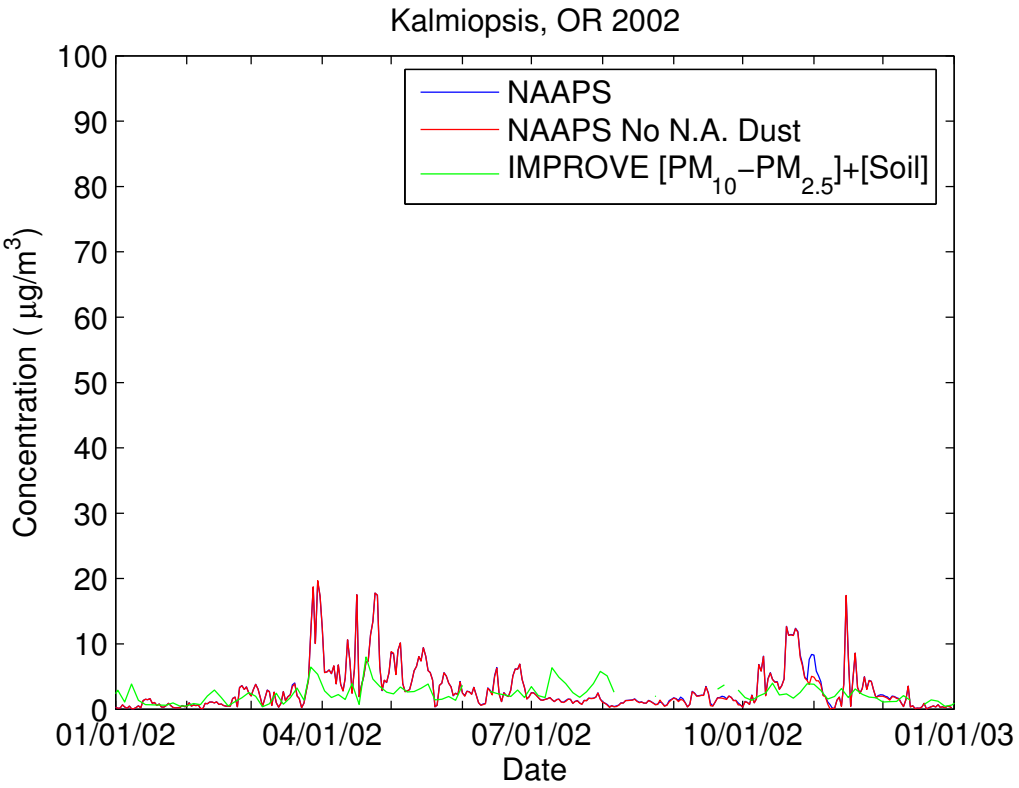
Kalmiopsis, OR 2002
NAAPS
NAAPS No N.A. Dust
IMPROVE [PM10−PM2.5]+[Soil]
Concentration ( µg/m3)
0
10
20
30
40
50
60
70
80
90
100
01/01/02
04/01/02
07/01/02
10/01/02
01/01/03
Date

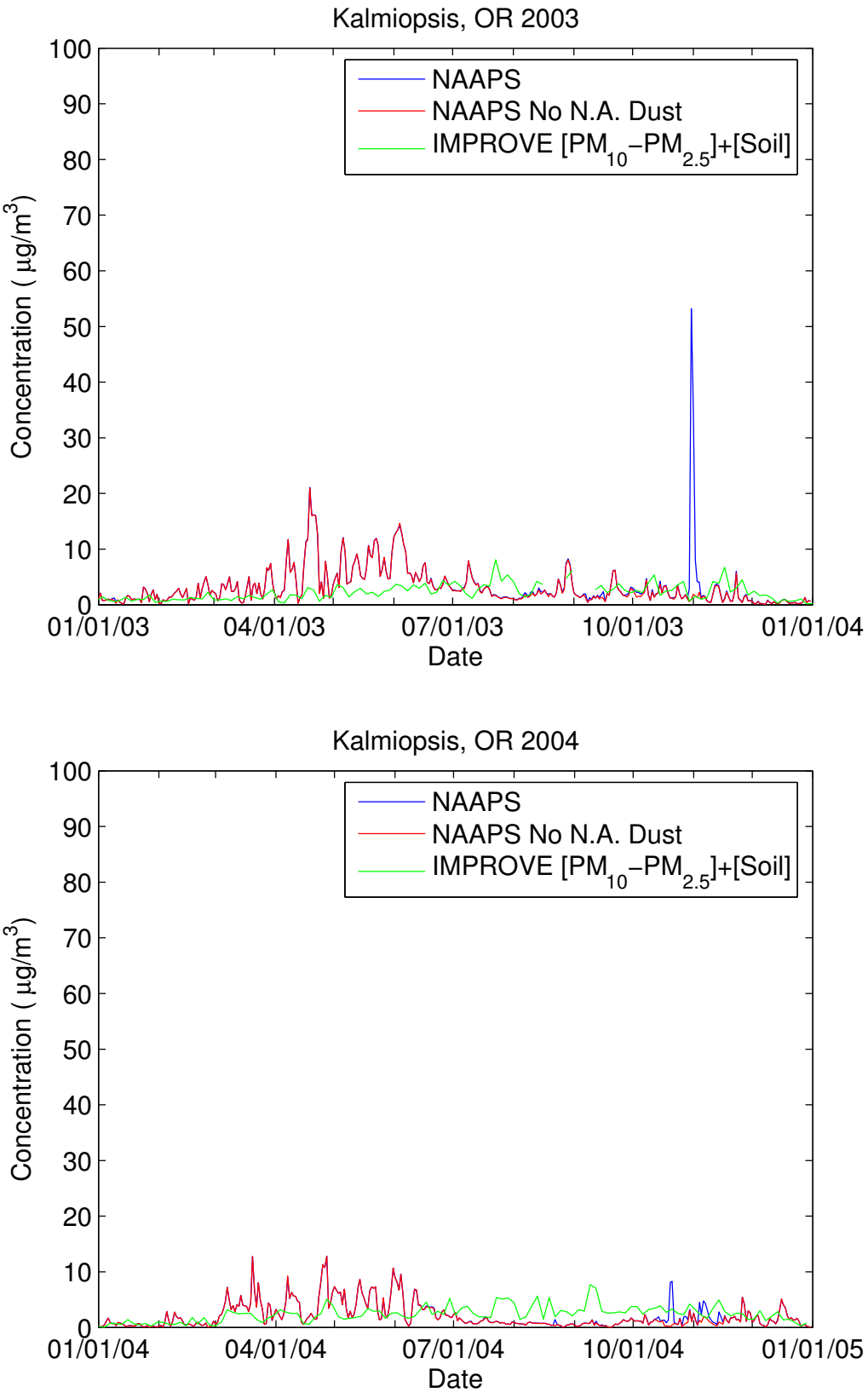


**Figure 3.10: 2001-2004 NAAPS and IMPROVE daily average timelines for Kalmiopsis, Oregon.**

could also be a result of Asian dust transport to the U.S., which would be consistent with studies that have diagnosed the presence of Asian dust in chemical measurements in the U.S. throughout the year (VanCuren and Cahill, 2002). An investigation of the typical Al/Ca ratio used by VanCuren and Cahill (2002) in their diagnosis might confirm this suspicion; however, aluminum is generally below detection limit at Kalmiopsis.

In a comparison with the IMPROVE measurements, it appears that NAAPS has some skill in reproducing the overall variability of soil dust measured at Kalmiopsis. Most of the spring and late fall episodic peaks in dust aerosol predicted by the model coincide with peaks in the IMPROVE data, though predictions of maximum soil in NAAPS tend to contain more mass than IMPROVE. In summer and early fall, on the other hand, the IMPROVE $[PM_{10}\text{-}PM_{2.5}]$+[Soil] tends to be consistently higher than the corresponding NAAPS predicted amounts. The implications of this behavior will be discussed in later sections.

| Season | Average Predicted Total Dust ($\mu g\ m^{-3}$) | Average Predicted Non-North Am. Dust ($\mu g\ m^{-3}$) | Predicted Non-North American Contribution (%) |
|---|---|---|---|
| DJF | 1.0 | 1.0 | 100 |
| MAM | 5.7 | 5.7 | 100 |
| JJA | 2.3 | 2.3 | 100 |
| SON | 2.4 | 1.9 | 79 |

**Table 3.3: Seasonal averages of total and non-North American surface dust concentrations predicted by NAAPS, and the corresponding seasonal non-North American contributions at Kalmiopsis, Oregon.**

#### 3.3.1.2 Death Valley National Park, California

Death Valley National Park, located in the arid region of California east of the Sierra Nevada Mountains, exhibits a somewhat different seasonal soil dust pattern than Kalmiopsis. Its location in the western U.S. also makes it a good site at which to investigate the seasonal trend and extent of Asian dust transport to the U.S. Timelines for the site are shown in Figure 3.11.

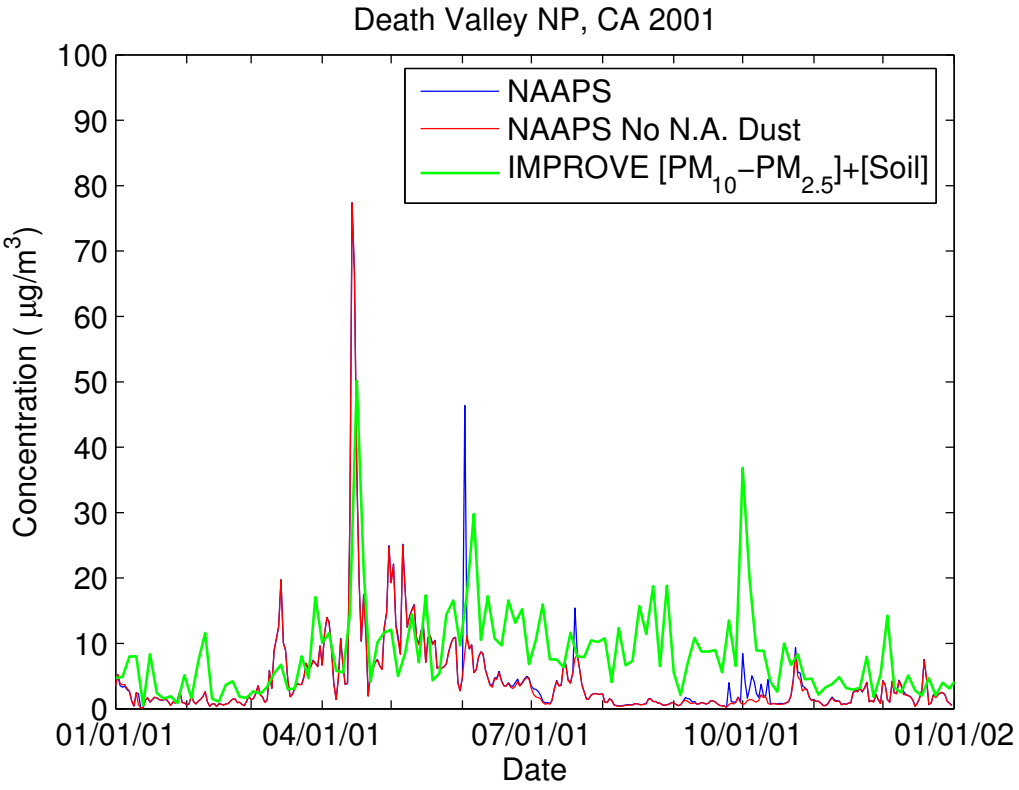
Death Valley NP, CA 2001
NAAPS
NAAPS No N.A. Dust
IMPROVE [PM10−PM2.5]+[Soil]
Concentration ( µg/m3)
Date
01/01/01
04/01/01
07/01/01
10/01/01
01/01/02

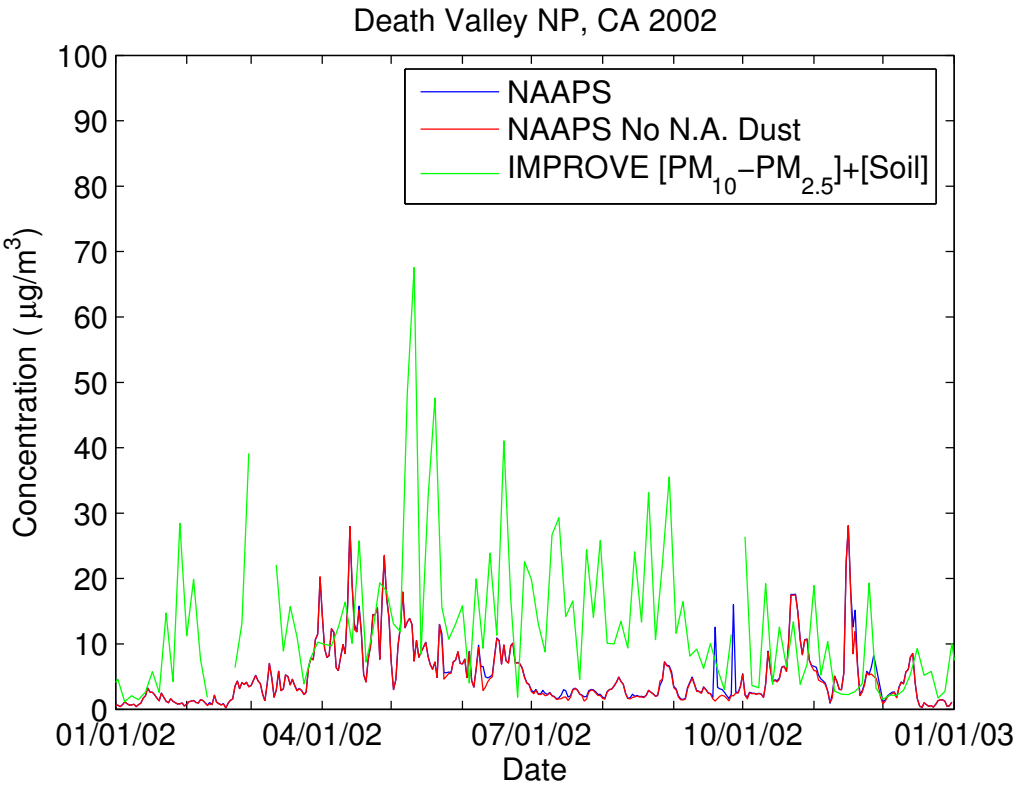
Death Valley NP, CA 2002
NAAPS
NAAPS No N.A. Dust
IMPROVE [PM10−PM2.5]+[Soil]
Concentration ( µg/m3)
Date
01/01/02
04/01/02
07/01/02
10/01/02
01/01/03

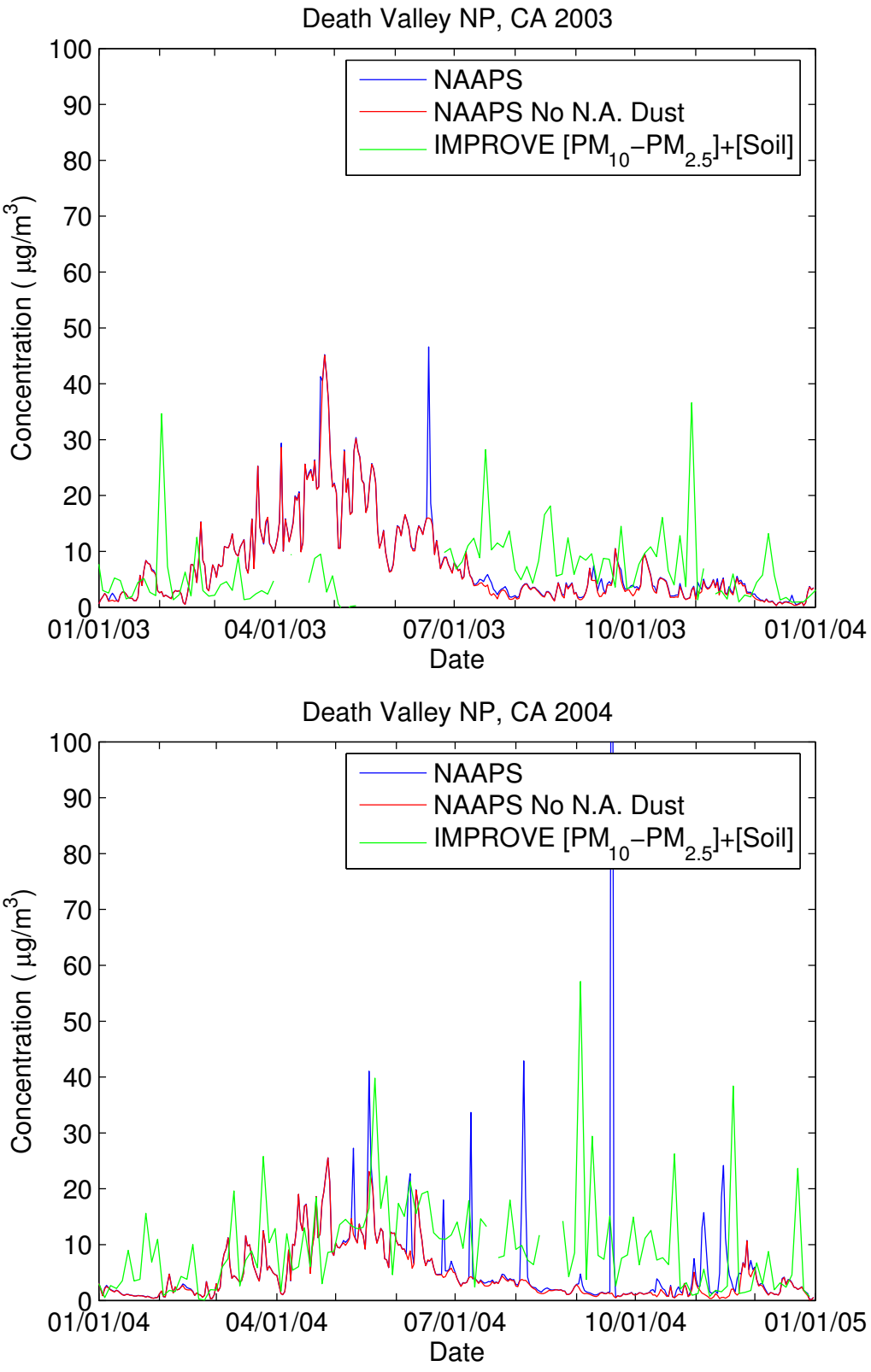


**Figure 3.11: 2001-2004 NAAPS and IMPROVE daily average timelines for Death Valley National Park, California.**

In general, NAAPS predicts higher total dust concentrations at Death Valley than at Kalmiopsis, from both North American and non-North American sources. Seasonally-averaged forecasted concentrations are roughly twice those predicted for Kalmiopsis (Table 3.4). As at Kalmiopsis, the model simulates low concentrations of non-North American dust at Death Valley in the winter and late summer/early fall, but it also simulates large periodic spikes of local dust in the spring, summer, and fall months. On average, North American dust sources are predicted to have the greatest impact at Death Valley in the fall; although the mass attributable to these sources is much less than the mass attributable to non-North American sources. The sustained springtime mass of non-North American dust predicted at Kalmiopsis is predicted each year in NAAPS at Death Valley as well, though the influence of long-range transport at this site begins to occur in February and lasts into June (perhaps even July in 2001) at higher concentrations than at the Oregon site. The observed Asian dust event on 14 April 2001 is quite pronounced in the NAAPS 2001 timeline for Death Valley, manifested in a 24-hour surface concentration peak of over 70 $\mu g\ m^{-3}$.

| Season | Average Predicted Total Dust ($\mu g\ m^{-3}$) | Average Predicted Non-North Am. Dust ($\mu g\ m^{-3}$) | Predicted Non-North American Contribution (%) |
|---|---|---|---|
| DJF | 2.1 | 2.0 | 95 |
| MAM | 11.7 | 11.5 | 98 |
| JJA | 5.2 | 4.4 | 85 |
| SON | 4.4 | 3.0 | 68 |

**Table 3.4: Seasonal averages of total and non-North American surface dust concentrations predicted by NAAPS, and the corresponding seasonal non-North American contributions at Death Valley National Park, California.**

It is interesting that NAAPS predicts a more prominent influence of Asian dust each year at Death Valley than at Kalmiopsis, despite the fact that Death Valley is located farther inland (and at roughly the same elevation). The reason for this requires a return to the discussion of transport patterns in Section 3.2.2. Kalmiopsis is located at 42.5º N,

roughly within the band of maximum spring trans-Pacific Asian dust transport, but Death Valley is located farther south, where subsidence and drier conditions favor higher surface concentrations of Asian dust. The suspected Asian dust transport at Kalmiopsis in October and November is also predicted in greater amounts at Death Valley National Park. The IMPROVE chemical data do not rule out the presence of Asian dust this time of year. The average IMPROVE Al/Ca ratio in the fine aerosol fraction at the site from 2001-2004 was ~1.4 (Figure 3.12), well below the VanCuren and Cahill (2002) Asian dust upper-limit ratio of 2.6. Although these data cannot necessarily confirm NAAPS predictions of non-North American dust at Death Valley National Park, they at least help to eliminate the possibility that calcium-depleted dusts are being transported to the site from North Africa. The apparent constancy of the Al-to-Ca ratio at the site also illustrates the difficulty in separating Asian dust from southwestern U.S. dust influences based only upon these variables, as was also noted by VanCuren and Cahill (2002).

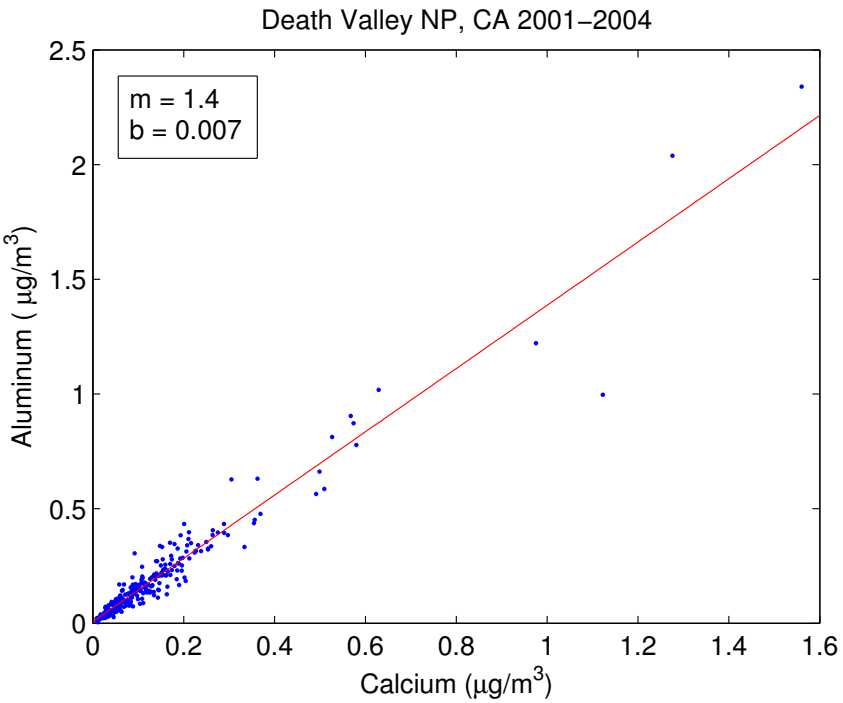


**Figure 3.12: IMPROVE aluminum vs. calcium mass measured from 2001-2004 at Death Valley National Park, California.**

There is general agreement between many of the features in the NAAPS dust and IMPROVE [$PM_{10}$-$PM_{2.5}$]+[Soil] concentration timelines for Death Valley, although a power outage and subsequent equipment problems at the site led to an unfortunate gap in the IMPROVE data in Spring 2003. The long-range dust transport events in NAAPS generally correspond well with the IMPROVE measurements at the site in springtime; however, the periods of sustained high soil mass reported by the IMPROVE network in the summer seem to be not well-resolved in the model, especially the large IMPROVE spikes in Summer of 2002 that corresponded with a period in which the Palmer drought severity index (PDSI) was as low as it had been in the previous 100 years (Figure 3.13, van der Schrier et al., 2006). Periodic pulses of local dust are generated by NAAPS at magnitudes that are on the order of the measurements, but they do not occur with the frequency necessary to be entirely consistent with the IMPROVE data. On the other hand, the fact that the IMPROVE network only samples every three days means that some pulses of locally- or regionally-generated dust could be missed in the data record.

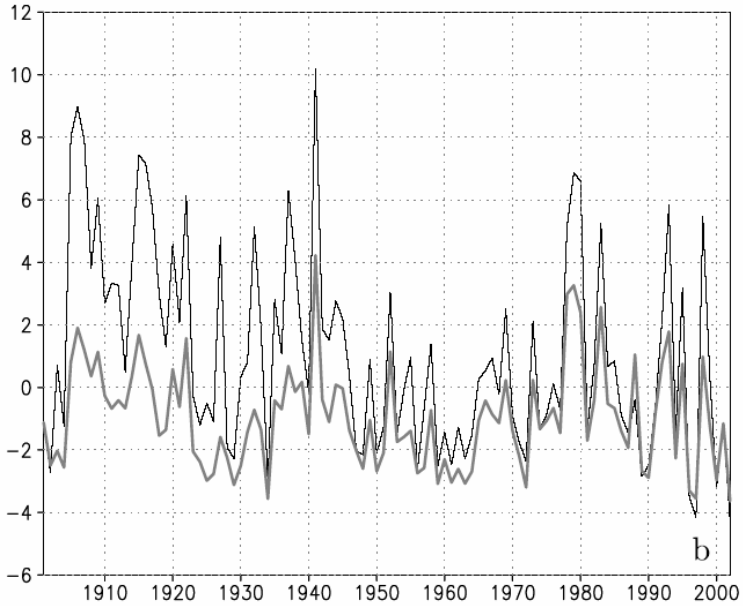


**Figure 3.13: Mean summer PDSI values (thin line) and summer self-calibrating PDSI values (shaded line) for southern California (van der Schrier et al., 2006).**

### 3.3.1.3 Brigantine National Wildlife Reserve, New Jersey

A third site that lends itself to an interesting comparison in this study is Brigantine National Wildlife Reserve in eastern New Jersey. Its location facilitates the examination of long-range transport from North African sources, as well as Asian and North American sources, to the eastern United States. Timelines of daily average NAAPS predictions and IMPROVE measurements for Brigantine National Wildlife Reserve are located in Figure 3.14.

As one might expect, NAAPS predicts low concentrations of soil dust at Brigantine for 2001-2004, less than 3 μg $m^{-3}$ on average in any season (Table 3.5). The majority of dust at Brigantine is predicted to be of non-North American origin in the spring, with more North American influence in the summer, fall and winter months. Interestingly, the small non-North American dust peaks predicted at the site each year in spring are consistent with studies that have found evidence of Asian aerosol in the eastern U.S. (VanCuren and Cahill, 2002). However, the small concentrations in NAAPS generally fall below the IMPROVE measurements, especially in the spring and fall. This has implications for the validity of our choice of comparison variables, especially the assumption that the aerosol coarse fraction consists entirely of soil. At a coastal site such as Brigantine, it is very likely that the $PM_{10}$ contains some mass due to sea salt. This possibility is explored more closely in Chapter 4.

| Season | Average Predicted Total Dust (μg $m^{-3}$) | Average Predicted Non-North Am. Dust (μg $m^{-3}$) | Predicted Non-North American Contribution (%) |
|---|---|---|---|
| DJF | 2.6 | 1.2 | 46 |
| MAM | 2.7 | 2.5 | 93 |
| JJA | 1.4 | 0.9 | 64 |
| SON | 2.7 | 1.2 | 44 |

**Table 3.5: Seasonal averages of total and non-North American surface dust concentrations predicted by NAAPS, and the corresponding seasonal non-North American contributions at Brigantine National Wildlife Reserve, New Jersey.**

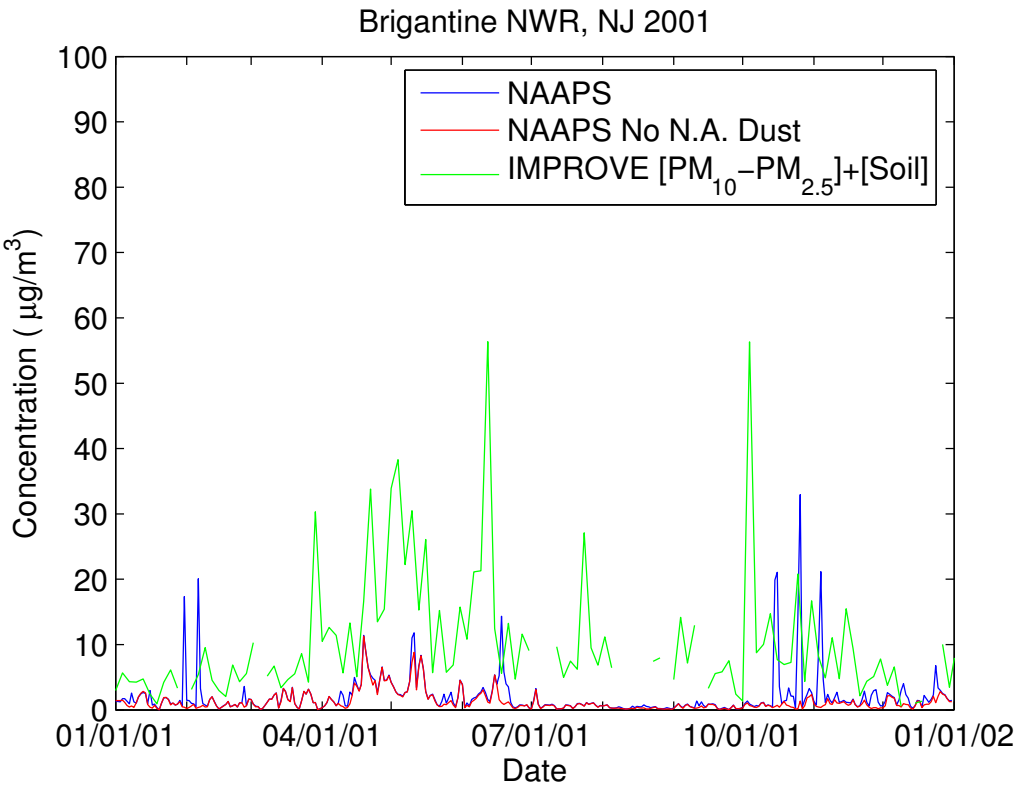
Brigantine NWR, NJ 2001
NAAPS
NAAPS No N.A. Dust
IMPROVE [PM10−PM2.5]+[Soil]
Concentration ( µg/m3)
Date
0
10
20
30
40
50
60
70
80
90
100
01/01/01
04/01/01
07/01/01
10/01/01
01/01/02

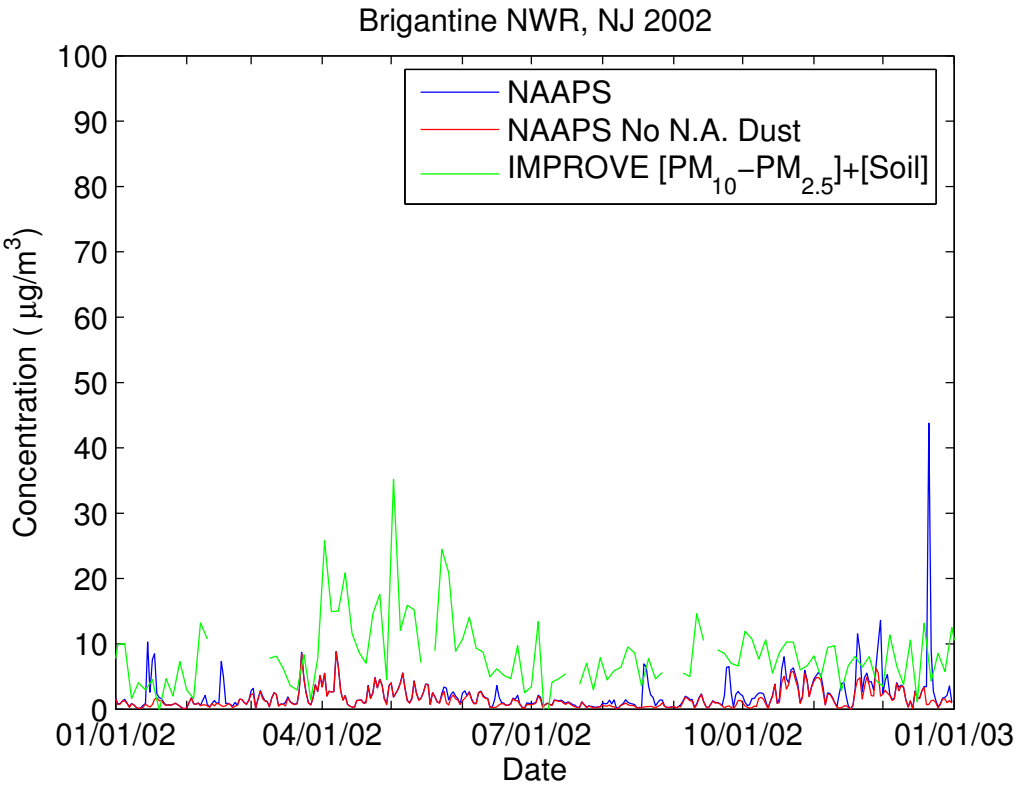
Brigantine NWR, NJ 2002
NAAPS
NAAPS No N.A. Dust
IMPROVE [PM10−PM2.5]+[Soil]
Concentration ( µg/m3)
Date
0
10
20
30
40
50
60
70
80
90
100
01/01/02
04/01/02
07/01/02
10/01/02
01/01/03

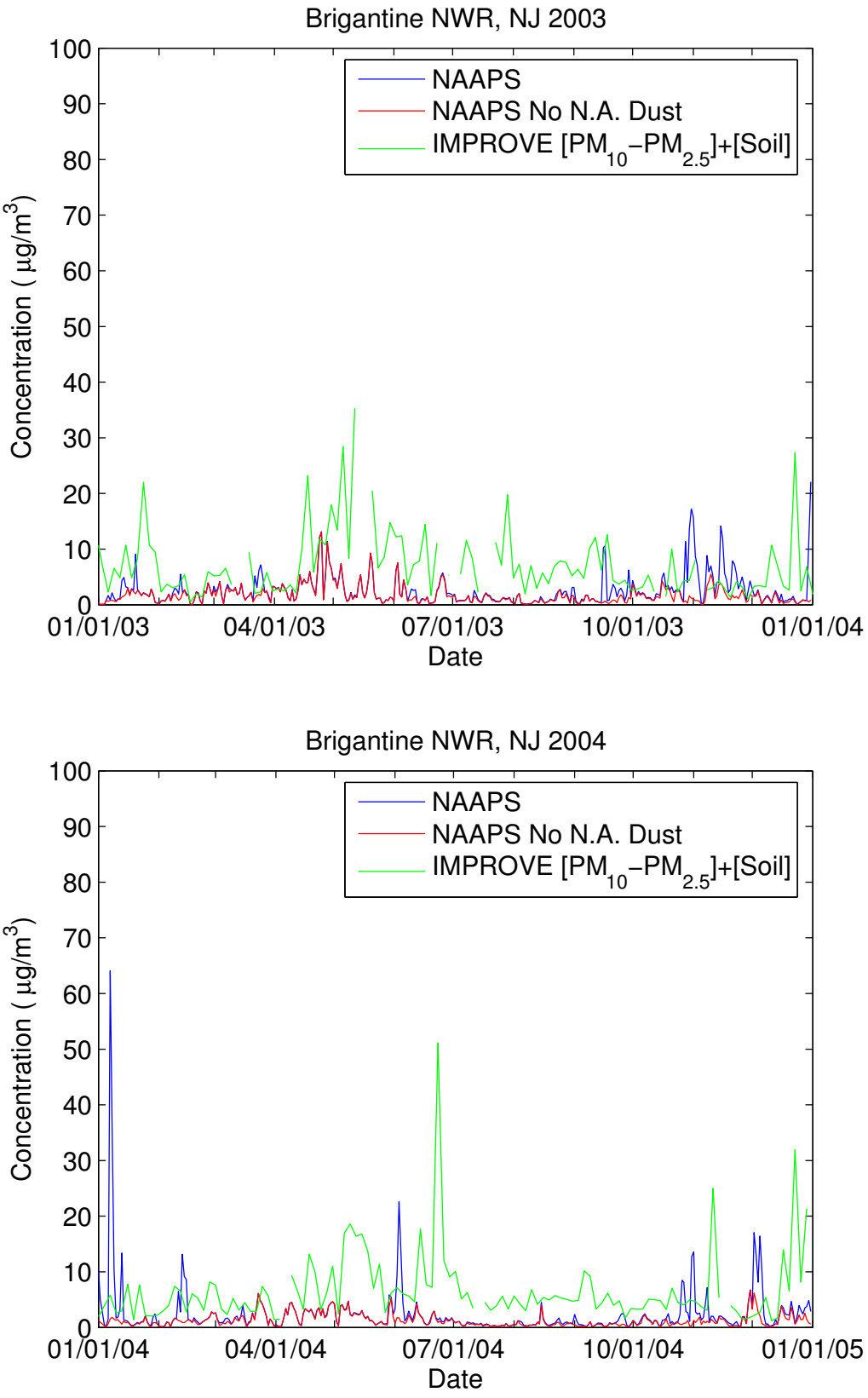


**Figure 3.14: 2001-2004 NAAPS and IMPROVE daily average timelines for Brigantine National Wildlife Reserve, New Jersey.**

#### 3.3.1.4 Theodore Roosevelt, North Dakota

Theodore Roosevelt was chosen as a site for comparison due to its location in western North Dakota, near the region of maximum North American surface dust concentrations predicted by NAAPS. The timelines in Figure 3.15 indicate that the model predicts a strong, frequent influence of North American dust sources at Theodore Roosevelt throughout the fall and winter, with a periodic influence predicted in spring and summer. Average seasonal surface concentrations predicted by NAAPS were between 13 and 35 μg $m^{-3}$ (Table 3.6) but daily average concentrations exceeding 1000 μg $m^{-3}$ were sometimes predicted at the site in the winter and late fall months.

With North American sources removed, a background amount of soil dust is still predicted at Theodore Roosevelt, with a large peak in spring (extending into summer) and a lesser peak in the fall. Peak non-North American soil amounts predicted at the site are on the same order or higher than those predicted at Kalmiopsis in spring. This highlights the potential role of surface elevation in the spatial distribution of dust concentration (Theodore Roosevelt is located at about 850 m). The IMPROVE [$PM_{10}$-$PM_{2.5}$]+[Soil] values have a reasonably similar trend to the NAAPS non-North American dust predictions, and also exhibit some larger peaks in the summer, but not generally of the magnitude of NAAPS predictions of North American dust concentration. Such mass concentrations would actually be well above national ambient air quality standards (150 μg $m^{-3}$ for 24-hour average $PM_{10}$). The behavior of this region in the model will also be discussed in more detail in the following chapter.

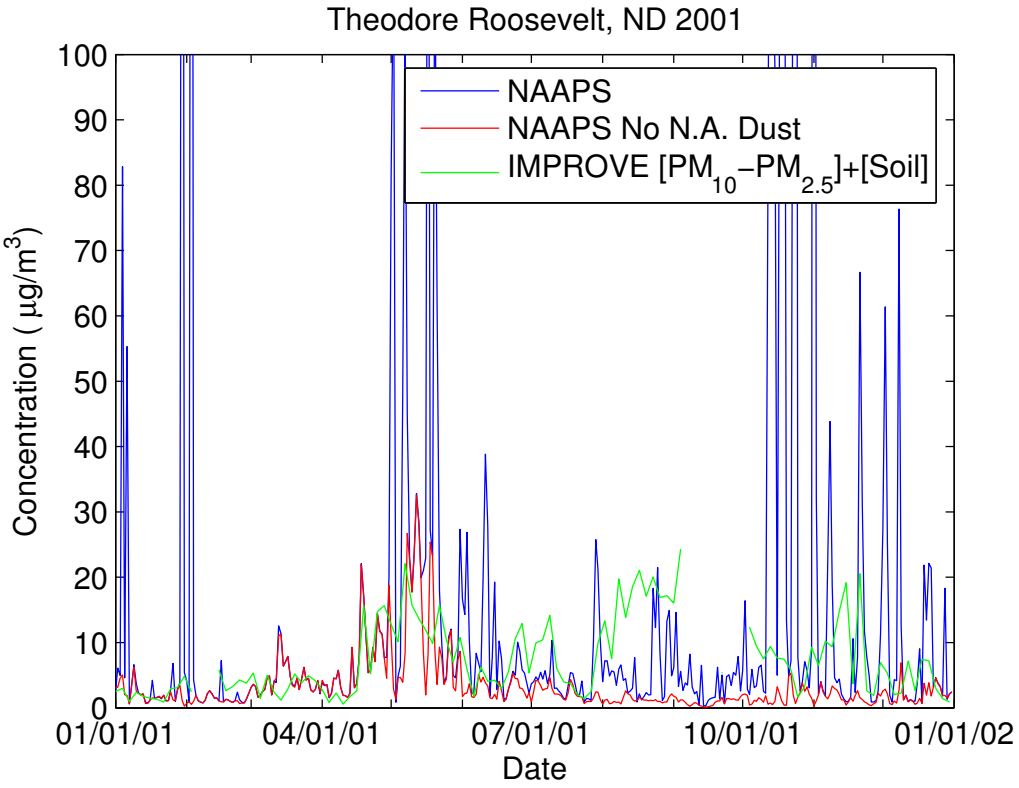
Theodore Roosevelt, ND 2001
NAAPS
NAAPS No N.A. Dust
IMPROVE [PM10−PM2.5]+[Soil]
Concentration ( µg/m3)
Date
01/01/01
04/01/01
07/01/01
10/01/01
01/01/02

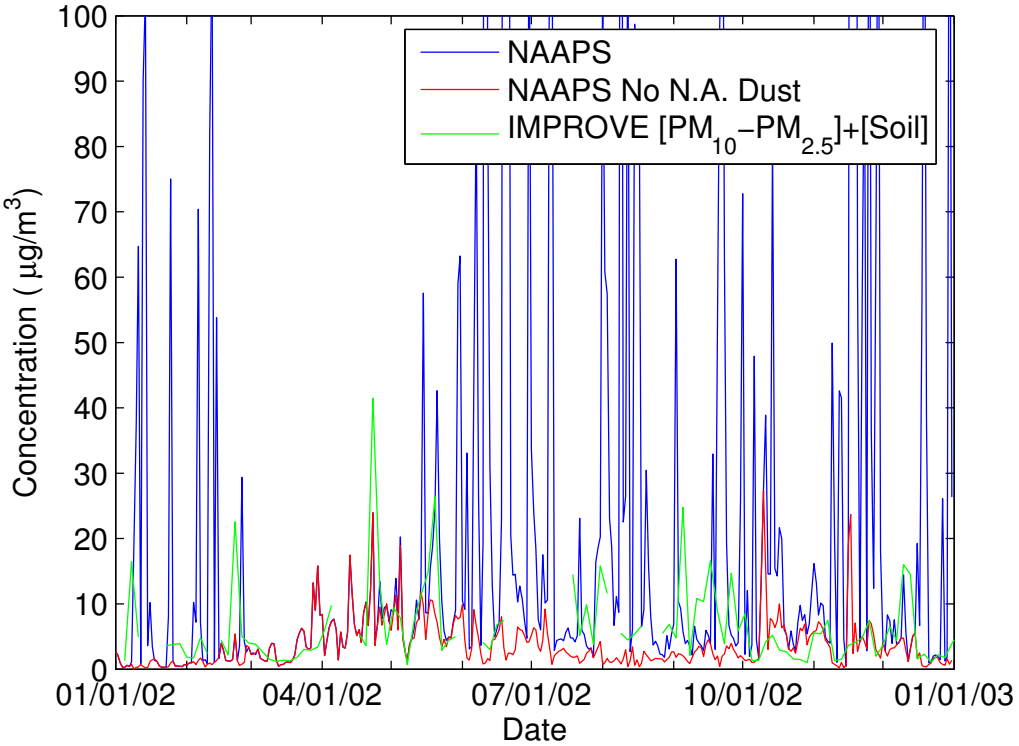
Theodore Roosevelt, ND 2002
NAAPS
NAAPS No N.A. Dust
IMPROVE [PM10−PM2.5]+[Soil]
Concentration ( µg/m3)
Date
01/01/02
04/01/02
07/01/02
10/01/02
01/01/03

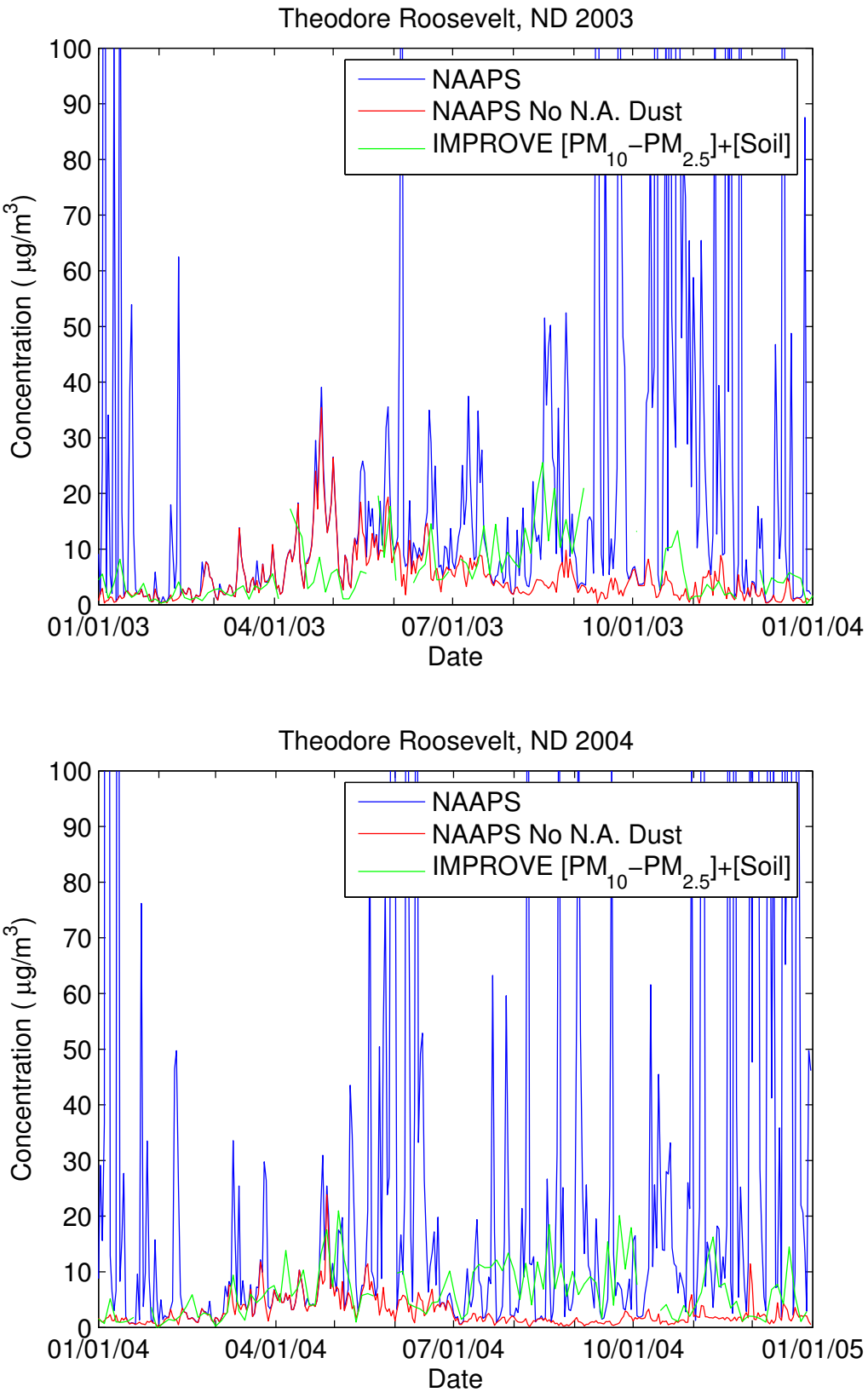


**Figure 3.15: 2001-2004 NAAPS and IMPROVE daily average timelines for Theodore Roosevelt, North Dakota.**

| Season | Average Predicted Total Dust ($\mu g\ m^{-3}$) | Average Predicted Non-North Am. Dust ($\mu g\ m^{-3}$) | Predicted Non-North American Contribution (%) |
|---|---|---|---|
| DJF | 26.1 | 1.7 | 6.5 |
| MAM | 13.2 | 7.0 | 53 |
| JJA | 20.5 | 3.2 | 16 |
| SON | 35.0 | 2.7 | 8 |

**Table 3.6: Seasonal averages of total and non-North American surface dust concentrations predicted by NAAPS, and the corresponding seasonal non-North American contributions at Theodore Roosevelt, North Dakota.**

### 3.3.2 Assessment of NAAPS Predicted Surface Soil Aerosol Mass

Although timelines of NAAPS and IMPROVE data give a qualitative sense of both the seasonal soil dust distribution and year-to-year differences of local versus long-range soil dust amounts at specific sites in the U.S., they do not facilitate a more rigorous assessment of NAAPS surface predictions. A regression of NAAPS predictions against IMPROVE $[PM_{10}\text{-}PM_{2.5}]$+[Soil] for each season of the four-year simulation was carried out as a first attempt at such an examination. In this analysis, if NAAPS predictions are higher than the IMPROVE measurements, the influence of local or long-range dust transport is probably overestimated by the model. If, on the other hand, NAAPS dust concentrations are below IMPROVE $[PM_{10}\text{-}PM_{2.5}]$+[Soil] amounts, some dust source regions are not resolved in NAAPS or the IMPROVE aerosol coarse fraction is not comprised solely of soil particles. These issues will all be addressed in Chapter 4.

Figure 3.16 summarizes this analysis for all IMPROVE sites evaluated in this study. The color levels represent the percent of NAAPS daily average soil dust predictions that are within a factor of two above or below the IMPROVE "soil" amount, a range that was arbitrarily chosen as a reasonable range of expected agreement between the model predictions and the measurements. Definite spatial patterns emerge in Figure 3.16. The frequency of NAAPS predictions that are within a factor of two of the IMPROVE measurements is consistently low at near-coastal sites such as Brigantine

DJF Percent NAAPS Dust Within x2 of IMPROVE [$PM_{10}$-$PM_{2.5}$]+[Soil]

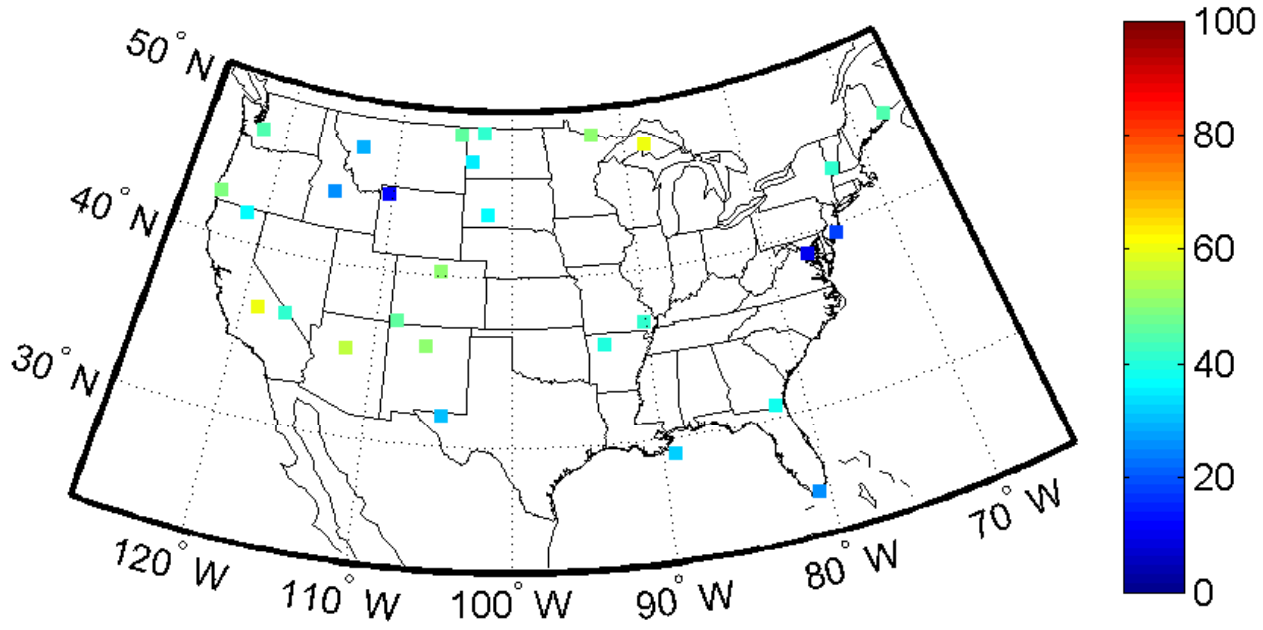


MAM Percent NAAPS Dust Within x2 of IMPROVE [$PM_{10}$-$PM_{2.5}$]+[Soil]

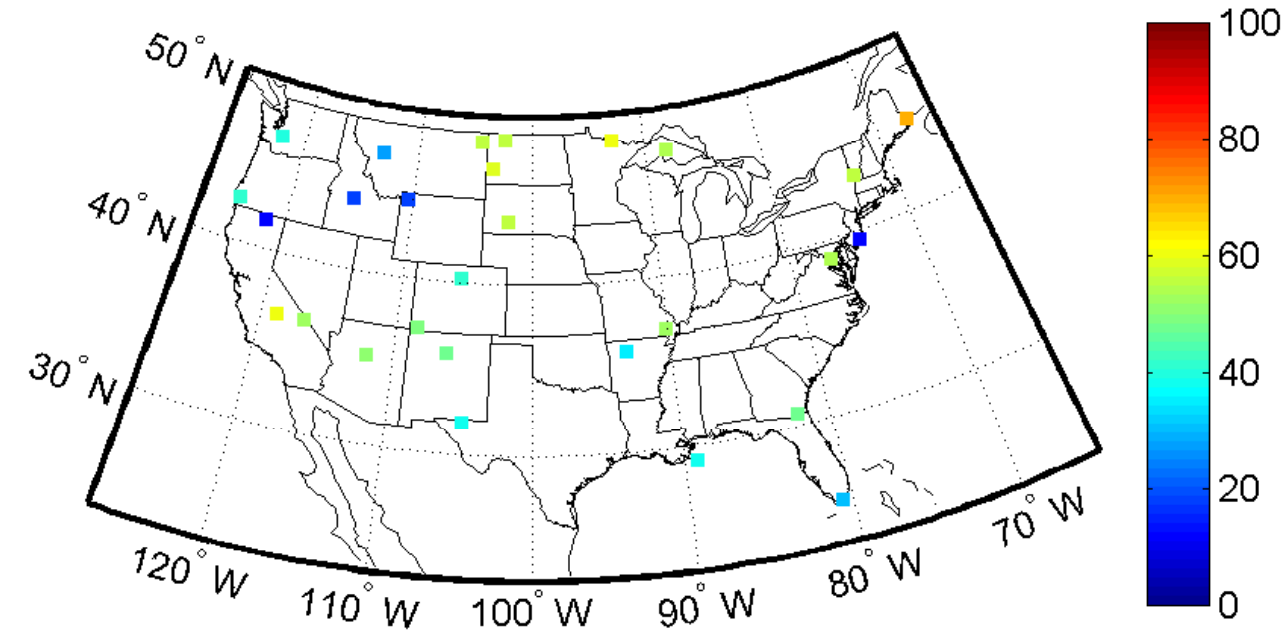

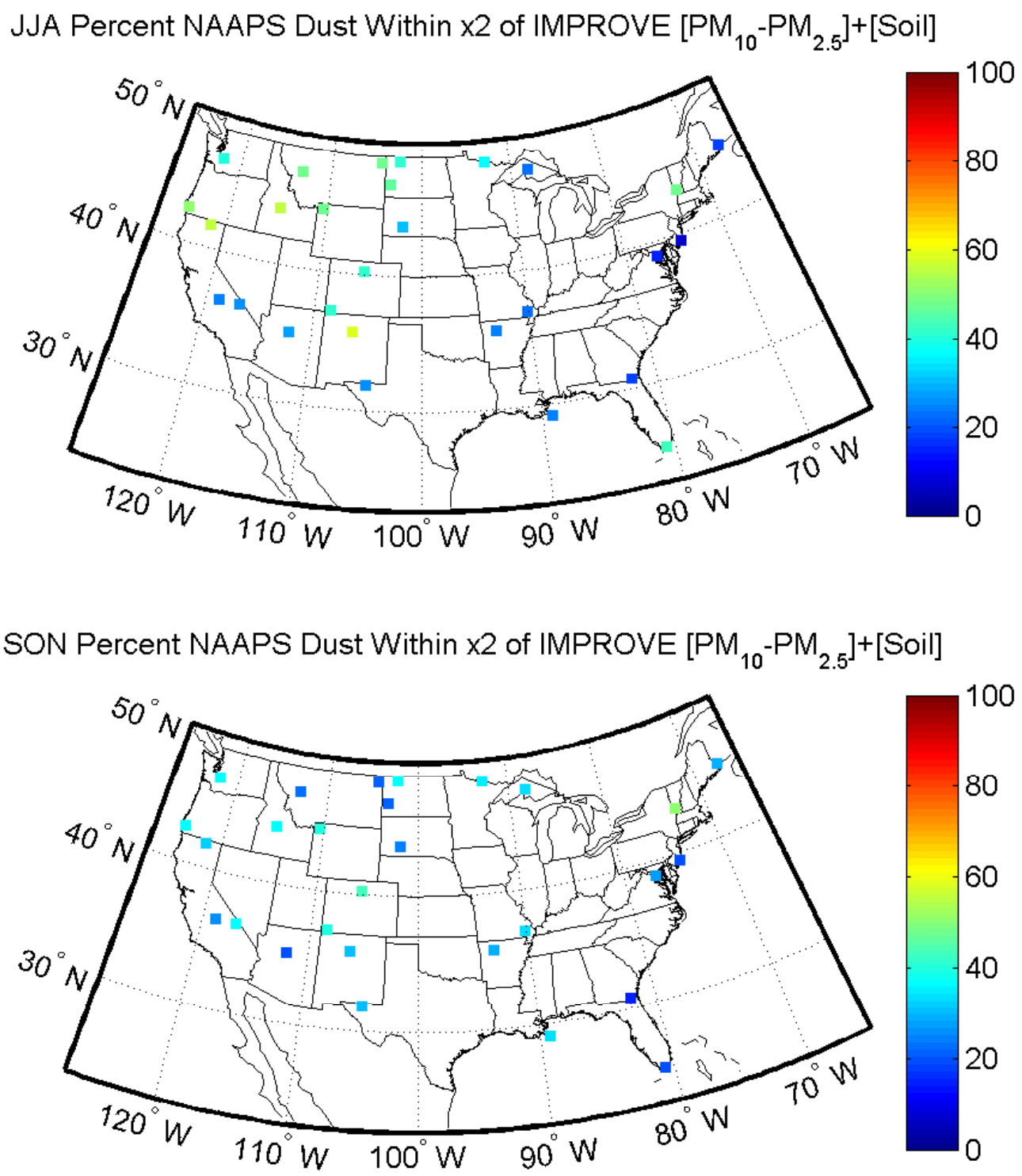


**Figure 3.16: Seasonal comparisons of the frequency (%) of NAAPS predictions falling within 2:1 and 1:2 of IMPROVE [$PM_{10}$-$PM_{2.5}$]+[Soil].**

National Wildlife Reserve, New Jersey; Everglades National Park, Florida; and Breton, Louisiana. It is also low in the Montana/Wyoming/Idaho cluster of sites in the spring, fall, and winter months. In the southwestern U.S., NAAPS predictions are frequently within a factor of two of IMPROVE during the winter and spring months; however, this is not the case during the summer and fall. The same holds true for sites in the central U.S. and Great Lakes regions. At sites near the active NAAPS U.S. dust site in Montana, frequencies of agreement between the model and measurements are ≥ 50%, despite the fact that the model produces a lot of dust here throughout the year. NAAPS is not as often within a factor of two of IMPROVE at these sites in the fall and winter months. Few NAAPS predictions fall within a factor of two of IMPROVE $[PM_{10}\text{-}PM_{2.5}]$+[Soil] in the fall, with the exception of Lye Brook Wilderness, Vermont.

The maps in Figure 3.16 do not indicate whether a bias exists in the comparison, that is, if NAAPS or IMPROVE is consistently the higher value at a certain site. To examine the seasonal variation of biases, scatter plots of the NAAPS-to-IMPROVE comparisons at the four sites discussed in Section 3.3 are shown in Figure 3.17. At Kalmiopsis, the scatter is fairly evenly distributed around the 1:1 line in all seasons. At Theodore Roosevelt; however, many of the NAAPS predictions are well above the IMPROVE measurements. Two populations appear in the comparisons at Death Valley and Brigantine with very few points falling along the 1:1 line. At Death Valley National Park, the NAAPS forecasts generally contain less mass than reported by the IMPROVE network, but the reverse is true for many NAAPS predictions at the site in spring. NAAPS predictions are nearly always below 1:1 with the IMPROVE data at Brigantine, with the exception of a small grouping of points in fall and winter.

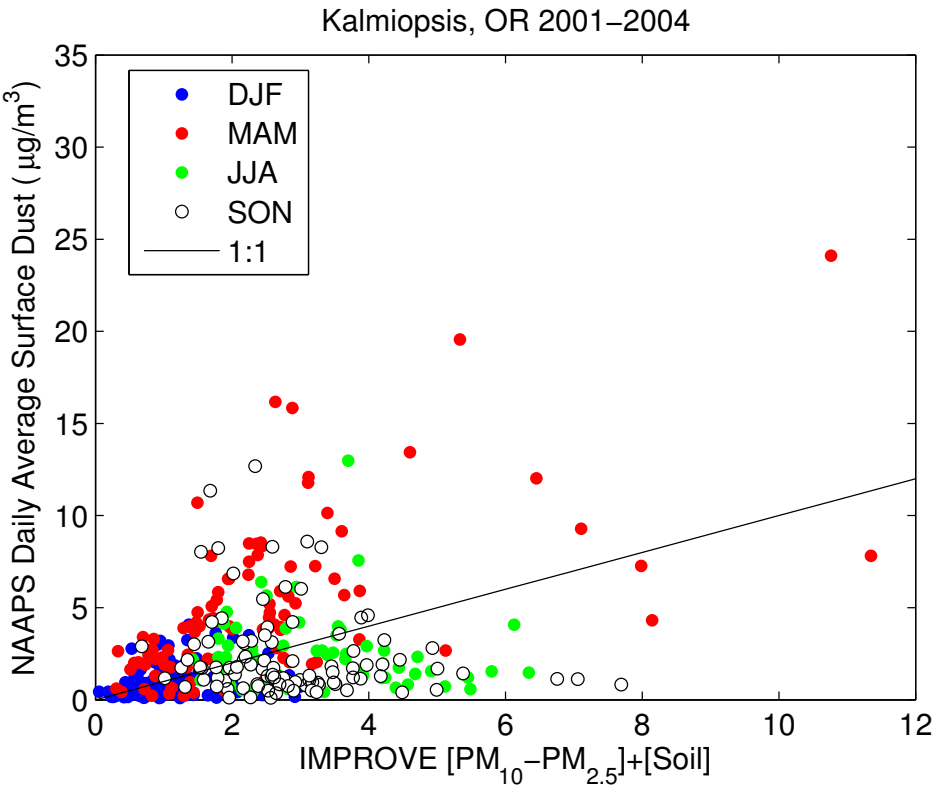
Kalmiopsis, OR 2001–2004
DJF
MAM
JJA
SON
1:1
NAAPS Daily Average Surface Dust (μg/m3)
IMPROVE [PM10–PM2.5]+[Soil]
0
5
10
15
20
25
30
35
0
2
4
6
8
10
12

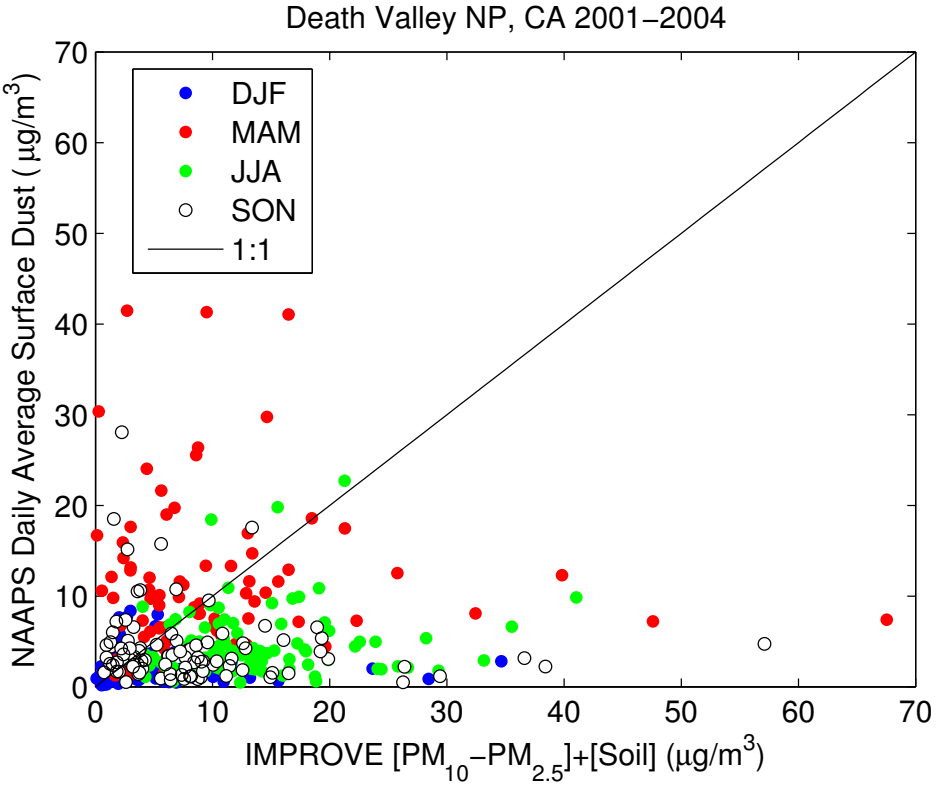
Death Valley NP, CA 2001–2004
DJF
MAM
JJA
SON
1:1
NAAPS Daily Average Surface Dust (μg/m3)
IMPROVE [PM10–PM2.5]+[Soil] (μg/m3)
0
10
20
30
40
50
60
70
0
10
20
30
40
50
60
70

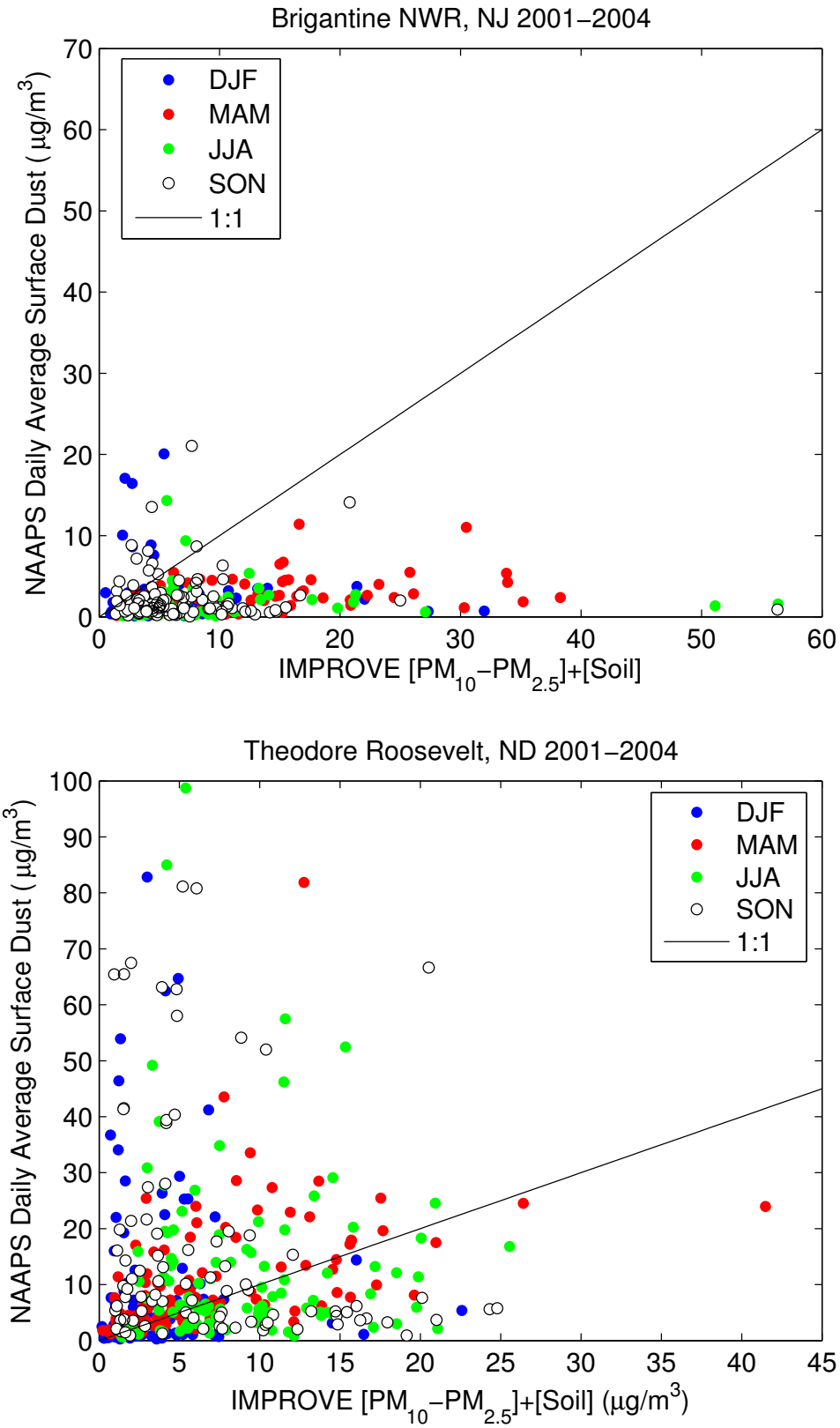


**Figure 3.17: NAAPS daily average surface dust versus IMPROVE [$PM_{10}$-$PM_{2.5}$]+[Soil] for each season at Kalmiopsis, Oregon; Death Valley National Park, CA; Brigantine National Wildlife Reserve, New Jersey; and Theodore Roosevelt, North Dakota.**

To separately examine the seasonal variation of comparisons between NAAPS and IMPROVE that is suggested by these scatter plots, frequency distributions of NAAPS/IMPROVE ratios were constructed for all 28 sites in this study. In order to not introduce biases due to very low IMPROVE concentrations, days with measurements of fine soil less than 0.1 μg $m^{-3}$ (a value equal to roughly three times the sum of the average minimum detections limits of aluminum and calcium) were excluded when computing the ratios. The distributions were constructed using bins of width $\Delta\log_{10}$ ratio = 0.2. The median ratio and standard deviation of each distribution are listed in each plot. Results for Death Valley National Park are shown in Figure 3.18.

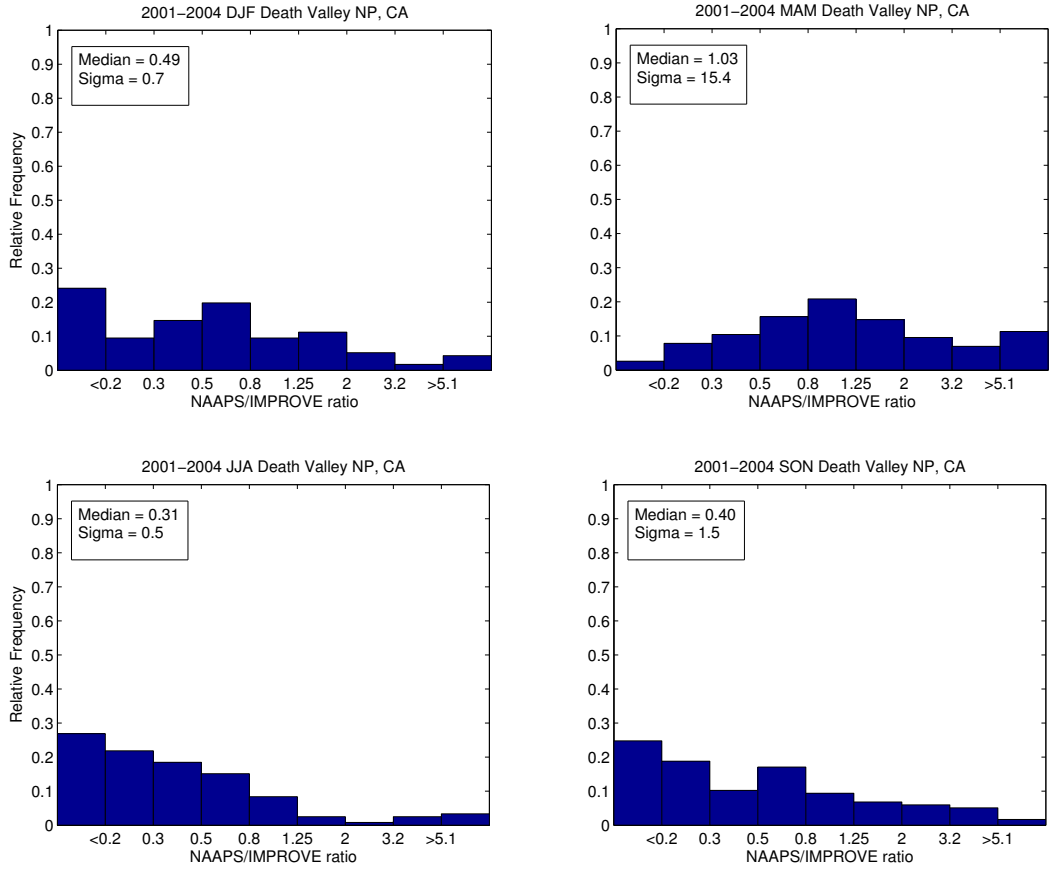


**Figure 3.18: Seasonal frequency distributions of the ratio of NAAPS predicted surface dust to IMPROVE [$PM_{10}$-$PM_{2.5}$]+[Soil] for 2001-2004 at Death Valley National Park, California.**

The frequency distribution is centered near a ratio of one at Death Valley in the spring, but exhibits a bias toward smaller ratios in other seasons, especially in summer. The figure demonstrates clearly what was seen qualitatively in the timelines in Figure 3.11; namely, that the correspondence is good between NAAPS and IMPROVE during the period of maximum Asian dust transport to the U.S., but there appears to be significant local or regional sources of dust in the summer and early fall whose influences on aerosol concentration at Death Valley are not captured in the model.

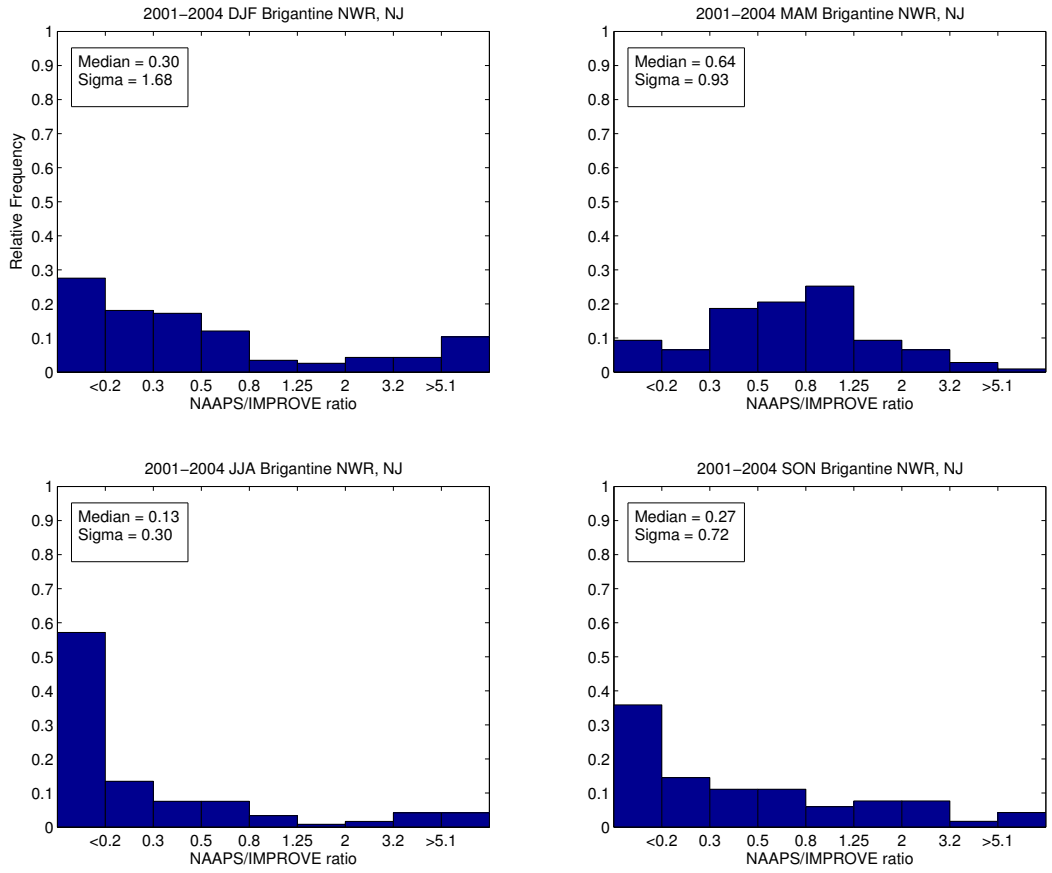


**Figure 3.19: Seasonal frequency distributions of the ratio of NAAPS predicted surface dust to IMPROVE [$PM_{10}$-$PM_{2.5}$]+[Soil] for 2001-2004 at Brigantine National Wildlife Reserve, New Jersey.**

Seasonal frequency distributions of NAAPS/IMPROVE ratios for Brigantine are shown in Figure 3.19. The distributions indicate a bias toward ratios less than one at all seasons, although there is a second mode in the spring distribution centered between 0.3

and 0.5. The bias in the IMPROVE data is due to the presence of non-soil particles (likely sea salt) in the aerosol coarse fraction throughout the year. The Asian dust influence in the spring results in a second mode that is shifted toward (but still below) a ratio of one.

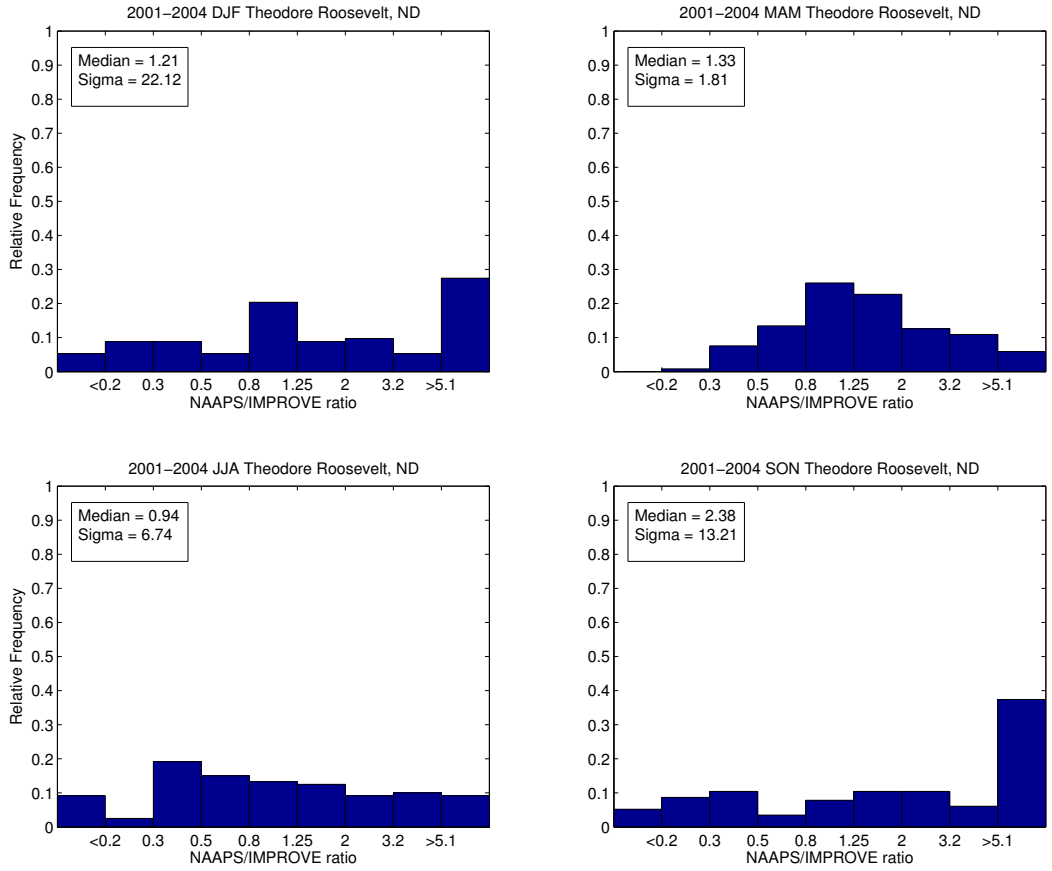


**Figure 3.20: Seasonal frequency distributions of the ratio of NAAPS predicted surface dust to IMPROVE [$PM_{10}$-$PM_{2.5}$]+[Soil] for 2001-2004 at Theodore Roosevelt, North Dakota.**

The spring frequency distribution for Theodore Roosevelt (Figure 3.20) confirms what the timelines in Figure 3.15 suggested: that the comparison between NAAPS and IMPROVE is reasonable when mostly non-North American dust is predicted at the site. Spring is the only season when non-North American sources dominate at the site, and thus exhibits a distribution centered on a ratio of one. During the winter months there is a mode centered at a ratio of one, but, as in the fall months, the winter distribution also contains a larger peak at ratios greater than 5.1 due to the frequent generation of local

dust events in the model. Surprisingly, the summer distribution of NAAPS/IMPROVE ratios at Theodore Roosevelt is somewhat biased toward ratios less than one, despite the frequent impact of regional dust sources predicted by NAAPS. A closer look at the timelines suggests that perhaps the IMPROVE measurements indicate a more persistent influence of soil dust than the periodic spikes predicted by NAAPS. This could be due to the influence of agricultural dust sources in the region.

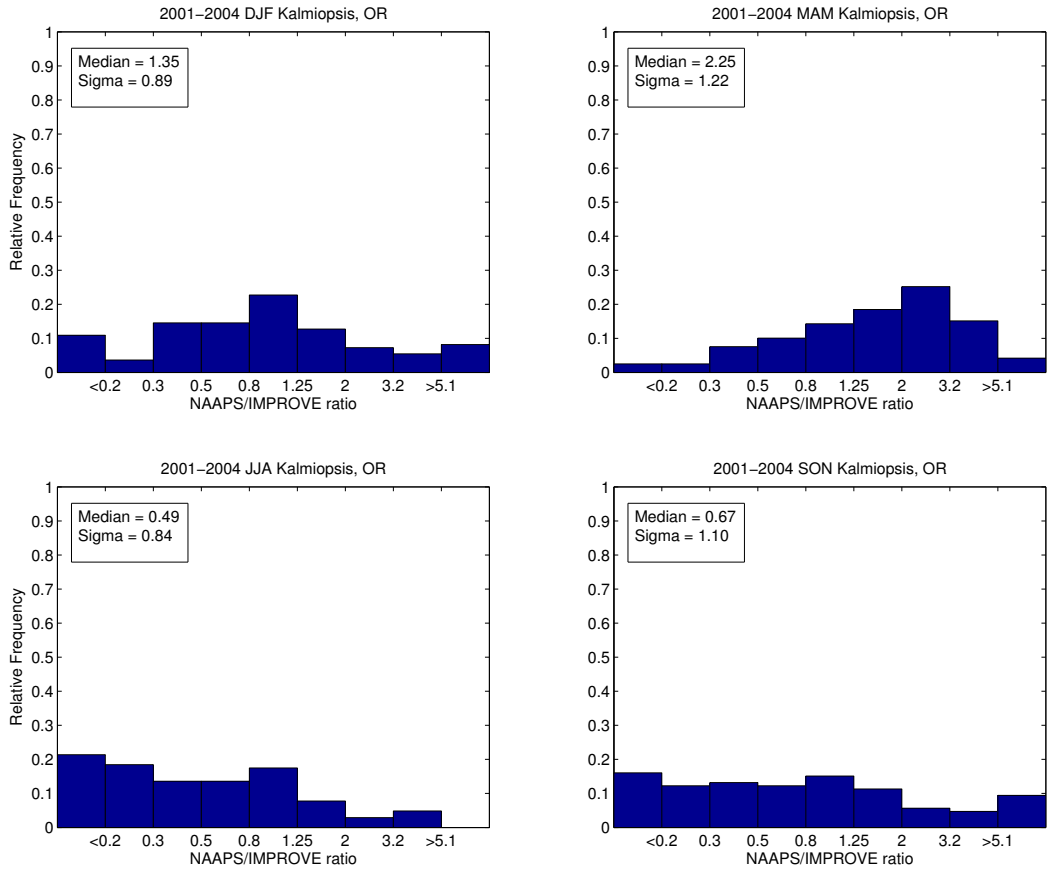


**Figure 3.21: Seasonal frequency distributions of the ratio of NAAPS predicted surface dust to IMPROVE [$PM_{10}$-$PM_{2.5}$]+[Soil] for 2001-2004 at Kalmiopsis, Oregon.**

At Kalmiopsis, the distributions are broad, but are roughly centered at a ratio of one in fall and winter (Figure 3.21). Opposite biases exist in the comparison in both spring and summer. In spring, a bias towards higher ratios indicates that the NAAPS predictions tend to contain more mass than the IMPROVE measurements at Kalmiopsis.

Since NAAPS predicts the exclusive influence of long-range transport at the site in spring, the bias could be due to an underestimation of atmospheric soil dust removal during transport. In summer, the comparison bias is toward smaller ratios, most likely due to the presence of other species (i.e. smoke or sea salt) in the aerosol coarse fraction.

Median ratios of NAAPS predictions to IMPROVE $[PM_{10}\text{-}PM_{2.5}]$+[Soil] by season for 2001-2004 at all IMPROVE sites examined in this study are plotted in Figure 3.22. In the plots, yellow shades indicate a median value close to one, warmer shades indicate median ratios larger than one, and cooler shades indicate median ratios smaller than one. The spatial patterns of high or low NAAPS/IMPROVE median ratios give some insight into possible explanations for their existence. For instance, coastal sites in the eastern U.S. exhibit ratios less than one throughout the year, as do inland sites that might be impacted by marine air from the Gulf of Mexico. This pattern supports the theory that sea salt makes up a significant portion of the coarse aerosol mass at these sites.

In spring, the period of maximum predicted Asian dust influence, NAAPS/IMPROVE ratios greater than one are realized at nearly all sites in the western U.S. In the summer months, many sites in the intermountain West have ratios close to one, although ratios smaller than one at sites in the central, northwestern, and southwestern U.S. reveal the impact of non-soil particles on the coarse mode, or of mineral dust sources that are not resolved by NAAPS. Similar distributions appear in the fall and winter months, but large NAAPS/IMPROVE ratios at sites in the northern Great Plains and northern Rocky Mountains indicate a persistent source of mineral dust in NAAPS that is greater than that reported by the IMPROVE network. These issues will be explored in detail in the following chapter.

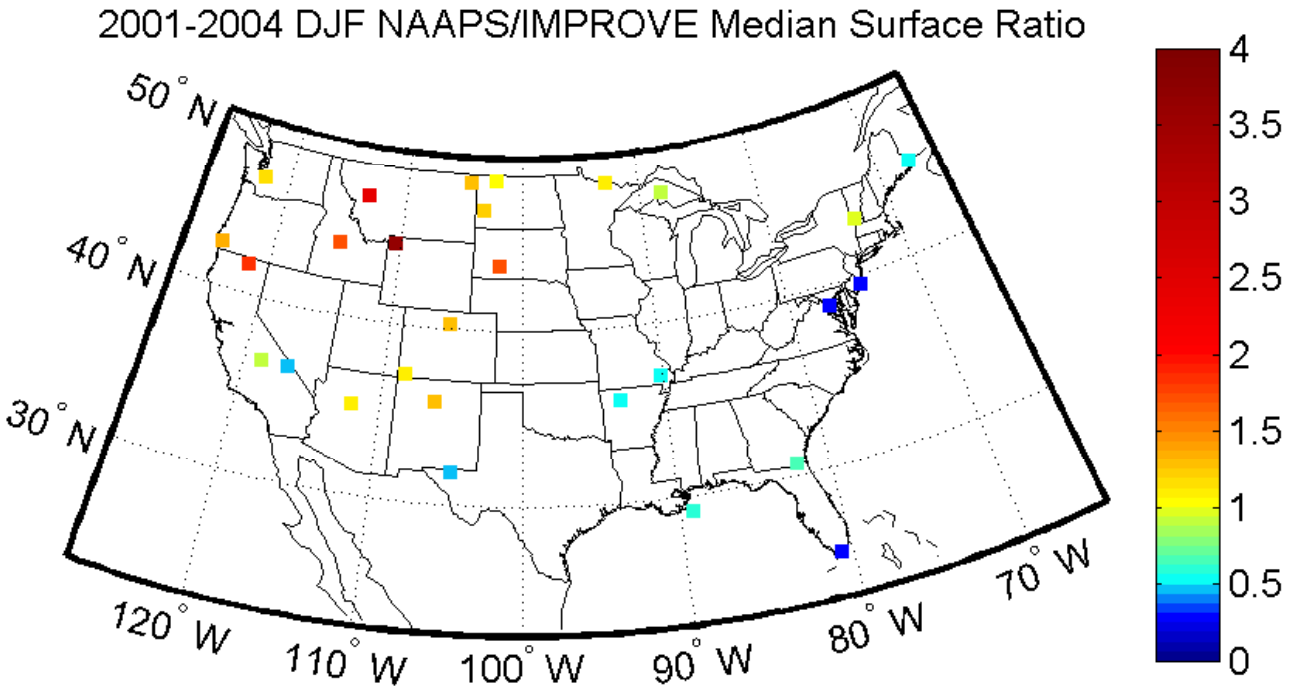
2001-2004 DJF NAAPS/IMPROVE Median Surface Ratio
50°N
40°N
30°N
120°W
110°W
100°W
90°W
80°W
70°W
4
3.5
3
2.5
2
1.5
1
0.5
0

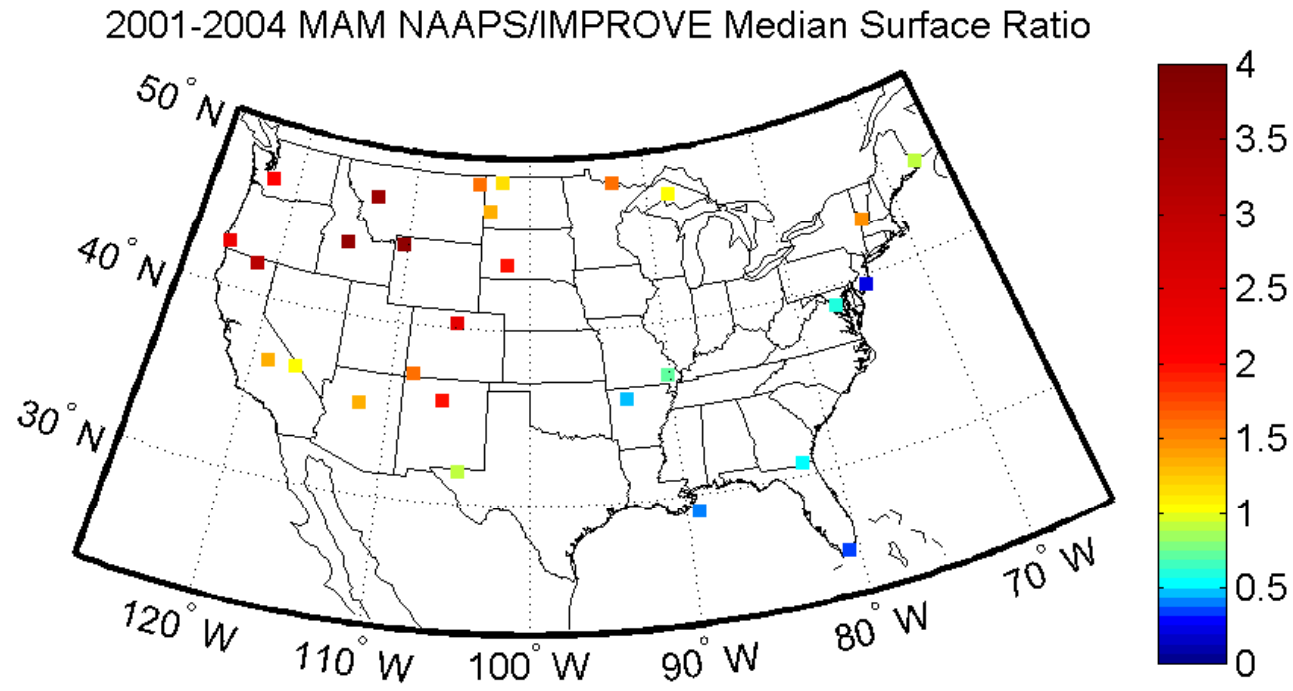
2001-2004 MAM NAAPS/IMPROVE Median Surface Ratio
50°N
40°N
30°N
120°W
110°W
100°W
90°W
80°W
70°W
4
3.5
3
2.5
2
1.5
1
0.5
0

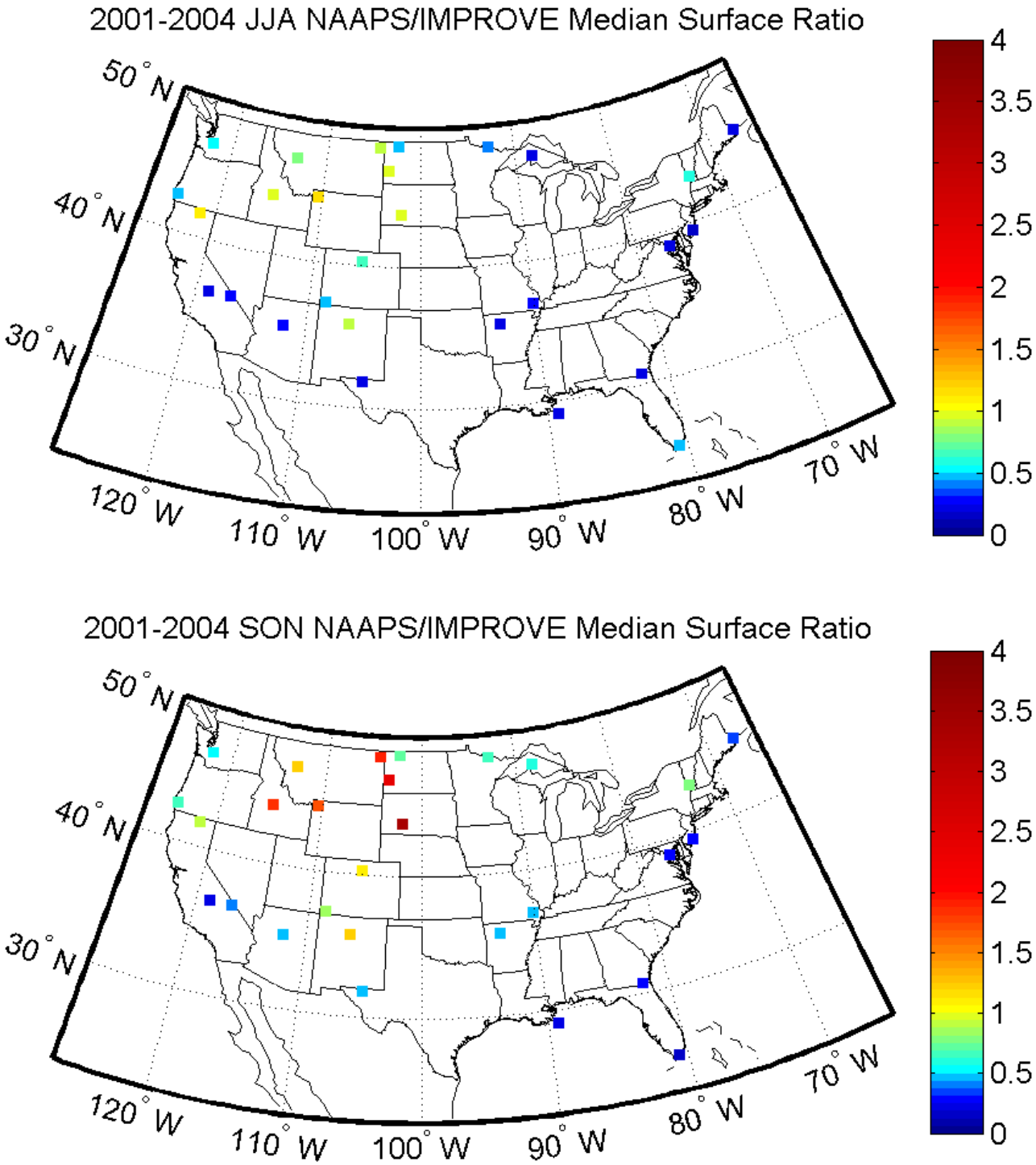


**Figure 3.22: Seasonal median ratios of NAAPS to IMPROVE [$PM_{10}$-$PM_{2.5}$]+[Soil] for 28 IMPROVE measurement sites.**

# 4 Discussion of Soil Dust Aerosol Results

## 4.1 Evaluation of IMPROVE "Soil"

In 2004 (and Fall 2003 at some sites), analysis for chemical composition was performed on the $PM_{10}$ filters for select IMPROVE sites. Since this is not standard IMPROVE practice, the dataset provides a unique opportunity to investigate the validity of assumptions used in the IMPROVE network, specifically the assumption that the coarse fraction, [$PM_{10}$-$PM_{2.5}$], contains only insoluble soil particles. An evaluation of the $PM_{10}$ soil estimation used for this study was performed at four sites in different regions of the U.S., applying the IMPROVE fine soil formula to the speciated total $PM_{10}$ mass.

### 4.1.1 Brigantine National Wildlife Reserve, New Jersey

The results for Brigantine are shown in Figure 4.1. For 2004, the $PM_{10}$ soil estimation used for this study overshoots the $PM_{10}$ soil mass obtained using the fine soil formula. This pattern is consistent throughout the year. Thus, there must be something else in the aerosol coarse fraction at this site that is always present in significant amounts. The seasonal compositions of the major coarse fraction constituents for the IMPROVE speciation period are plotted in Figure 4.2. In 2004, soil particles only accounted for approximately 1/3 of the total coarse fraction in any one season. Organic carbon (OC), ammonium nitrate, and ammonium sulfate together comprised another 1/4 to 1/3 of the

coarse fraction, leaving 30 to over 40% of the coarse fraction unaccounted for by major aerosol species considered in the IMPROVE network.

It is likely that sea salt is a major contributor to the "other" category of coarse fraction mass at Brigantine, given that the site is located near the Atlantic coast at only 5 meters above sea level. Sea salt is a difficult species to measure; the detection of sodium using PIXE and XRF is poor given that it fluoresces at a very low energy with a high probability of being re-absorbed by the particle. The average minimum detection limit for sodium measured in the IMPROVE network is 0.013 μg $m^{-3}$ (California-Davis, 1995). Furthermore, the chloride ion is often reacted away by sulfate or nitrate in urban environments; thus, its usefulness as a sea salt tracer is questionable.

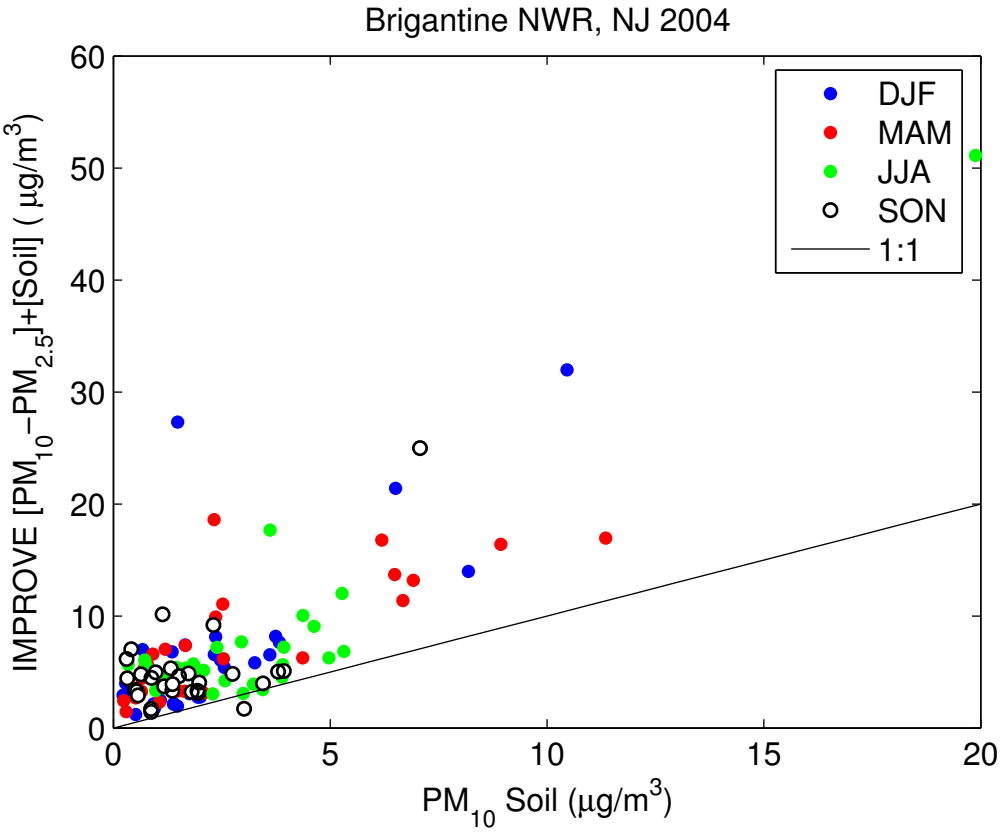


**Figure 4.1: IMPROVE [$PM_{10}$-$PM_{2.5}$]+[Soil] versus $PM_{10}$ soil as computed using the IMPROVE fine soil formula for Brigantine National Wildlife Reserve, New Jersey.**

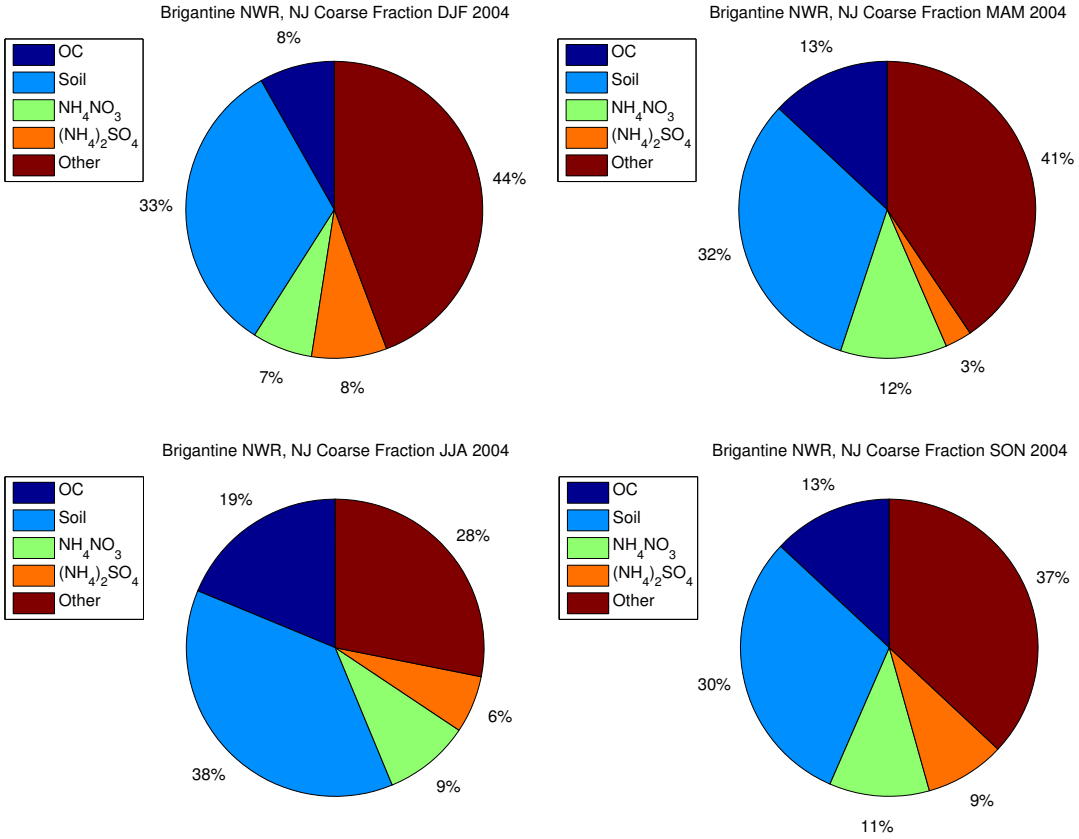


**Figure 4.2: Seasonal composition of major components of IMPROVE coarse fraction aerosol for Brigantine National Wildlife Reserve, New Jersey.**

By scaling the seasonal coarse mass concentrations by their corresponding average soil fractions, one can assess whether or not the seasonal averages are a good representation of the daily ambient aerosol composition at Brigantine, or whether large excursions from the mean state are common. A comparison of the sum of fine soil and the scaled coarse fraction with $PM_{10}$ soil from the IMPROVE formula is shown in Figure 4.3. The scaled data compare better with the $PM_{10}$ soil than the un-scaled data shown in Figure 4.1, but higher concentrations of $PM_{10}$ soil tend to be underestimated by this method, whereas concentrations less than ~3 μg $m^{-3}$ are still commonly overestimated. Perhaps, since dust incursions are episodic at Brigantine, the coarse fraction actually

contains a higher-than-average percentage of soil mass on days when $PM_{10}$ soil mass is elevated. The reverse is likely true on days in which less dust is present at Brigantine.

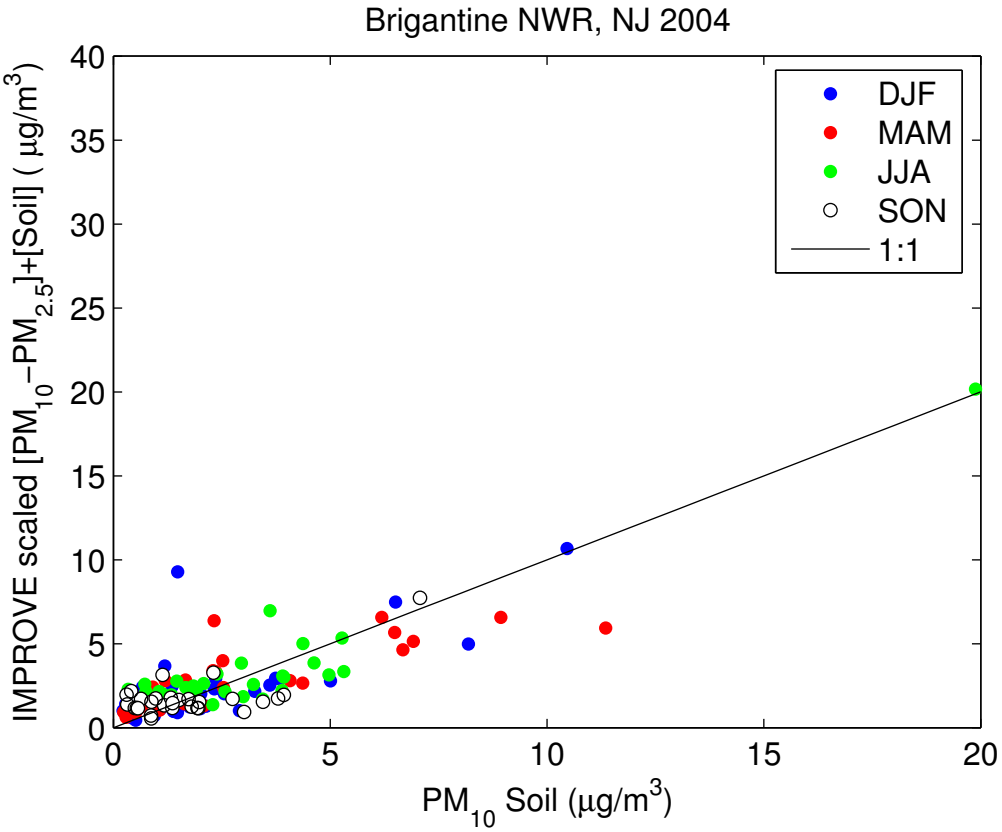


**Figure 4.3: IMPROVE scaled [$PM_{10}$-$PM_{2.5}$]+[Soil] versus $PM_{10}$ soil as computed using the IMPROVE fine soil formula for Brigantine National Wildlife Reserve, New Jersey.**

Nonetheless, comparing the NAAPS predictions for the four years against the scaled IMPROVE data at Brigantine does reduce biases in the comparison of the datasets, resulting in median ratios that are much closer to one in fall and winter (Figure 4.4). In spring, however, when NAAPS predicts the highest influence of non-North American dust at Brigantine, a comparison with the scaled data shifts the bias to higher NAAPS/IMPROVE ratios; scaling by the average spring soil composition at Brigantine likely removes too much mass from the IMPROVE data in the presence of dust events. On the other hand, a bias toward ratios less than one is still evident in the summer

months. This could be due to an underprediction of North African dust transport to the site in NAAPS; a suspected instance of this will be examined in subsequent sections.

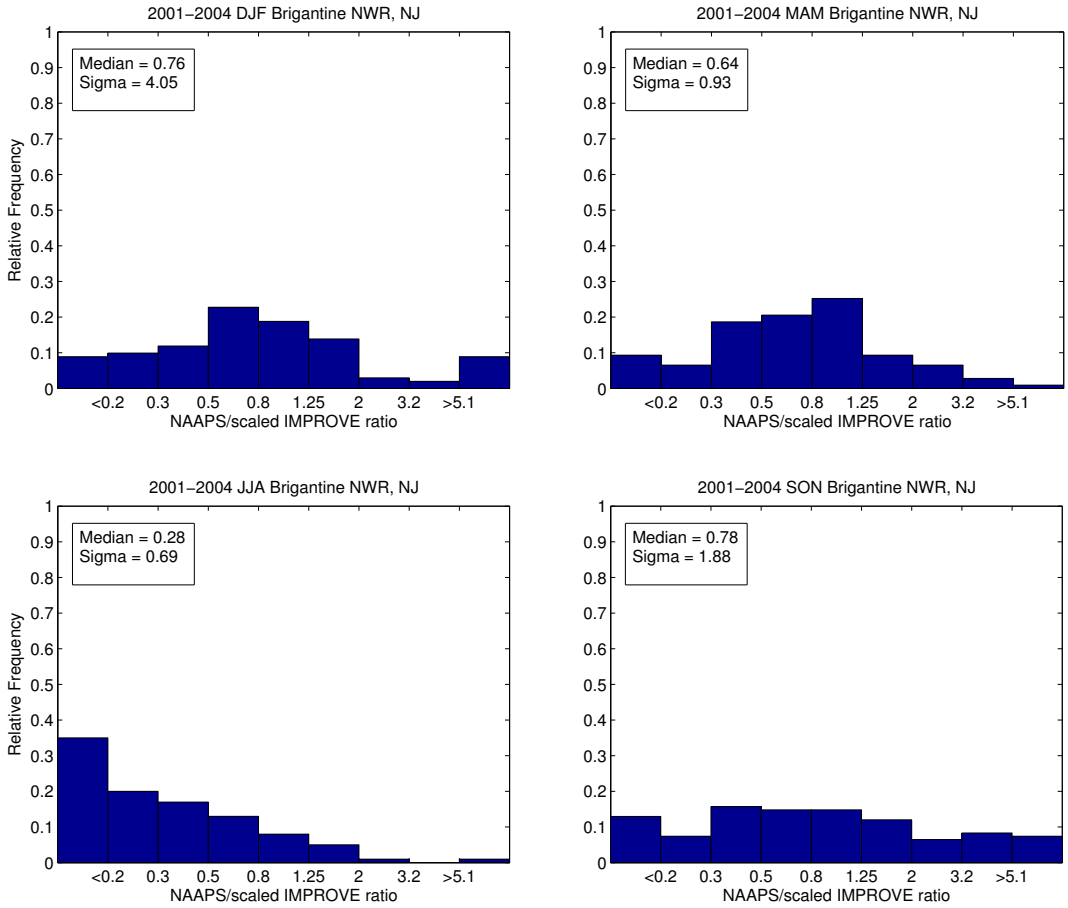


**Figure 4.4: Seasonal frequency distributions of the ratio of NAAPS predicted surface dust to IMPROVE scaled [$PM_{10}$-$PM_{2.5}$]+[Soil] for 2001-2004 at Brigantine National Wildlife Reserve, New Jersey.**

### 4.1.2 Mount Rainier National Park, Washington

Chemical analysis was not performed on the $PM_{10}$ filters at Kalmiopsis, but data were available for another site in the Pacific Northwest. The aerosol sampler at Mount Rainier National Park is located farther inland than at Kalmiopsis, at an elevation of 427 meters. A comparison of IMPROVE estimated $PM_{10}$ soil versus that obtained with the soil formula is shown in Figure 4.5. Like at Brigantine, [$PM_{10}$-$PM_{2.5}$]+[Soil] at Mount Rainier consistently exceeds the estimation obtained with the fine soil formula applied to

the $PM_{10}$ samples. However, the overestimation at this site varies strongly with season. In spring and summer, the slope of the comparison is roughly 1:1 with $PM_{10}$ soil, but is offset by 1-2 µg $m^{-3}$ due to other species that are consistently present in the ambient coarse aerosol. In fall and winter, the comparison yields a much higher slope.

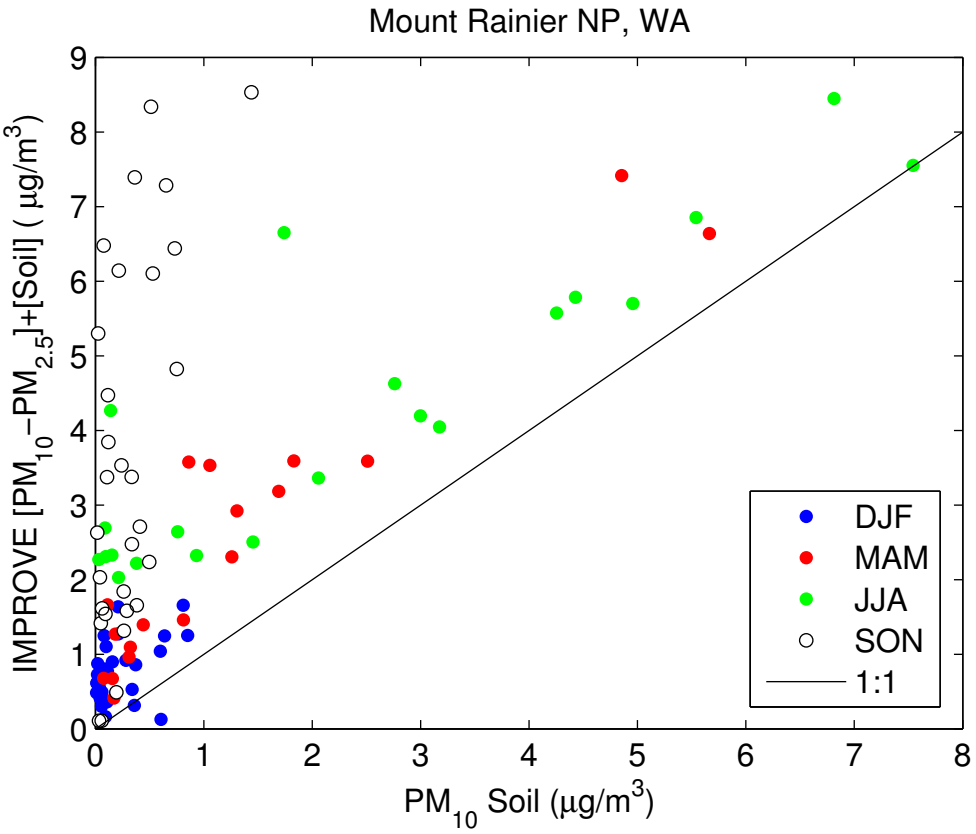


**Figure 4.5: IMPROVE [$PM_{10}$-$PM_{2.5}$]+[Soil] versus $PM_{10}$ soil as computed using the IMPROVE fine soil formula for Mount Rainier National Park, Washington.**

The seasonal composition of the 2004 coarse fraction mass at Mount Rainier is located in Figure 4.6. In spring, only about 50% of the coarse fraction mass could be attributed to soil particles; in summer the fraction was about 60%. OC constituted about 1/4 of the coarse fraction mass in both seasons, sulfates and nitrates made up another 8-9%, while the remaining 10-40% was left unaccounted for. Sea salt from marine air parcels could explain some of this unresolved mass. In fall and winter, the major component of the coarse fraction mass was not soil, but organic carbon. Soil particles

actually constituted a very small fraction of the coarse mass in fall, leading to the strong slope of the SON comparison of [$PM_{10}$-$PM_{2.5}$]+[Soil] versus $PM_{10}$ soil. The influence of a series of small eruptions from Mount St. Helens, located just southwest of Mount Rainier, beginning ~ 1 October 2004, could have influenced the aerosol coarse mode, as could a series of fires that occurred in the vicinity of Mount Rainier in August and September 2004 (http://www.ncdc.noaa.gov/oa/climate/research/2004/fire04.html).

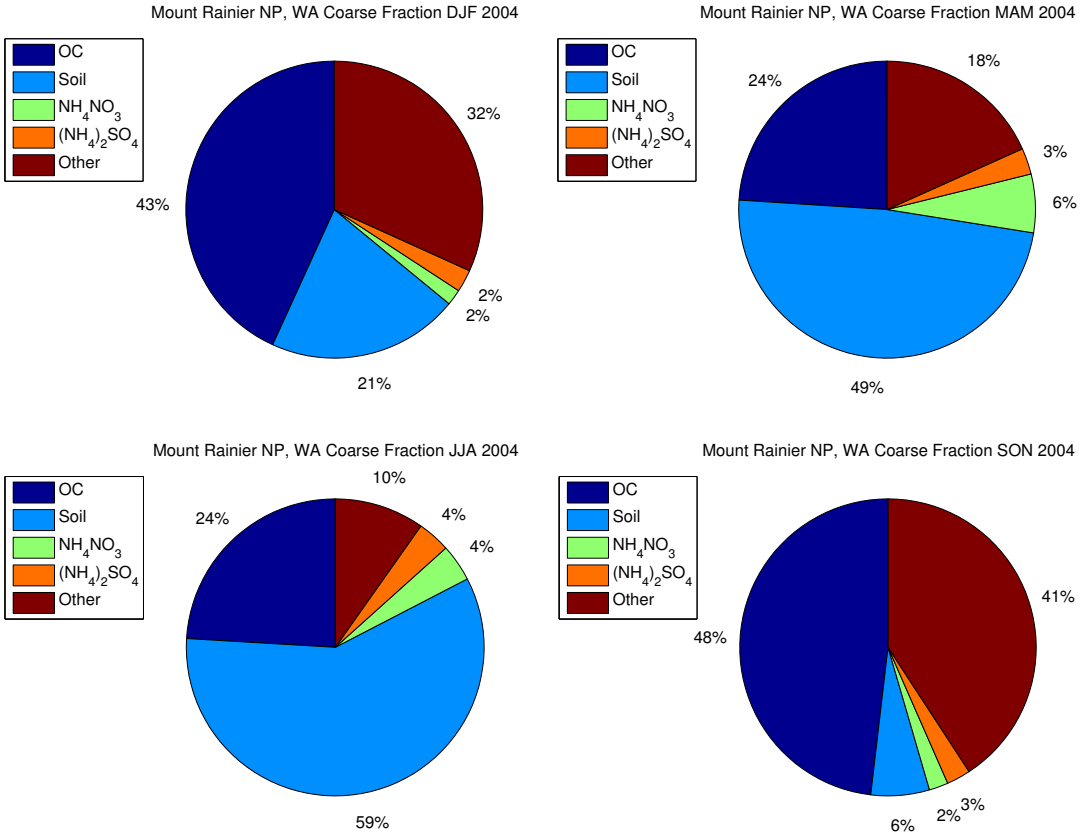


**Figure 4.6: Seasonal composition of major components of IMPROVE coarse fraction aerosol for Mount Rainier National Park, Washington.**

OC likely constitutes a large portion of aerosol mass in the western United States, especially at elevated sites. Using aircraft measurements made off the coast of Japan from April-May 2001 during the ACE-Asia campaign, Heald et al. (2005) found that OC concentrations averaged 4 μg $m^{-3}$ in the 2-6.5 km column of the troposphere, a value that is 10-100 times higher than current model estimates. Since mixed marine/Asian air

masses are thought to impact sites in the western U.S. throughout the year (Jaffe et al., 2005), it would make sense for OC to make up a substantial fraction of background aerosol mass in this region. In an analysis of Asian dust incursions over North America, VanCuren (2003) often found an increase in OC in conjunction with Asian dust events.

It is important to note that the relative coarse mass contribution of OC by season at Mount Rainier could be underestimated in Figure 4.6. The mass of organic compounds measured by IMPROVE is estimated by multiplying the measured organic carbon mass by a factor of 1.4. However, some argue that this is the lowest reasonable estimate for organic molecular weight per carbon weight for urban aerosol (Turpin and Lim, 2001). Non-urban aerosol tends to be more oxygenated, so the measured OC mass at Mount Rainier National Park would likely be due to more high-molecular weight compounds. Turpin and Lim (2001) suggest implementing a factor of $2.1 \pm 0.2$ to estimate the total mass due to organic compounds from the measured mass of OC at remote sites. An even higher ratio is suggested for sites with frequent fire impact. Seasonal compositions using the 2.1 factor for OC at Mount Rainier are shown in Figure 4.7.

Multiplying the OC mass at Mount Rainier by a factor of 2.1 accounts for the entire coarse fraction mass that was left previously unexplained by major aerosol species in 2004. In fact, the sum of OC, soil, ammonium sulfate, and ammonium nitrate is 8-15% larger in each season than the total coarse fraction measured on the Teflon filter when the 2.1 OC factor is used. This could mean that the 2.1 factor is slightly larger than the average organic molecular weight-to-carbon weight ratio at Mount Rainier; this could also be due to uncertainties in the actual mass of sulfate and nitrate present (IMPROVE assumes the species are fully neutralized by ammonia), or in uncertainties in the soil

formula itself. Such uncertainties in the attribution of mass to individual species could have implications for the reconstructed coarse fraction at all sites in this study.

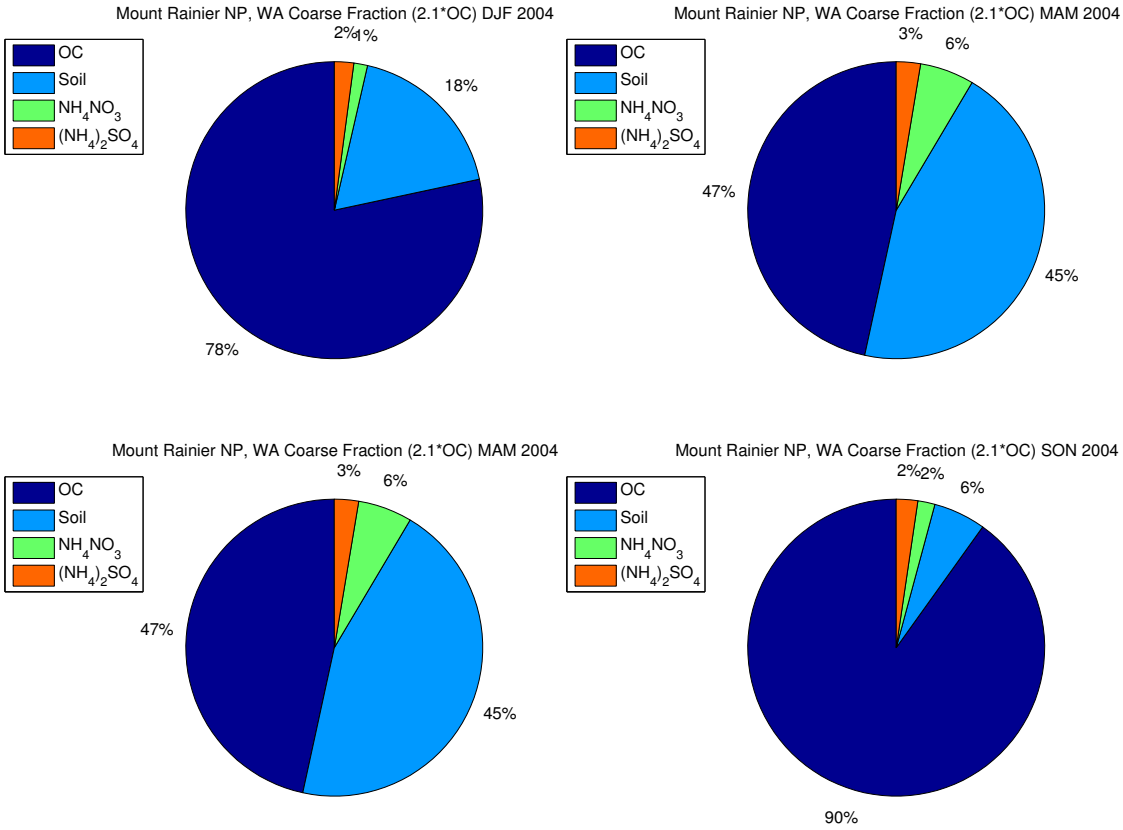


**Figure 4.7: Seasonal composition of major components of IMPROVE coarse fraction aerosol (with a factor of 2.1 for organic mass) for Mount Rainier National Park, Washington.**

Figure 4.8 contains a comparison of the sum of fine soil and the coarse fraction, scaled by the seasonal soil contribution at Mount Rainier, to the $PM_{10}$ soil determined using the fine soil formula for 2004. As at Brigantine, this method leads to an underestimation of soil mass when the $PM_{10}$ soil is larger than ~3 μg $m^{-3}$. Thus, since soil dust events are often episodic in nature, the total coarse fraction on days with higher $PM_{10}$ soil is probably composed of a larger-than-average fraction of soil dust at Mount Rainier as well.

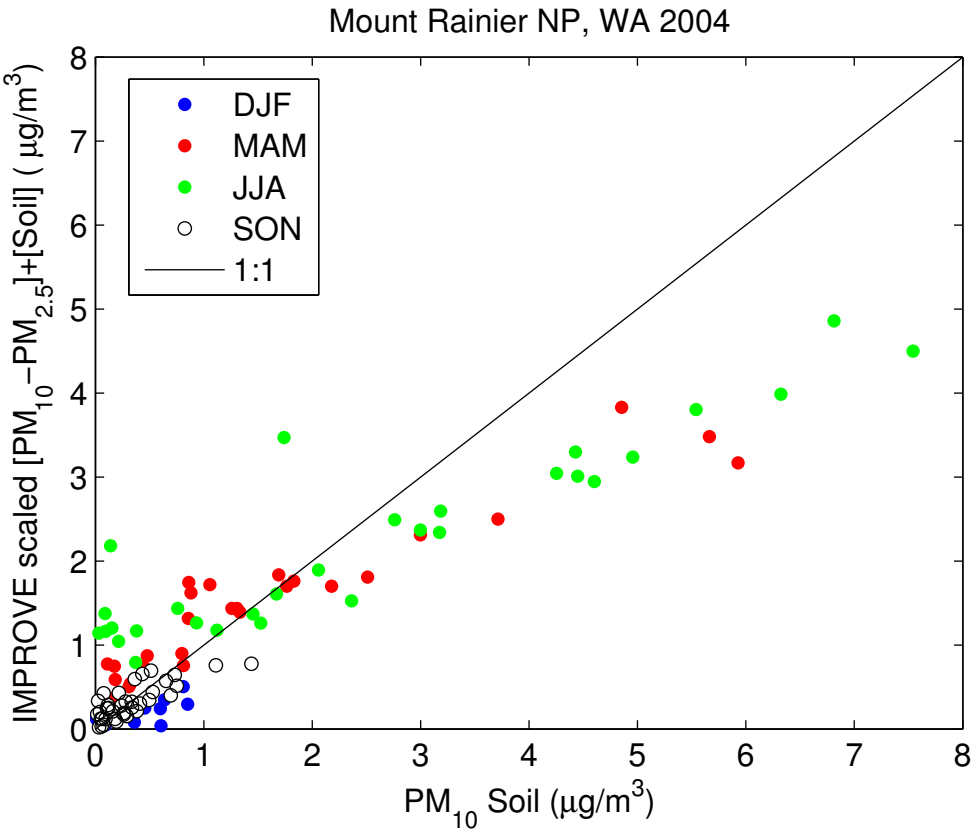


**Figure 4.8: IMPROVE scaled [$PM_{10}$-$PM_{2.5}$]+[Soil] versus $PM_{10}$ soil as computed using the IMPROVE fine soil formula for Mount Rainier National Park, Washington.**

Scaling the coarse mode by the average seasonal soil fraction measured at Mount Rainier in 2004 leads to a median ratio close to one in the summer (Figure 4.9), but it introduces strong biases toward NAAPS/IMPROVE ratios greater than one in winter, spring, and fall. Fire and volcanic influences during 2004 may have resulted in an aerosol composition that is unrepresentative of typical fall aerosol at Mount Rainier, leading to a subsequent underestimation of soil dust mass in other years. In winter, the comparison is also problematic because total aerosol mass is so low during the season (the coarse fraction mass was only 0.7 µg $m^{-3}$ on average in 2004), leading to an estimated dust mass that is very inconsequential. In spring, episodic Asian dust transport events would be underestimated in the scaling of the IMPROVE data, resulting in larger NAAPS/IMPROVE ratios; however, since the un-scaled data were already biased high in

spring (with a median ratio of 2), NAAPS may overestimate mass concentrations in Asian dust plumes that reach the U.S.

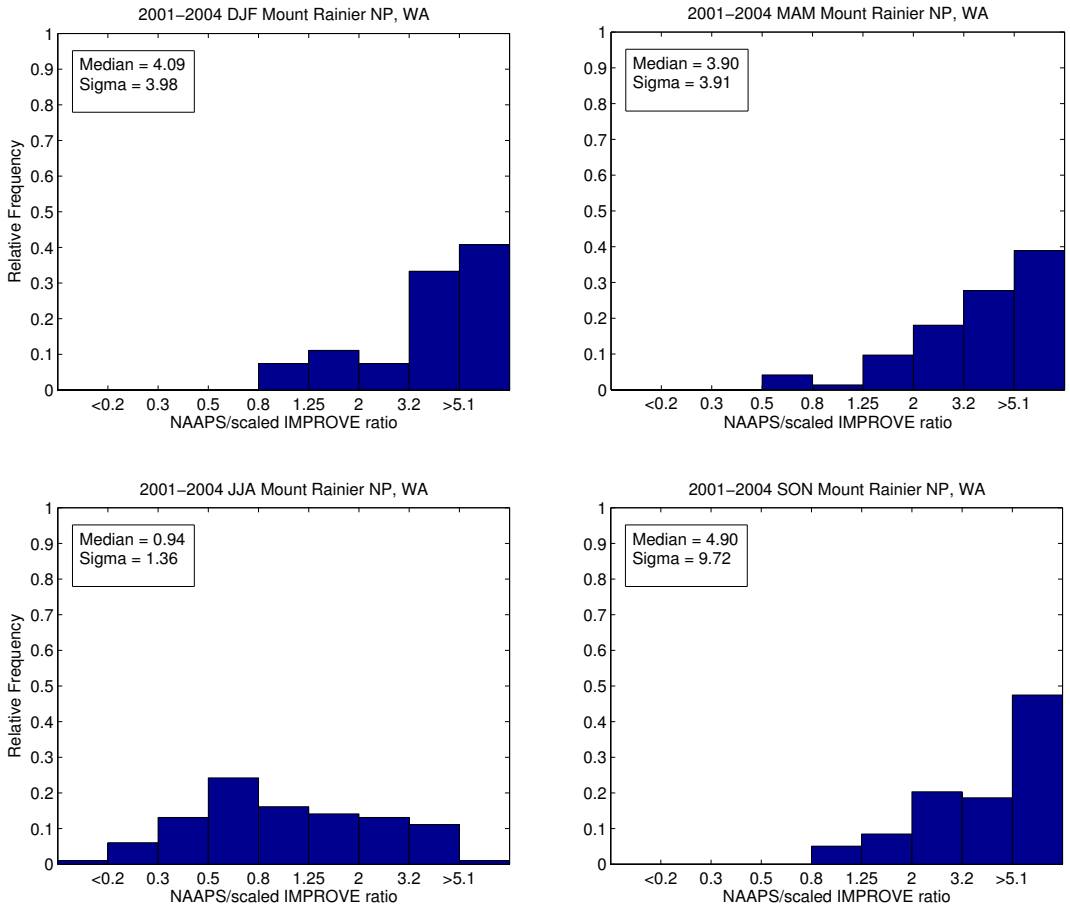


**Figure 4.9: Seasonal frequency distributions of the ratio of NAAPS predicted surface dust to IMPROVE scaled [$PM_{10}$-$PM_{2.5}$]+[Soil] for 2001-2004 at Mount Rainier National Park, Washington.**

### 4.1.3 Sequoia National Park, California

Sequoia National Park is located west of Death Valley National Park in California, though the former is elevated about 400 meters above the latter in the southern region of the Sierra Nevadas. As can be seen in Figure 4.10, the IMPROVE soil estimation used in this study at Sequoia National Park is arguably the most representative of actual $PM_{10}$ soil amounts than at the other three sites. In the summer months, the

correspondence is reasonably good at all $PM_{10}$ soil levels. This makes sense, since the average summer coarse fraction during 2004 was composed of 83% soil (Figure 4.11).

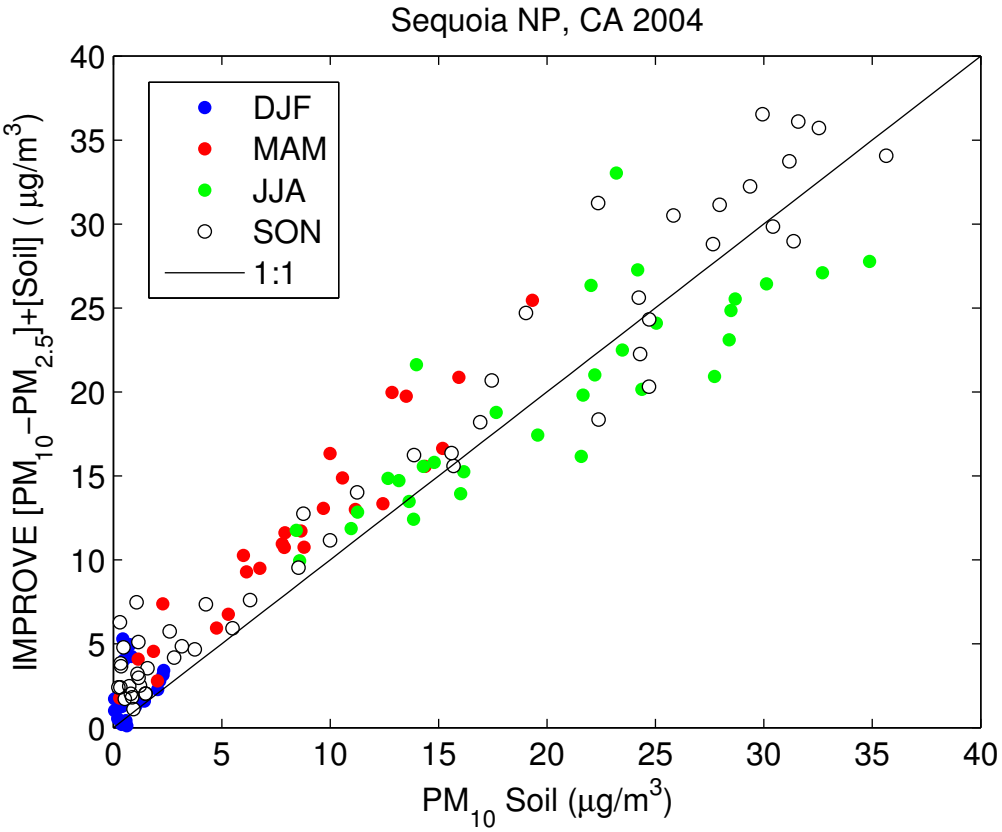


**Figure 4.10: IMPROVE [$PM_{10}$-$PM_{2.5}$]+[Soil] versus $PM_{10}$ soil as computed using the IMPROVE fine soil formula for Sequoia National Park, California.**

The $PM_{10}$ soil is overestimated during spring, fall, and winter by the [$PM_{10}$-$PM_{2.5}$]+[Soil] parameter, most dramatically when $PM_{10}$ soil is present at concentrations below ~3 µg $m^{-3}$. Although soil dust still made up the most significant portion of the coarse mass at Sequoia during the spring and fall, about 25-30% of the mass was attributable to other species. As at Mount Rainier, OC made up the largest fraction of this remaining mass, especially in the winter months. The higher unresolved mass in winter could be comprised of sea salt, given that sea salt production is highest during this season (Section 4.1.5); the low aerosol mass in winter months at the site could indicate the influence of clean marine air. A fair amount of nitrate was also present in each season.

Because the site is located to the east of the San Joaquin Valley, much of this could be due to agricultural emissions that impact the site during the day (Chow et al., 1992). The impact of local emissions on the seasonal cycle of soil dust will be addressed in subsequent sections.

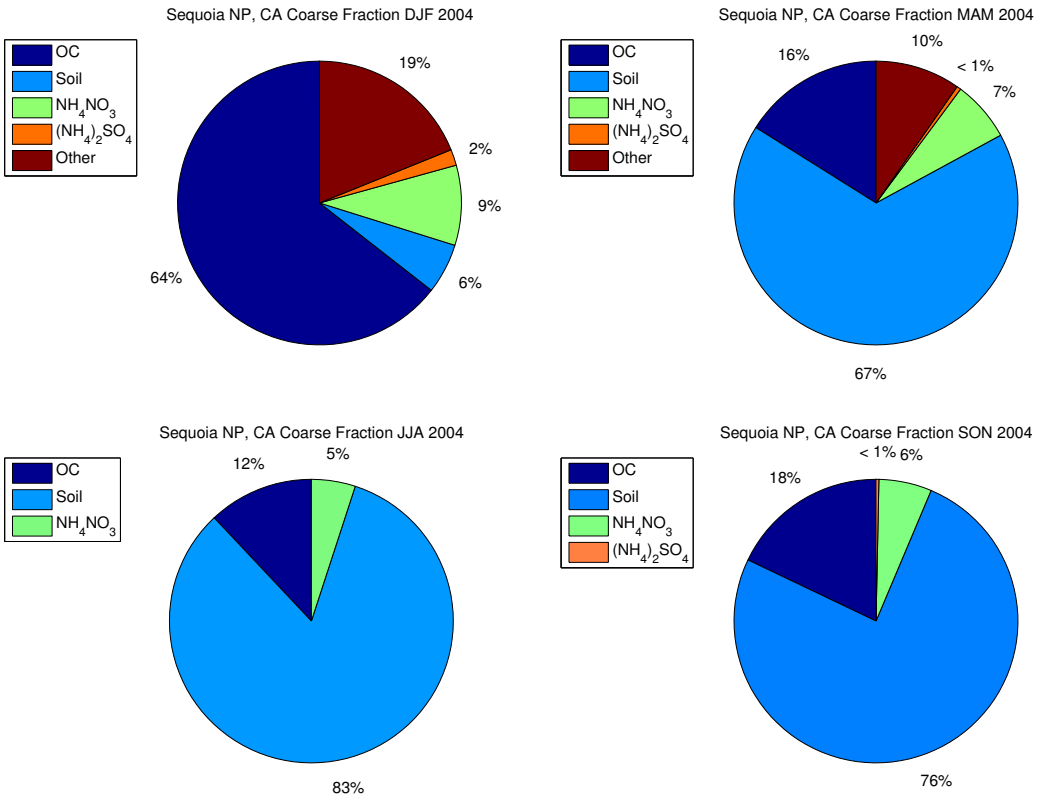


**Figure 4.11: Seasonal composition of major components of IMPROVE coarse fraction aerosol for Sequoia National Park, California.**

Figure 4.12 contains frequency distributions of the ratio of NAAPS to IMPROVE with the aerosol coarse fraction scaled by 2004 seasonal dust amounts at Sequoia National Park, CA. The winter and spring distributions at this site reveal biases similar to those at Mount Rainier: toward ratios significantly greater than one due to very clean overall conditions in winter, and toward ratios slightly above one due to potential underestimations in the scaled IMPROVE data (over overestimations in NAAPS) of Asian dust events in spring. Biases toward NAAPS/IMPROVE ratios smaller than one in

the summer and fall demonstrate a potential influence of local dust production that is not resolved in the model.

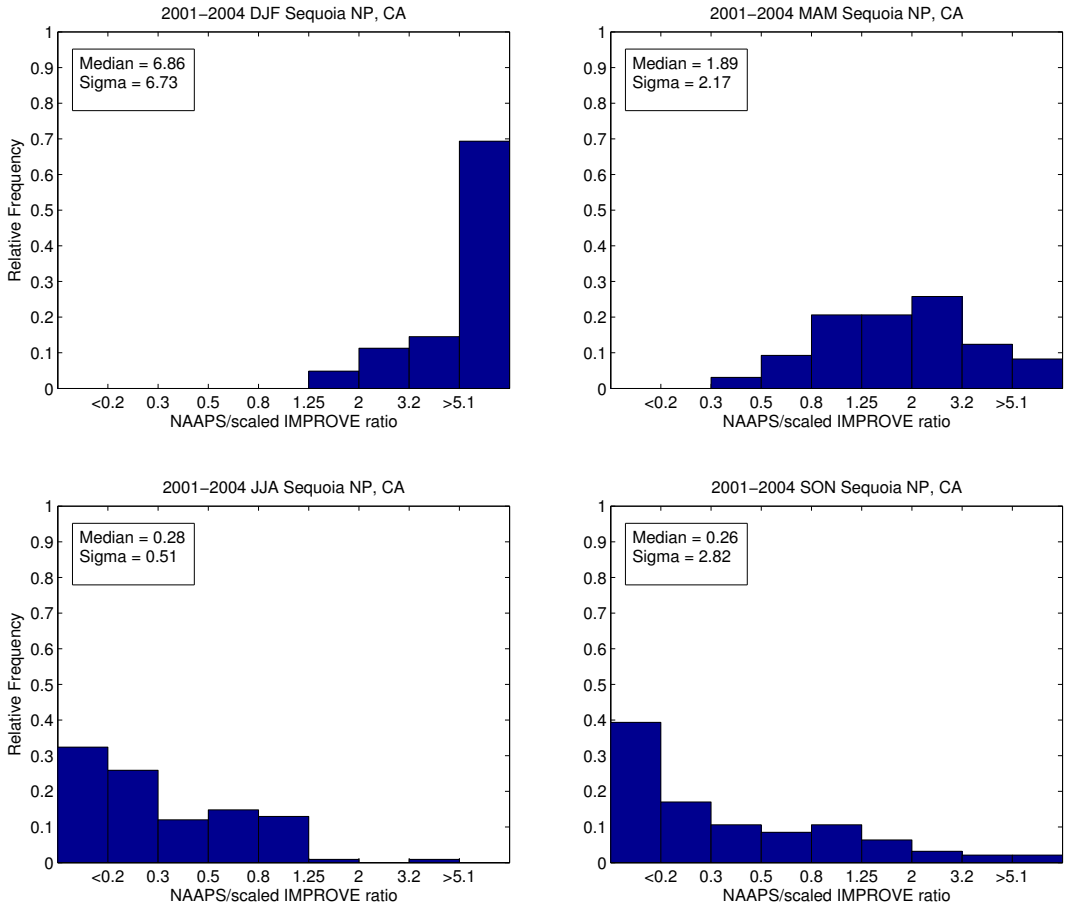


**Figure 4.12: Seasonal frequency distributions of the ratio of NAAPS predicted surface dust to IMPROVE scaled [$PM_{10}$-$PM_{2.5}$]+[Soil] for 2001-2004 at Sequoia National Park, California.**

### 4.1.4 Upper Buffalo Wilderness, Arkansas

Upper Buffalo Wilderness in Arkansas is another site at which the $PM_{10}$ soil amounts determined using the IMPROVE soil formula are overestimated by the sum of the IMPROVE aerosol coarse fraction and fine soil. Like at Brigantine, this occurs in all seasons (Figure 4.13), meaning that soil only makes up a portion of the coarse aerosol mass throughout the year. Soil dust aerosol made up ~40-50% of the total coarse fraction mass during 2004 at this site (Figure 4.14); OC accounted for another 10-30% depending

upon the season. Surprisingly, nearly 1/3 of the coarse fraction fell into the "other" category in spring, summer and fall, revealing just how complicated a characterization of ambient particles can be. Some of this could be due to an underestimation of organic mass, but sea salt (and residual water) could well be a component of the coarse fraction at Upper Buffalo, due to the impact of maritime air masses from the Gulf of Mexico. The distribution of sodium ion wet deposition for 2004 shown in Figure 4.15 suggests that, at least on an annual basis, Arkansas is impacted by air masses containing sea salt particles.

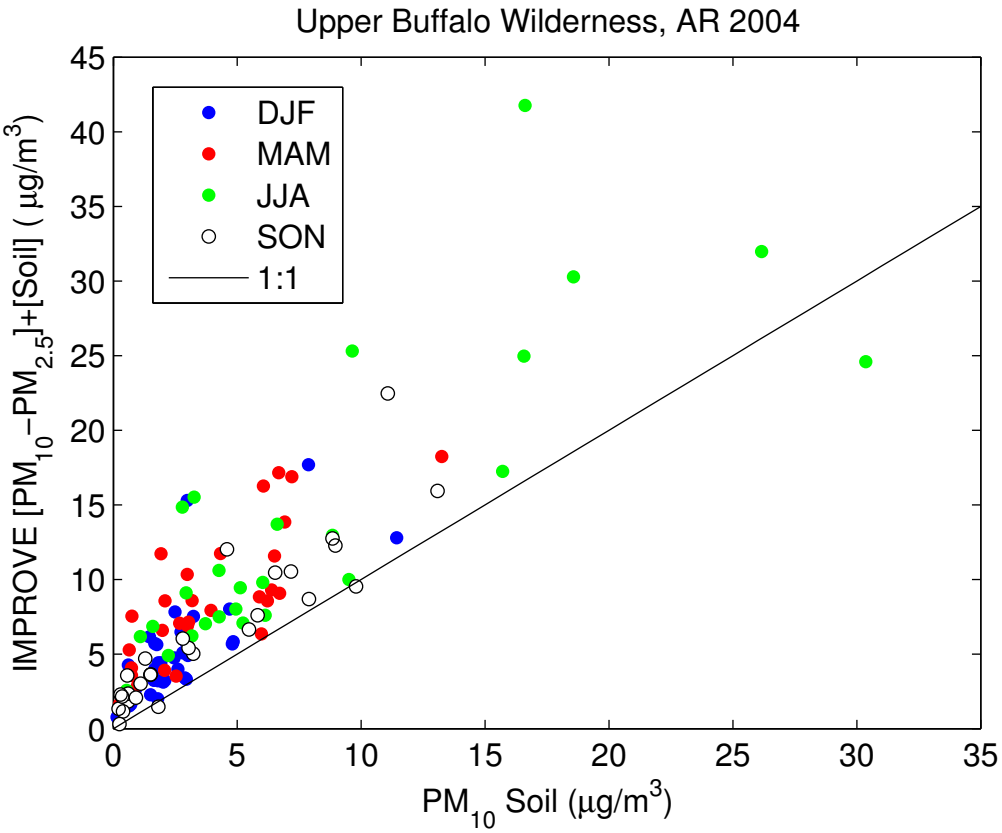


**Figure 4.13: IMPROVE [$PM_{10}$-$PM_{2.5}$]+[Soil] versus $PM_{10}$ soil as computed using the IMPROVE fine soil formula for Upper Buffalo Wilderness, Arkansas.**

The comparison of the scaled IMPROVE data versus the $PM_{10}$ soil from the fine soil formula in Figure 4.16 yields better agreement than that in Figure 4.13; although, as at other sites, scaling the coarse fraction by the 2004 average seasonal soil composition underestimates the $PM_{10}$ soil mass at higher soil amounts. Despite this, the comparison of

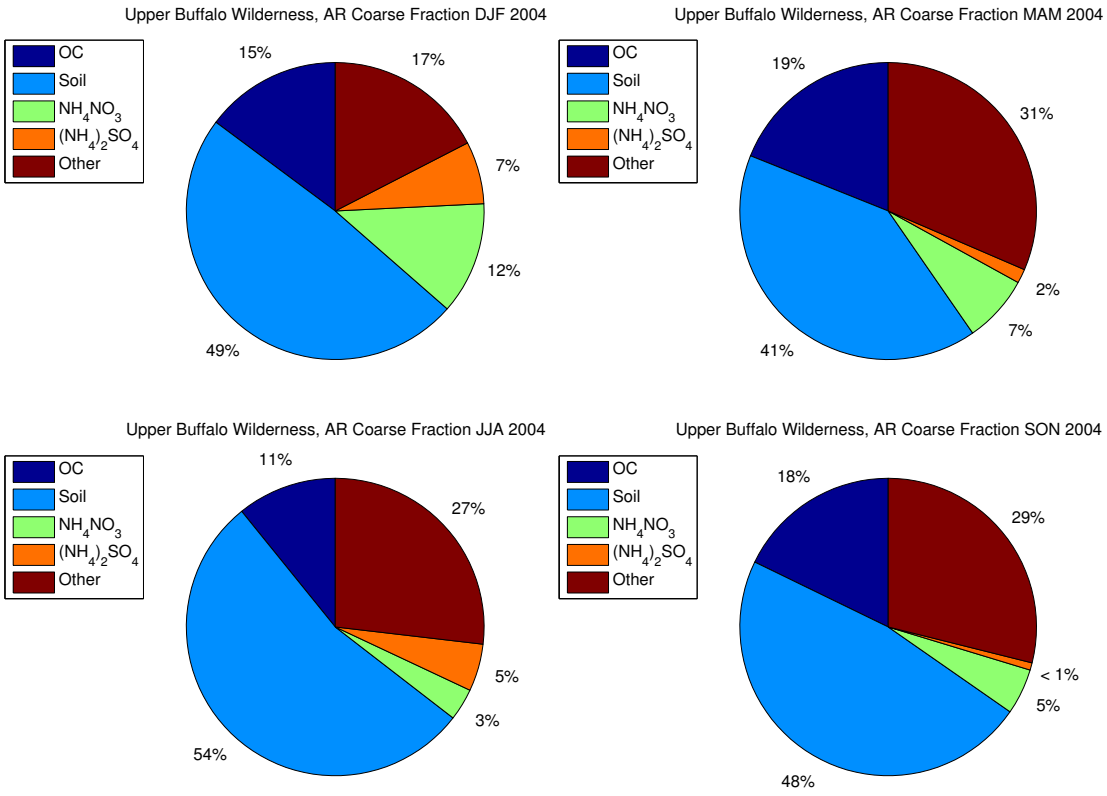


**Figure 4.14: Seasonal composition of major components of IMPROVE coarse fraction aerosol for Upper Buffalo Wilderness, Arkansas.**

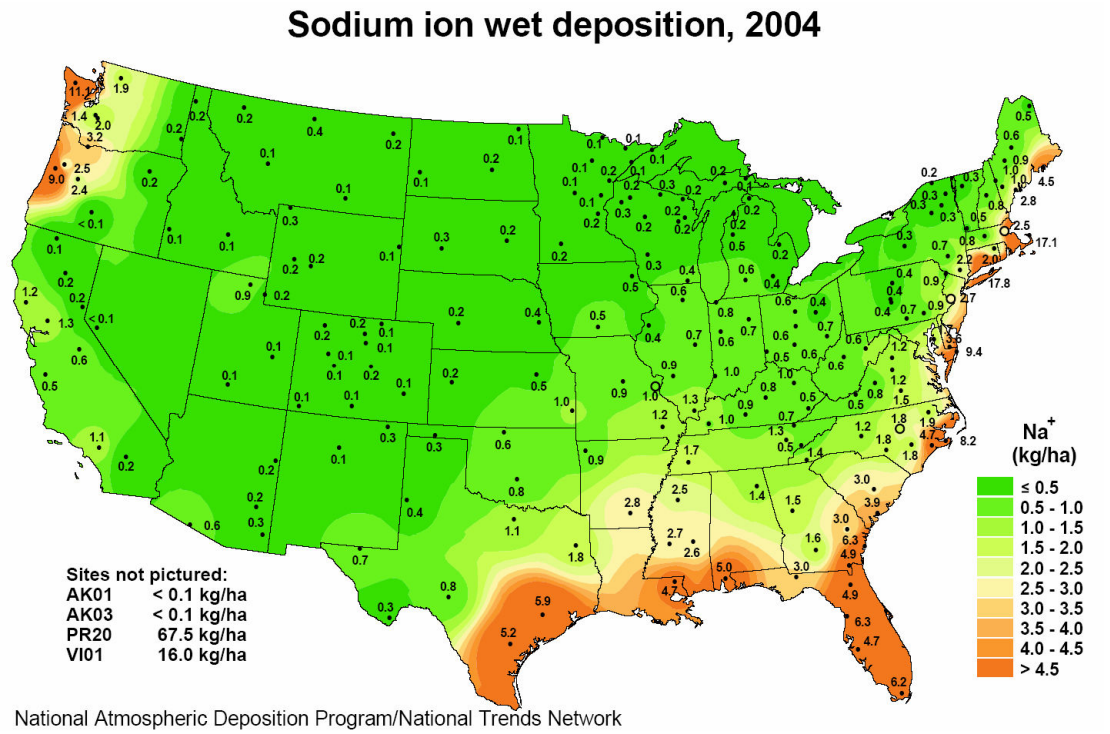


**Figure 4.15: Sodium ion wet deposition for 2004 (kg/ha). (Source: National Atmospheric Deposition Program/National Trends Network (http://nadp.sws.uiuc.edu)).**

NAAPS to the scaled IMPROVE data at Upper Buffalo Wilderness for 2001-2004 (Figure 4.17) yields median ratios close to one in winter, spring, and fall, with a bias toward ratios smaller than one in the summer. The frequency distributions are broad, but are centered at a median ratio of one in winter and spring, revealing generally good agreement between NAAPS and IMPROVE soil dust amounts (especially in spring). It has been shown that sea salt particles may well be found in the aerosol coarse mass fraction at Upper Buffalo Wilderness; the bias toward ratios less than one in the summer months could be due to this, or to the influence of episodic regional or Saharan dust transport that is not captured by NAAPS. The influence of North American sources in the model leads to secondary peaks in the fall and winter distributions at ratios much greater than one.

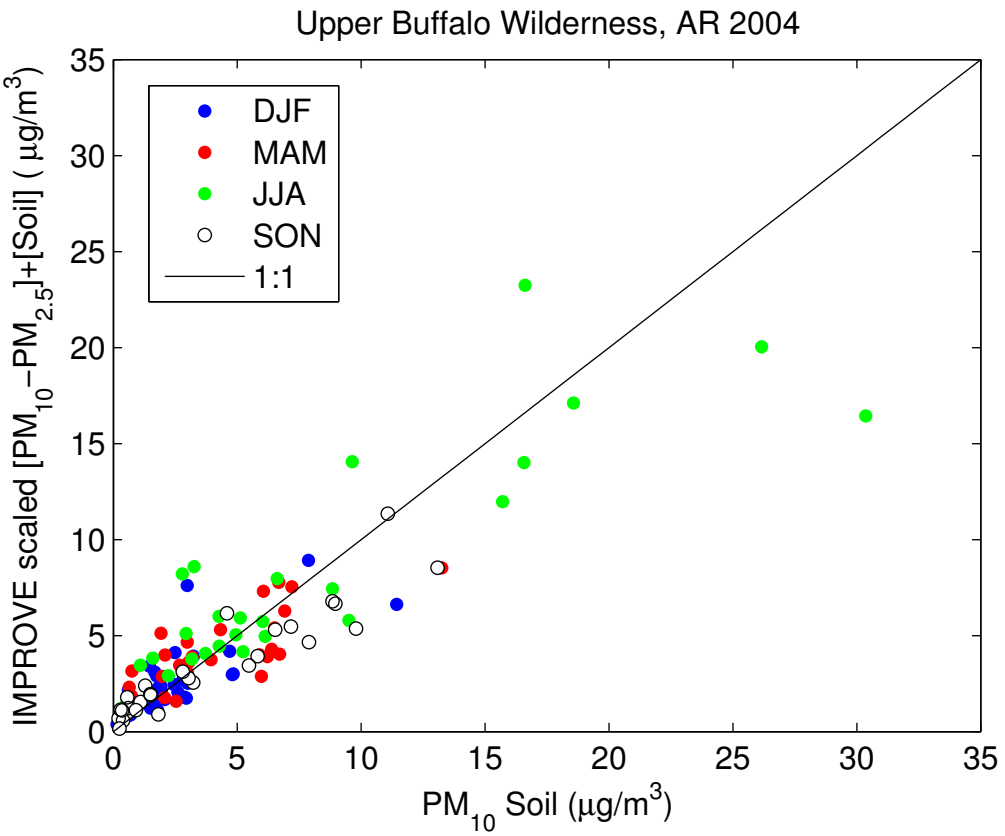


**Figure 4.16: IMPROVE scaled [$PM_{10}$-$PM_{2.5}$]+[Soil] versus $PM_{10}$ soil as computed using the IMPROVE fine soil formula for Upper Buffalo Wilderness, Arkansas.**

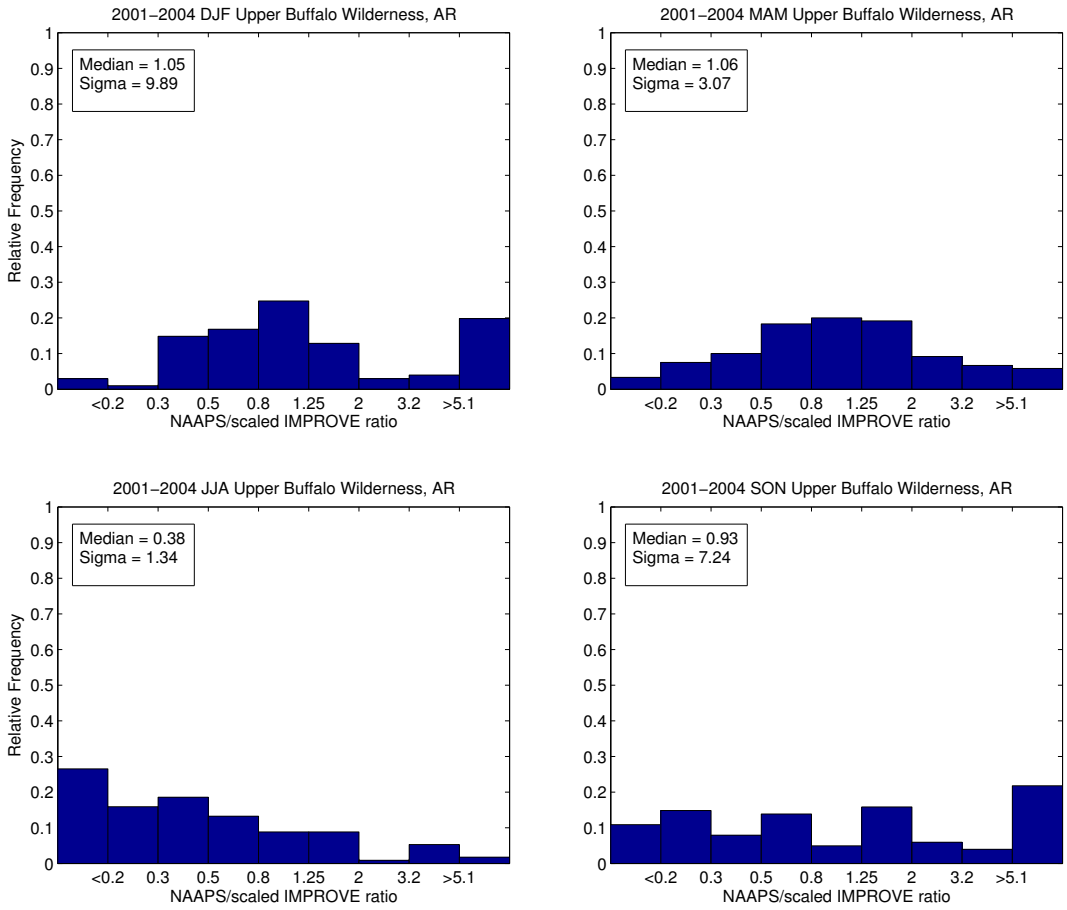


**Figure 4.17: Seasonal frequency distributions of the ratio of NAAPS predicted surface dust to IMPROVE scaled [$PM_{10}$-$PM_{2.5}$]+[Soil] for 2001-2004 at Upper Buffalo Wilderness, Arkansas.**

### 4.1.5 Sea Salt Aerosol in NAAPS

The speciated coarse fraction data discussed in the previous sections reveal that, in many portions of the U.S., it is not realistic to assume the aerosol coarse fraction is composed only of crustal material. Furthermore, they illustrate just how much mass at any one site could be due to species other than soil, OC, sulfate, or nitrate. Certainly sea salt must be a significant component of the coarse aerosol mass at coastal sites, and possibly also at those which are frequently impacted by air masses of marine origin. At Brigantine National Wildlife Reserve in New Jersey, for example, the sum of the aerosol coarse fraction and fine soil masses consistently overestimates the $PM_{10}$ soil reconstructed with the IMPROVE formula, presumably due to the presence of sea salt in

the coarse mode. As a result, if NAAPS correctly simulated the transport of $PM_{10}$ dust aerosol to Brigantine all the time, the predicted mass would always be less than that measured by IMPROVE if one works under the assumption that [$PM_{10}$-$PM_{2.5}$] is only due to soil particles.

The distribution of median NAAPS-to-IMPROVE [$PM_{10}$-$PM_{2.5}$]+[Soil] ratios (Chapter 3, Section 3.3.2) showed that low median ratios occurred consistently at coastal sites and at some inland sites which might be frequently impacted by the transport of sea salt. Sea salt particles can play an important role in global climate; they can serve as giant CCN, potentially enhancing precipitation processes at high CCN concentrations, (Feingold et al., 1999) and they can serve as an interface for atmospheric chemical reactions of halogenated compounds (Finlayson-Pitts and Hemminger, 2000). We have already discussed how sea salt is a difficult species to quantify using IMPROVE measurements, and that its detection is often associated with large errors. Thus, it is valuable to implement a sea salt parameterization into a global model such as NAAPS to better understand the production and distribution of sea salt aerosol. Here, we present results for one parameterization as described in Witek et al. (in preparation).

Figure 4.18 contains seasonal averages of NAAPS predicted total column sea salt amounts for 2001-2004. The model predicts a large amount of sea salt in the vicinity of the Icelandic and Aleutian lows, where strong surface winds exist over the open ocean. The largest mass loadings are simulated in the winter months; an overall minimum occurs in the summer months. Over the continental U.S., NAAPS predicts the most prominent influence of sea salt aerosol during any season along the Pacific coastline, with the Gulf Coast, the Great Lake states, and the eastern seaboard exhibiting large amounts as well.

2001-2004 DJF Average NAAPS Sea Salt Column (mg/m$^2$)

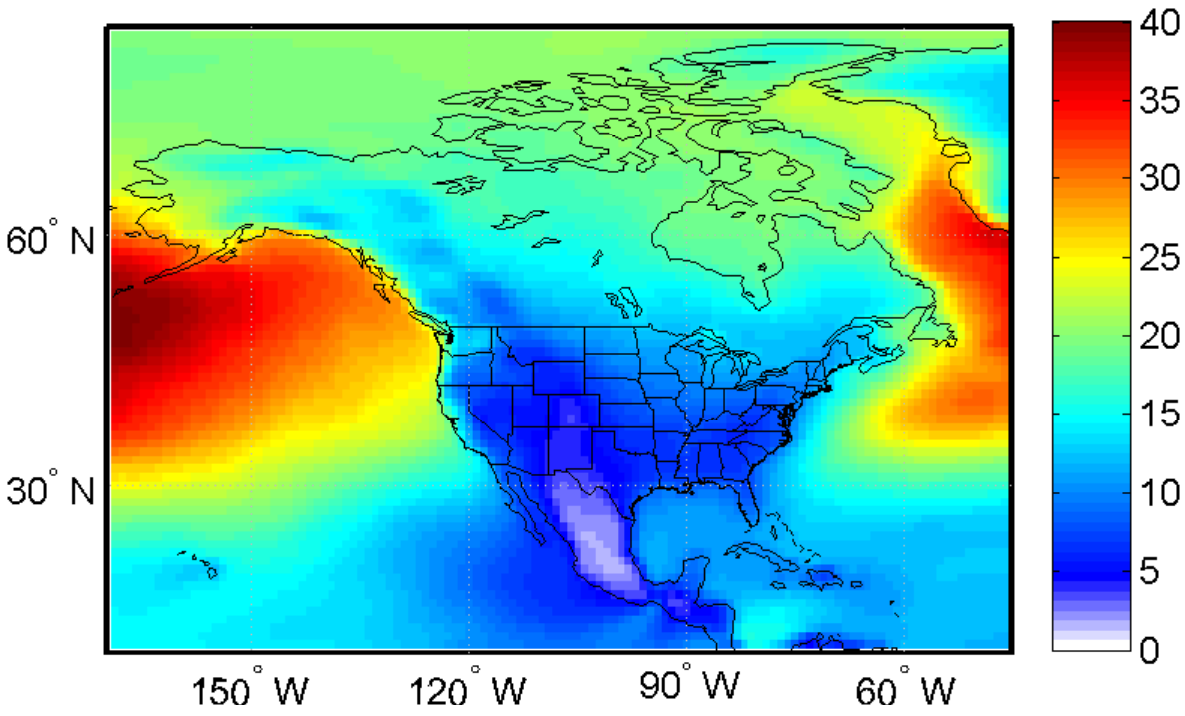


2001-2004 MAM Average NAAPS Sea Salt Column (mg/m$^2$)

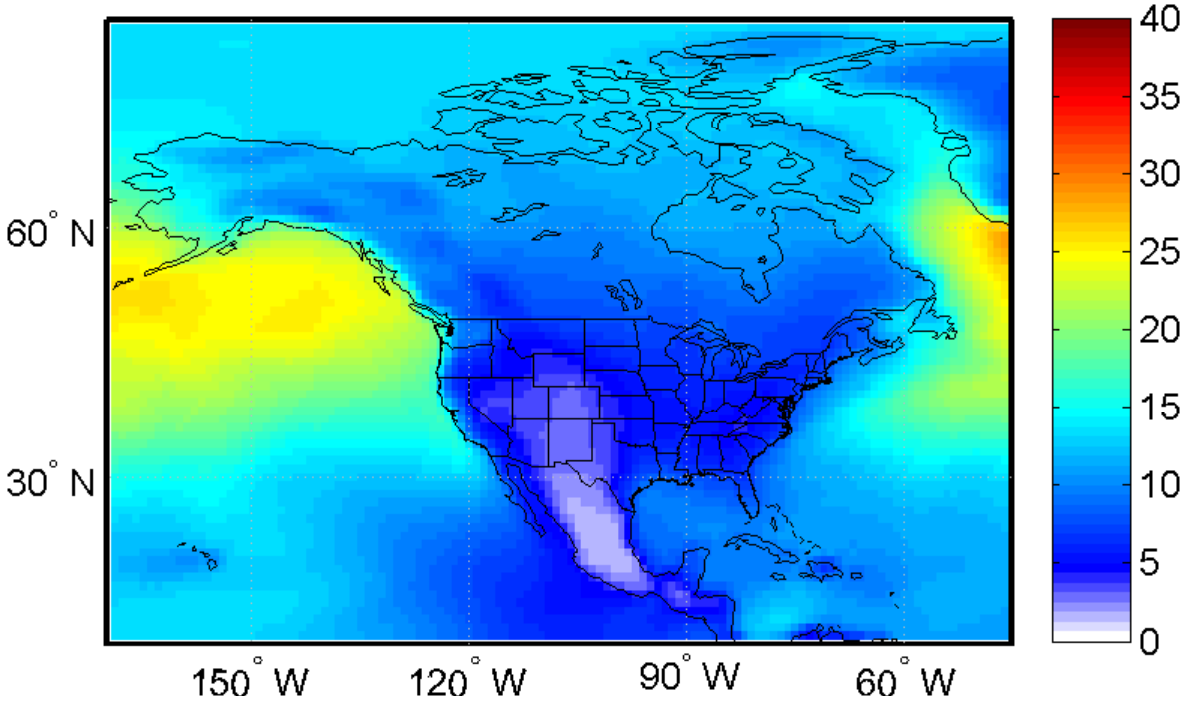

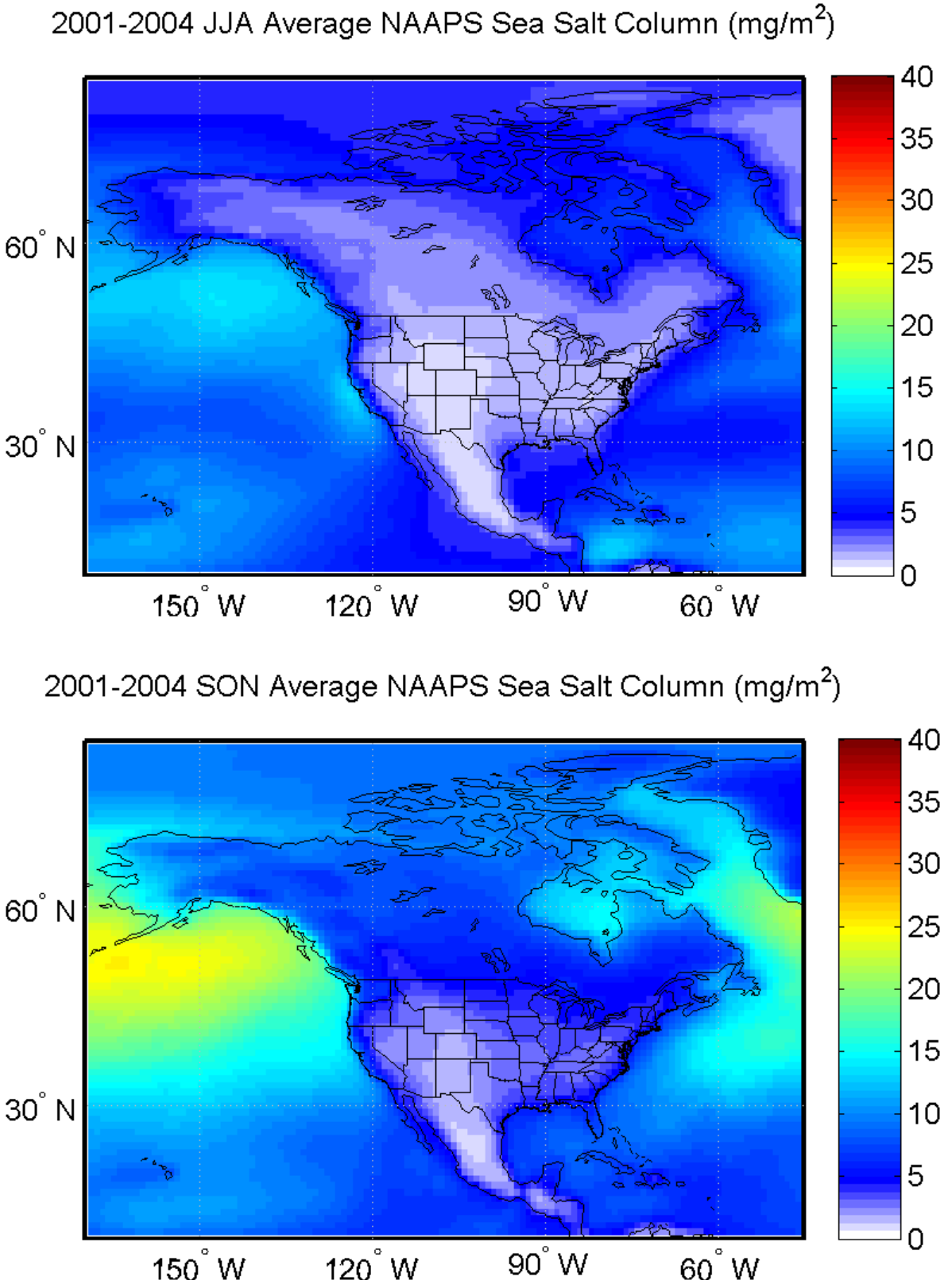


**Figure 4.18: 2001-2004 average seasonal NAAPS sea salt column (mg $m^{-2}$).**

The seasonality of sea salt predictions may explain some of the unresolved coarse fraction mass at coastal sites. The coarse mass composition at Brigantine National Wildlife Reserve contains large fractions of mass that are unaccounted for by the standard IMPROVE reconstructions in the wintertime, whereas a smaller fraction remains unaccounted for in the summer. Even at Sequoia National Park, the influence of marine air in the wintertime could result in the significant "other" fraction of the coarse mass in the winter months. At an inland site such as Upper Buffalo Wilderness, the presence of sea salt mass would be a strong function of the dominant transport patterns during a particular season, which could be one reason why the "other" category is larger in seasons other than winter at this site.

Frequency distributions of NAAPS dust to IMPROVE $[PM_{10}\text{-}PM_{2.5}]$+[Soil] for Everglades National Park, Florida (Figure 4.19) indicate a bias toward ratios less than one in all seasons; this bias is most strong in winter, spring and fall when Saharan dust transport to the U.S. is less pronounced. If we assume the aerosol coarse mass at this site is attributable only to dust or sea salt (which, as shown previously, is not necessarily the best assumption), a comparison of the sum of NAAPS predicted dust and sea salt to the IMPROVE $[PM_{10}\text{-}PM_{2.5}]$+[Soil] should resolve the low bias due to the IMPROVE measurements. This comparison for Everglades National Park is shown in Figure 4.20, which contains seasonal frequency distributions of NAAPS-to-IMPROVE ratios with the inclusion of NAAPS predicted sea salt mass.

Although the addition of sea salt to the NAAPS predictions results in a median NAAPS/IMPROVE ratio greater than one (greater than two in winter, when sea salt production is highest) throughout the year at Everglades National Park, it completely

eliminates NAAPS-to-IMPROVE ratios below 0.2. In fact, comparing the sum of NAAPS predicted dust and sea salt mass to IMPROVE [$PM_{10}$-$PM_{2.5}$]+[Soil] produces an almost normal frequency distribution for the summer months. The higher median NAAPS-to-IMPROVE ratios could be due to an overestimation of total sea salt production in NAAPS, the presence of organics or other aerosol species in the aerosol coarse mass, or to the fact that the IMPROVE mass contains no fine sea salt component. However, a further examination of sea salt production in NAAPS and $PM_{10}$ composition at coastal sites is necessary to confirm these ideas.

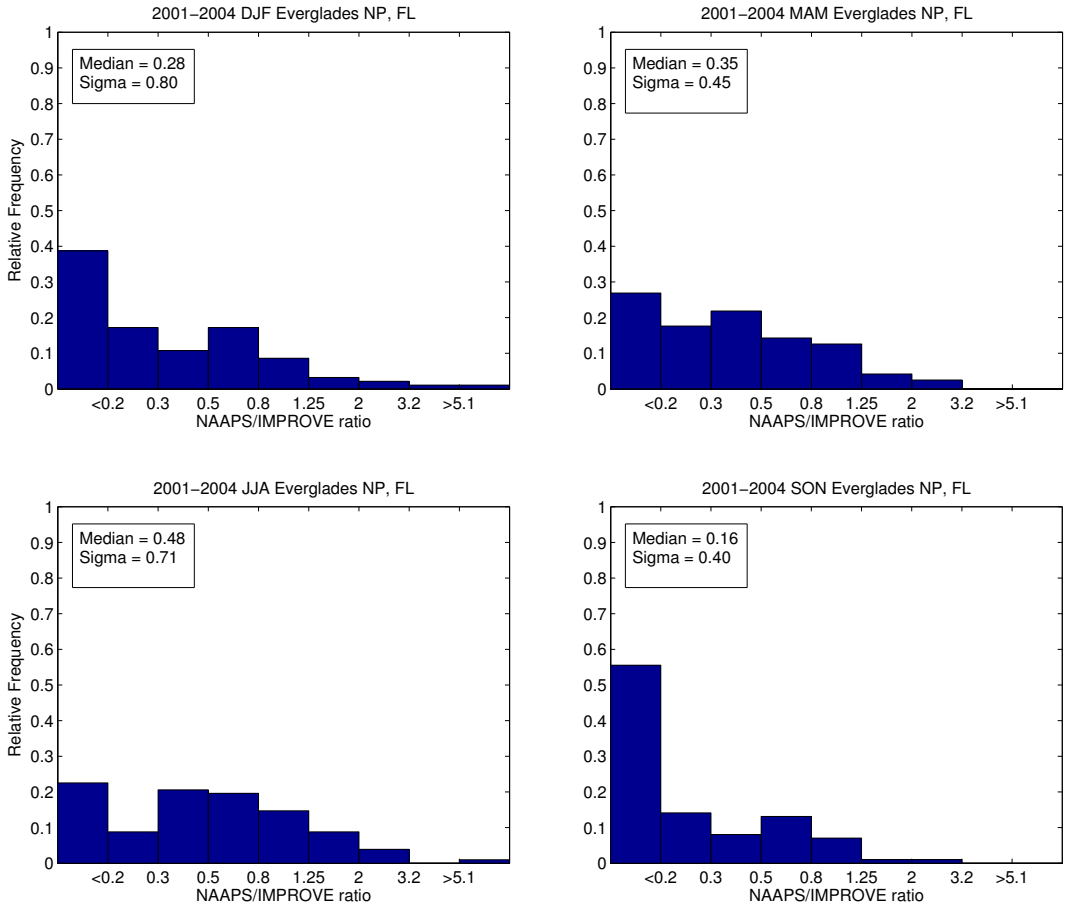


**Figure 4.19: Seasonal frequency distributions of the ratio of NAAPS predicted surface dust to IMPROVE [$PM_{10}$-$PM_{2.5}$]+[Soil] for 2001-2004 at Everglades National Park, Florida.**

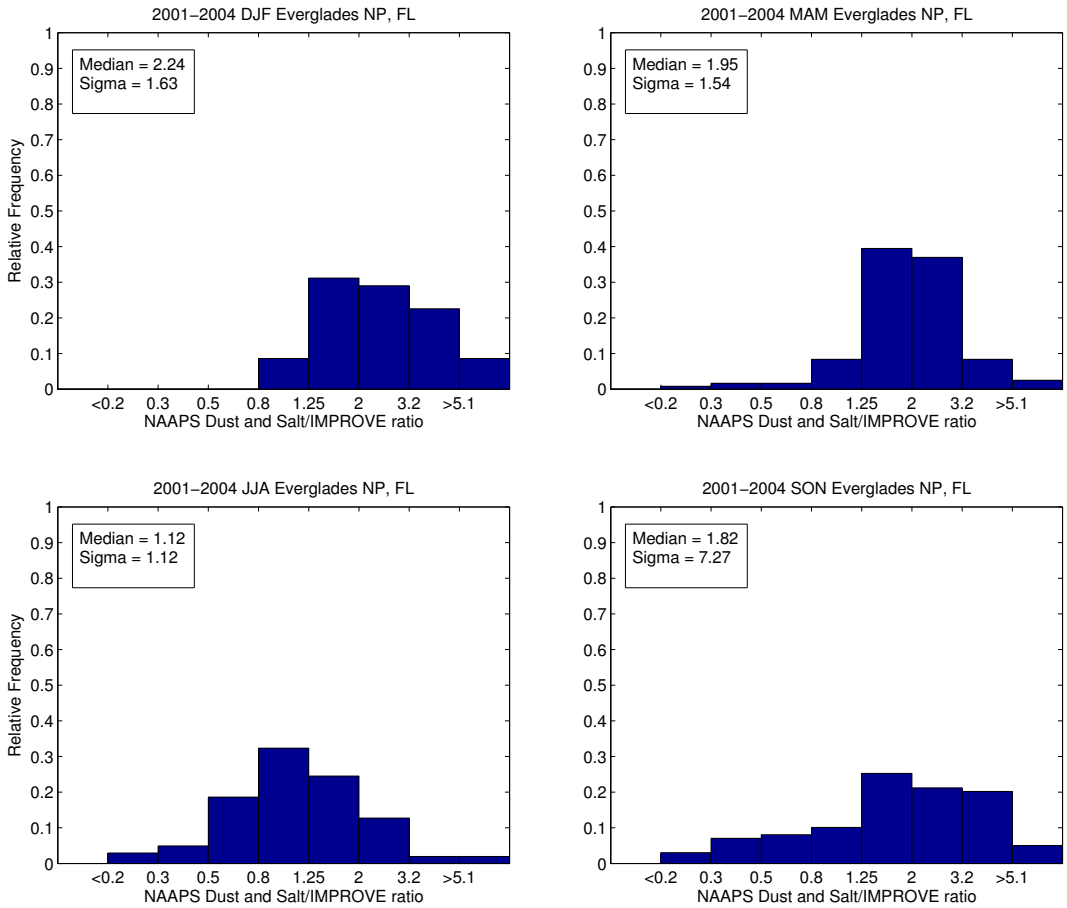


**Figure 4.20: Seasonal frequency distributions of the ratio of NAAPS predicted surface dust and sea salt to IMPROVE [$PM_{10}$-$PM_{2.5}$]+[Soil] for 2001-2004 at Everglades National Park, Florida.**

## 4.2 Special Study (2004) Comparison of NAAPS to IMPROVE

Results presented in the previous section reveal that $PM_{10}$ soil concentrations obtained with the soil formula are likely to be a better indicator of total soil mass than IMPROVE [$PM_{10}$-$PM_{2.5}$]+[Soil] due to the presence of non-crustal material in the aerosol coarse mode. However, speciated $PM_{10}$ data from the IMPROVE network are only available for a limited number of sites, and for only one of the four years examined in this study. This section presents comparisons involving this limited dataset for sites in different regions of the U.S., from which general conclusions on the NAAPS/IMPROVE comparison will be drawn. Figure 4.21 contains timelines of NAAPS and $PM_{10}$ soil measured during 2004 for the four sites examined in this chapter.

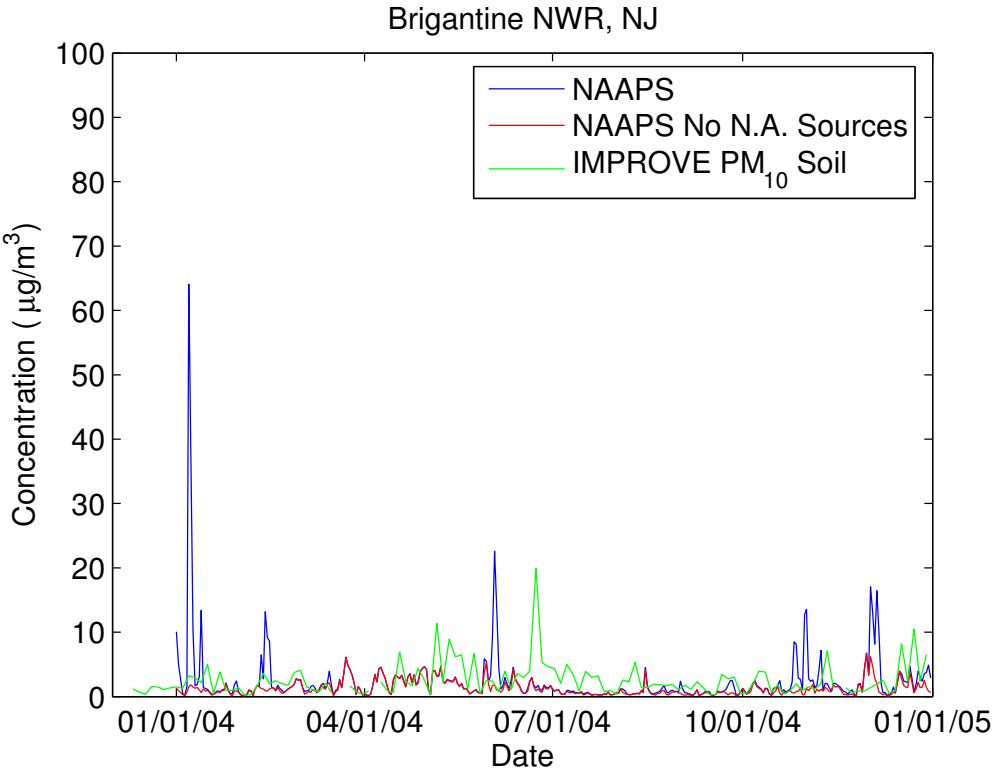
Brigantine NWR, NJ
NAAPS
NAAPS No N.A. Sources
IMPROVE PM10 Soil
Concentration ( µg/m3)
Date
0
10
20
30
40
50
60
70
80
90
100
01/01/04
04/01/04
07/01/04
10/01/04
01/01/05

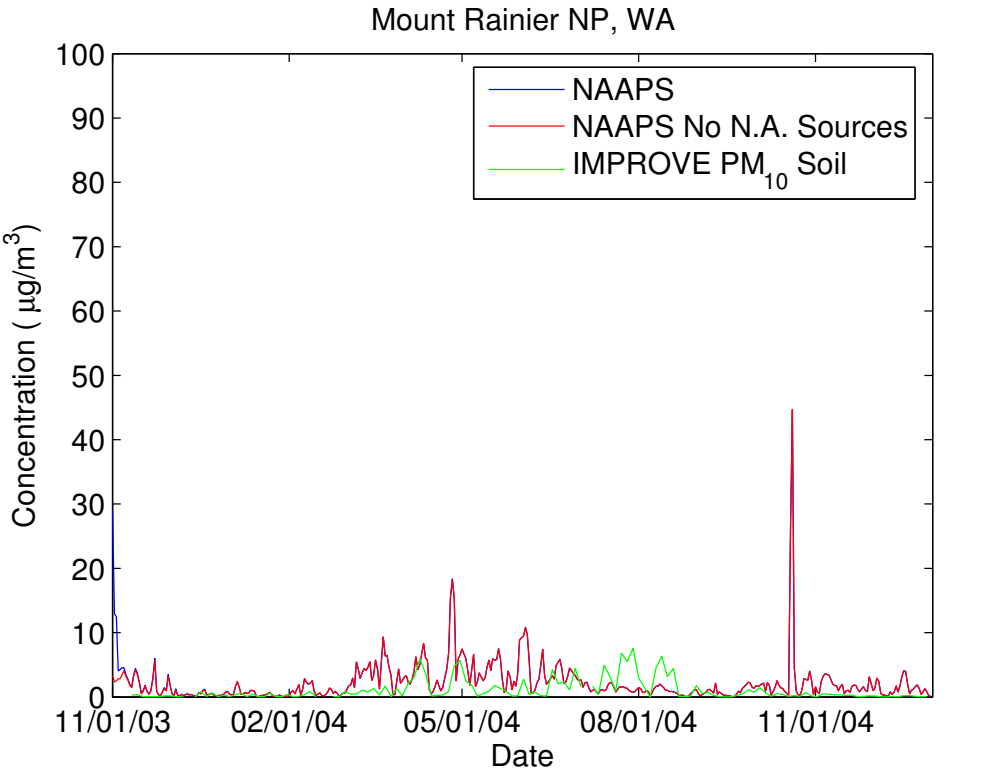
Mount Rainier NP, WA
NAAPS
NAAPS No N.A. Sources
IMPROVE PM10 Soil
Concentration ( µg/m3)
Date
0
10
20
30
40
50
60
70
80
90
100
11/01/03
02/01/04
05/01/04
08/01/04
11/01/04

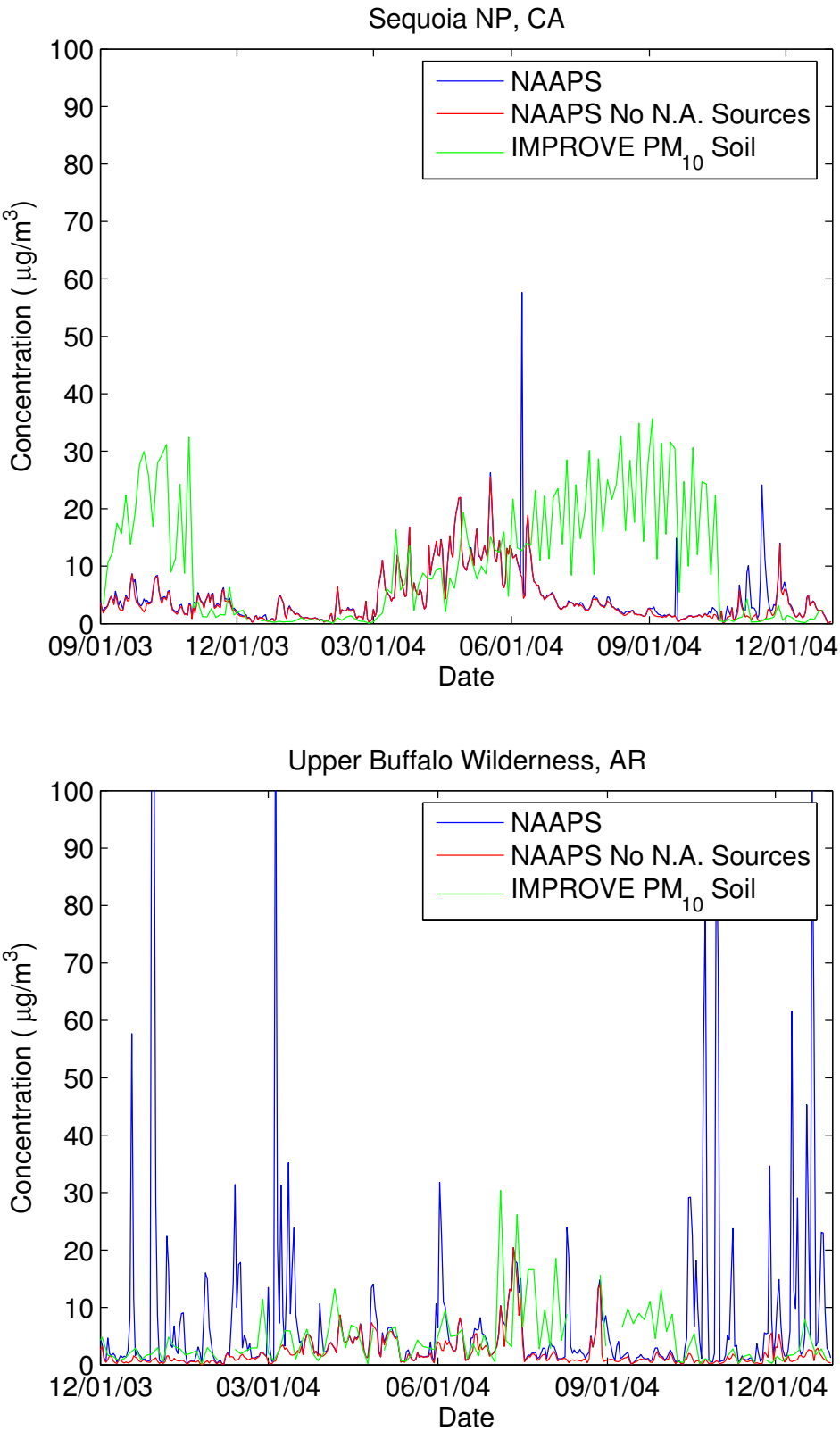


**Figure 4.21: NAAPS daily average soil dust and IMPROVE $PM_{10}$ soil timelines for Brigantine National Wildlife Reserve, New Jersey; Mount Rainier National Park, Washington; Sequoia National Park, California; and Upper Buffalo Wilderness, Arkansas.**

### 4.2.1 North American Dust Sources

At Brigantine National Wildlife Reserve and Mount Rainier National Park, the absence of a North American dust influence results in relative agreement between NAAPS predictions and IMPROVE $PM_{10}$ soil amounts for 2004. Although NAAPS predicted soil dust and IMPROVE $PM_{10}$ soil correspond well in winter and spring at Sequoia National Park, the timeline in Figure 4.21 indicates a large, persistent presence of $PM_{10}$ soil at the site during summer and fall that is not predicted by the model. The median NAAPS soil dust to IMPROVE $[PM_{10}\text{-}PM_{2.5}]$+[Soil] ratio is very low in the summer months at Sequoia and Death Valley National Parks in California, Sycamore Canyon, Arizona; and Guadelupe Mountains National Park, Texas, despite the fact that the surface is highly erodible in the vicinity of these sites (Figure 4.22), and TOMS AI values indicate a high frequency of absorbing aerosol in southern California/Arizona and southwestern Texas (Chapter 1, Section 1.1.2.2). Topographical smoothing may to blame for this. For instance, dust storms at Owens Dry Lake tend to occur in the presence of north-south flow forced by the Sierra Nevada and White-Inyo mountain ranges (Reid et al., 1994); such sub-grid scale processes would not be resolved in NAAPS.

Anthropogenic activities also play a large role in the seasonal cycle of soil dust aerosol at the measurement site in Sequoia National Park. A study of $PM_{10}$ source apportionment in the San Joaquin Valley (SJV) from 1988-1989 revealed that 54% of the summer and fall $PM_{10}$ mass in the valley was attributable to fugitive dust from tilling of fields, travel on unpaved roadways, and construction, whereas nitrate species were highest in the winter months (Chow et al., 1992). Since the measurement site in Sequoia National Park is at an elevation (535 m) that would often be impacted by the SJV

boundary layer during the day, it makes sense that the site exhibits persistently high $PM_{10}$ soil levels in the summer and fall. NAAPS has no anthropogenic or seasonal component in its source function, so it would not reproduce such a trend.

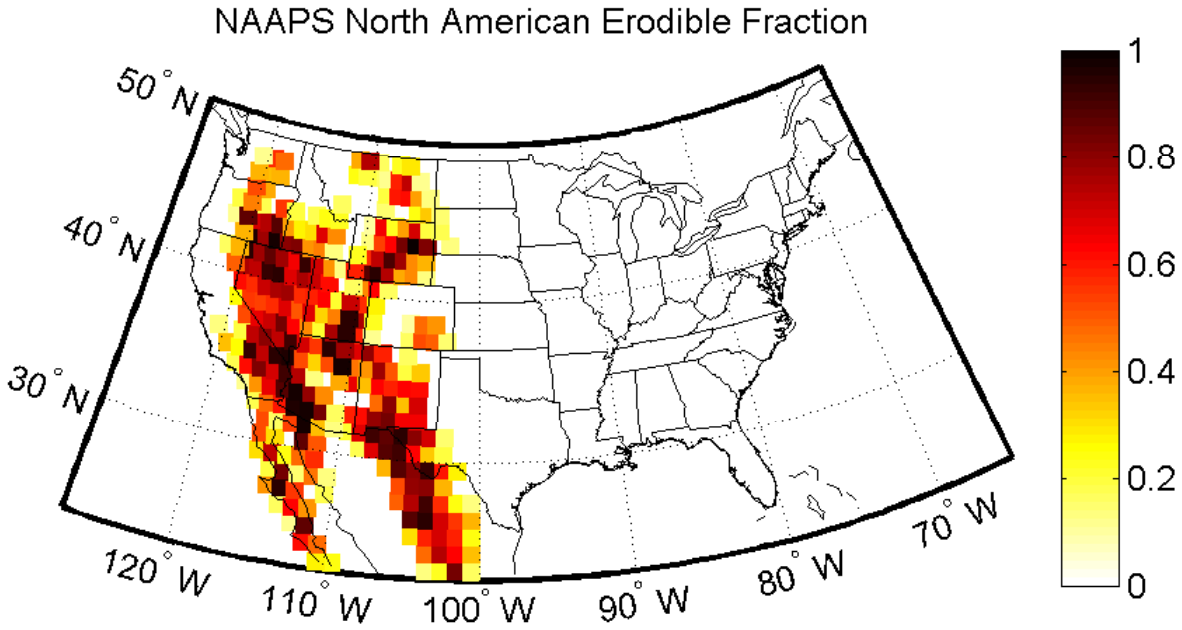


**Figure 4.22: Erodible fraction of NAAPS 1º x 1º gridboxes in North America.**

On the other hand, the timeline for Upper Buffalo Wilderness in Figure 4.21 contains NAAPS predicted North American soil peaks in late fall, winter, and early spring that are quite a bit higher than the IMPROVE $PM_{10}$ soil amounts. Some of this could be due to the absence of snow cover information in NAAPS; the production of dust aerosol on the High Plains in wintertime would likely be suppressed if snow cover were added to the model. Implementation of a variable threshold friction velocity would also likely reduce the frequency and magnitude of dust events generated in the High Plains, where katabatic winds and climatologically dry surface moisture values create conditions which are favorable for soil dust emission in NAAPS. However, as mentioned previously, the threshold friction velocity is currently set everywhere in the model to a value determined in a study of Saharan dust mobilization. The dominant surface type in

the High Plains of the U.S. is not characterized as bare desert in the USGS land cover database, but as semi-desert sage. Since the roughness height (the height at which the wind speed reaches zero) is higher over vegetated surfaces, a higher friction velocity threshold is probably more appropriate for dust sources in North America.

### 4.2.2 Removal processes

In addition to annual soil dust emission rates, Table 4.1 contains atmospheric soil dust burdens for the six models mentioned in Chapter 3. Despite being on the low end of annual emission estimates among the models, NAAPS has the highest simulated atmospheric soil dust burden—nearly double the burdens of other models on the low end of total emission estimates. This can be considered in terms of the particle lifetime, $\tau$, in NAAPS, which was computed assuming the dust aerosol to be in a steady state by using

$$\tau = \frac{M}{S} \tag{4.1}$$

where $M$ is the average atmospheric soil dust burden and $S$ represents the soil dust removal rate by wet or dry processes. The average wet lifetime of dust in NAAPS is within the range of the six models used for comparison; however, the average dry lifetime is nearly twice that of any of the other models (Figure 4.23), leading to a total dust aerosol lifetime in NAAPS that is 3-6 days longer than other estimates.

| Model | Emission (Tg $yr^{-1}$) | Atmospheric Burden (Tg) |
|---|---|---|
| NAAPS | 1306 | 36.7 |
| Miller et al. (2004) | 1019 | 14.6 |
| Ginoux et al. (2001) | 1814 | 35.9 |
| Tegen et al. (2002) | 1100 | 22.2 |
| Luo et al. (2003) | 1654 | 23.3 |
| Zender et al. (2003a) | 1490 | 17.4 |

**Table 4.1: Annual soil dust emission and atmospheric burden for six global models (adapted from Miller et al., 2004).**

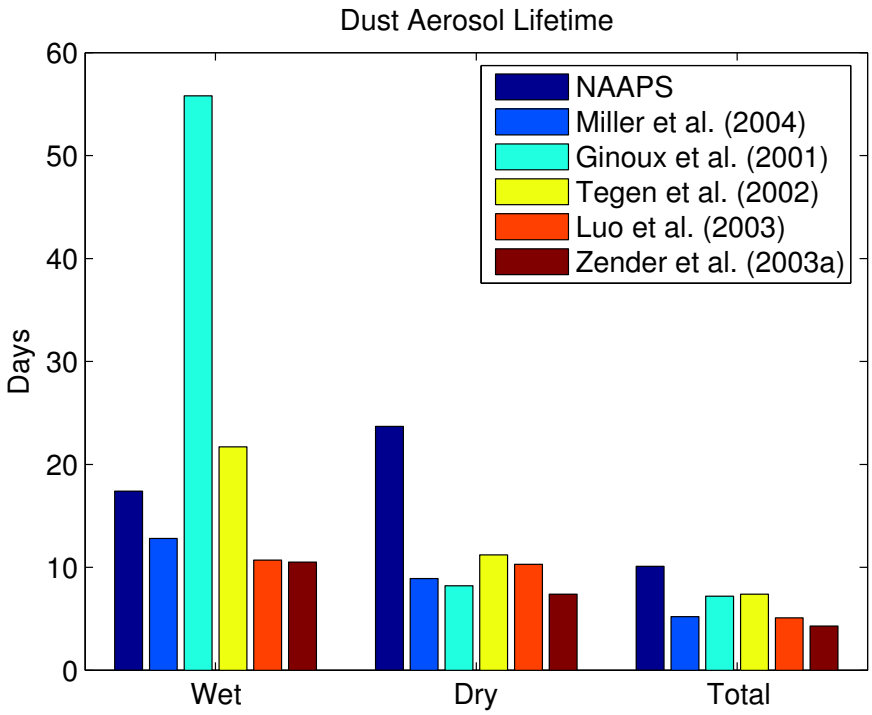


**Figure 4.23: Wet, dry, and total dust aerosol lifetimes (days) for six global models (adapted from Miller et al., 2004).**

In the absence of measurements of soil dust deposition with which to compare the removal of dust aerosol in NAAPS, one can do no more than speculate that perhaps dry deposition of dust is underestimated by the model based upon the long dry lifetime of dust computed for the four-year simulation. The hypothesis makes sense, given that soil dust deposition process are parameterized in NAAPS in the same manner as they are for sulfate particles (Chapter 2); in the absence of particle size-segregation, larger dust particles would not be removed as quickly in the model as they would in the real atmosphere. The exclusion of gravitational settling likely contributes to this trend. This could explain why very large concentrations are simulated in the vicinity of source regions, and why total non-North American dust amounts predicted over the U.S. during larger non-North American dust incursions are sometimes greater than in the IMPROVE measurements.

### 4.2.3 Saharan Dust Influence

At Brigantine National Wildlife Reserve, the timing and magnitude of peaks in NAAPS predicted non-North American soil correspond well with the IMPROVE $PM_{10}$ soil, especially in the fall and winter months, when background soil concentrations are predicted to be quite low. The predicted amounts of North American soil in NAAPS are above the IMPROVE measurements, though only the spike in January is of a magnitude that seems high when compared to the aerosol data (although the IMPROVE network can miss short-duration events given that it only samples every three days).

NAAPS predicts low concentrations of soil dust at Brigantine throughout the four year simulation, with the exception of a few larger peaks due to transport from North American source regions. Each year, however, there are a few summer peaks in the IMPROVE measurements that are not consistent with model predictions. Figure 4.24 contains the IMPROVE Al-to-Ca ratio and $PM_{10}$ soil timeline for 2004; the black dotted line indicates the lower limit of Al/Ca (3.8) used by Perry et al. (1997) to indicate the presence of North African dust in the U.S., while the red line indicates the upper limit of Al/Ca (2.6) used to identify Asian dust in the U.S. by VanCuren and Cahill (2002). The soil dust measured in the June 2004 peak at Brigantine is very calcium-depleted: the Al-to-Ca ratio measured that day is well above 3.8.

Since aluminum is often below the IMPROVE detection limit at Brigantine, the site's silicon-to-calcium ratio for 2001-2004 was examined for a potential Saharan dust signature. A scatter plot of the data is located in Figure 4.25; the red points correspond to days in which measured fine soil was above 2 $\mu g\ m^{-3}$. A linear best fit of the data reveals an average Si/Ca ratio of 5.0, but days with higher fine soil also saw even higher ratios.

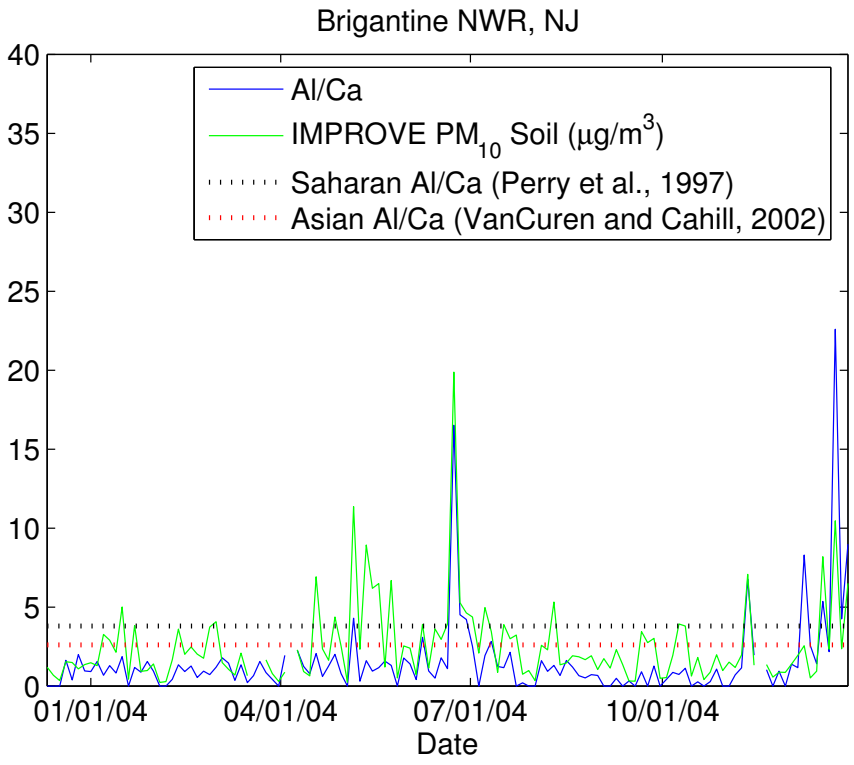


**Figure 4.24: IMPROVE Al-to-Ca ratio and $PM_{10}$ soil timeline for Brigantine National Wildlife Reserve, New Jersey.**

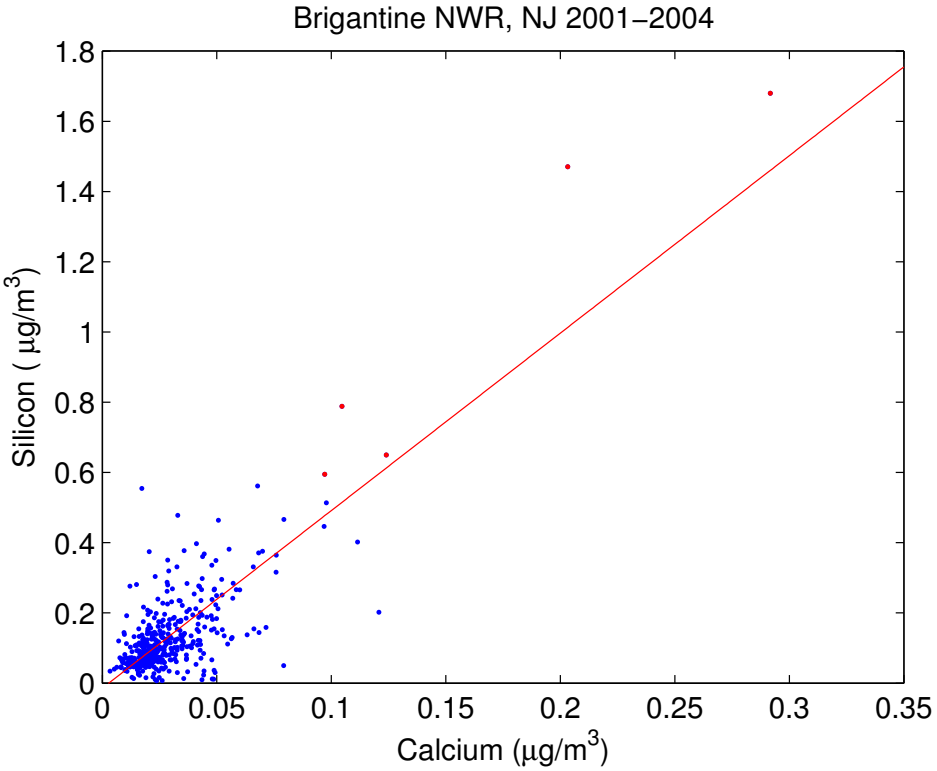


**Figure 4.25: IMPROVE silicon versus calcium mass measured from 2001-2004 at Brigantine National Wildlife Reserve, New Jersey. Red points correspond to days with fine soil mass > 2 µg $m^{-3}$.**

This could indicate the occasional influence of calcium-depleted dust from North Africa; the relatively large number of points at low Si-to-Ca ratios could be due to the influence of North American or Asian dust, both of which appear to be predicted at Brigantine by NAAPS.

## 4.3 Integrated Evaluation of NAAPS Dust Aerosol Predictions

The speciated $PM_{10}$ data presented in this chapter has helped reveal numerous issues in the comparison of NAAPS predictions to IMPROVE [$PM_{10}$-$PM_{2.5}$]+[Soil] at specific sites in the U.S. To apply these findings to a larger group of IMPROVE measurement sites, we return to two key distributions: the frequency of NAAPS predictions which fall within a factor of two of the IMPROVE measurements, and the median NAAPS-to-IMPROVE ratios.

### 4.3.1 DJF 2001 to 2004

The winter distribution of the frequency of NAAPS predictions within a factor of two of IMPROVE and median NAAPS/IMPROVE ratios are shown in Figure 4.26. On average, 39% of the NAAPS predictions fell within a factor of two of the IMPROVE measurements in winter at the 28 IMPROVE sites examined in this study. Higher frequencies of agreement (≥ 50%) occurred at sites in the southwestern U.S., the Great Lakes region and near the northern Pacific coast. Median ratios were greater than one in the northern Rockies, and less than one throughout the southeastern U.S. The comparison of NAAPS to IMPROVE in the winter months could be consistently biased toward high ratios at many sites in the western United States due to the fact that conditions are generally very clean at this time of year. 24-hour average $PM_{10}$ mass concentrations

below 1 μg $m^{-3}$ are not uncommon at sites such as Mount Rainier National Park; to expect a global aerosol model to reproduce such small concentrations is somewhat unrealistic (and unnecessary in terms of visibility considerations).

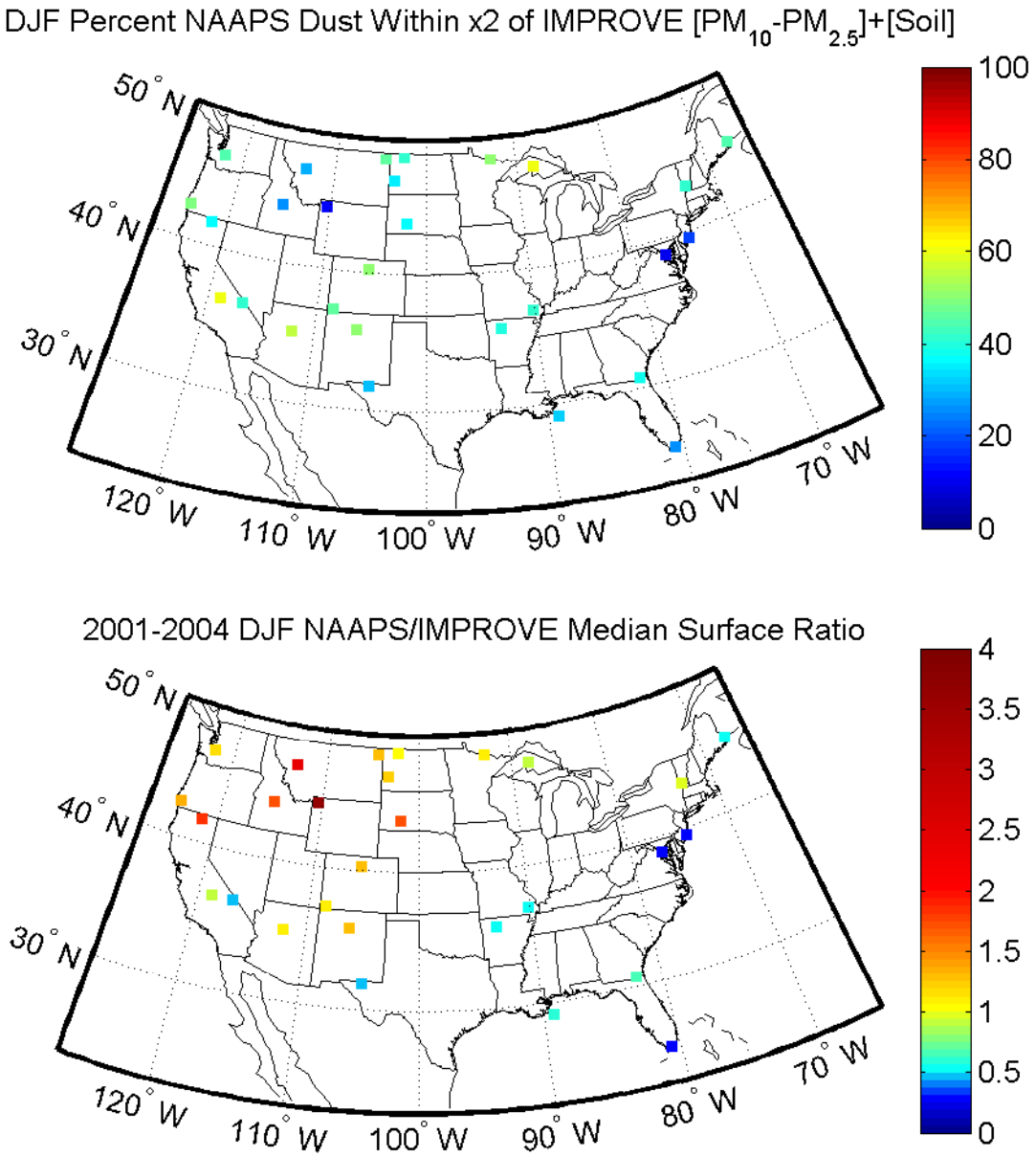


**Figure 4.26: DJF frequency (%) of NAAPS predictions falling within a factor of two of IMPROVE [$PM_{10}$-$PM_{2.5}$]+[Soil] (top) and DJF median ratios of NAAPS to IMPROVE (bottom).**

On the other hand, higher concentrations of $PM_{10}$ coarse mass are often evident in the central U.S. due to the influence of regional sources in winter months. The smaller

NAAPS/IMPROVE ratios at Upper Buffalo Wilderness, Arkansas and Mingo, Missouri during this season could be the result of an unresolved local influence in NAAPS, although this is inconclusive given the lack of measurement sites in the central U.S. The implementation of sites throughout the upper Great Plains of Nebraska, Kansas, Iowa, Minnesota, Illinois and Missouri as of 2004 could help to improve the characterization of $PM_{10}$ mass in this section of the country.

Simulated sea salt amounts in NAAPS were highest in the winter months due to high wind speeds over the open ocean. The presence of sea salt in the aerosol coarse fraction is the most likely explanation for NAAPS/IMPROVE ratios smaller than one at coastal sites. The speciated $PM_{10}$ data from 2004 indicated that 30 to over 40% of the coarse fraction mass at Brigantine could not be accounted for by soil, nitrate, sulfate, or organic aerosol depending upon the season, leading to the consistently low NAAPS/IMPROVE ratios at this and other sites in the vicinity of coastal regions.

### 4.3.2 MAM 2001 to 2004

In the most general sense, the comparison between NAAPS and IMPROVE fares best in the spring, when a widespread influence of Asian dust sources in the U.S. is predicted by the model. NAAPS predictions fell within a factor of two of the IMPROVE measurements an average of 45% of the time at U.S. sites in spring, as indicated by the large number of yellow and green points on the frequency map in Figure 4.27. Low frequencies occurred at coastal sites such as Brigantine, as expected, in addition to sites in northern California, Idaho, and the northern Rocky Mountains. Coastal sites (and Upper Buffalo Wilderness) exhibited low median ratios during spring due to the persistent influence of sea salt on the coarse mode, as previously discussed. Sites in the

northern Rockies (and throughout the western U.S.), however, had median NAAPS/IMPROVE ratios that were greater than one.

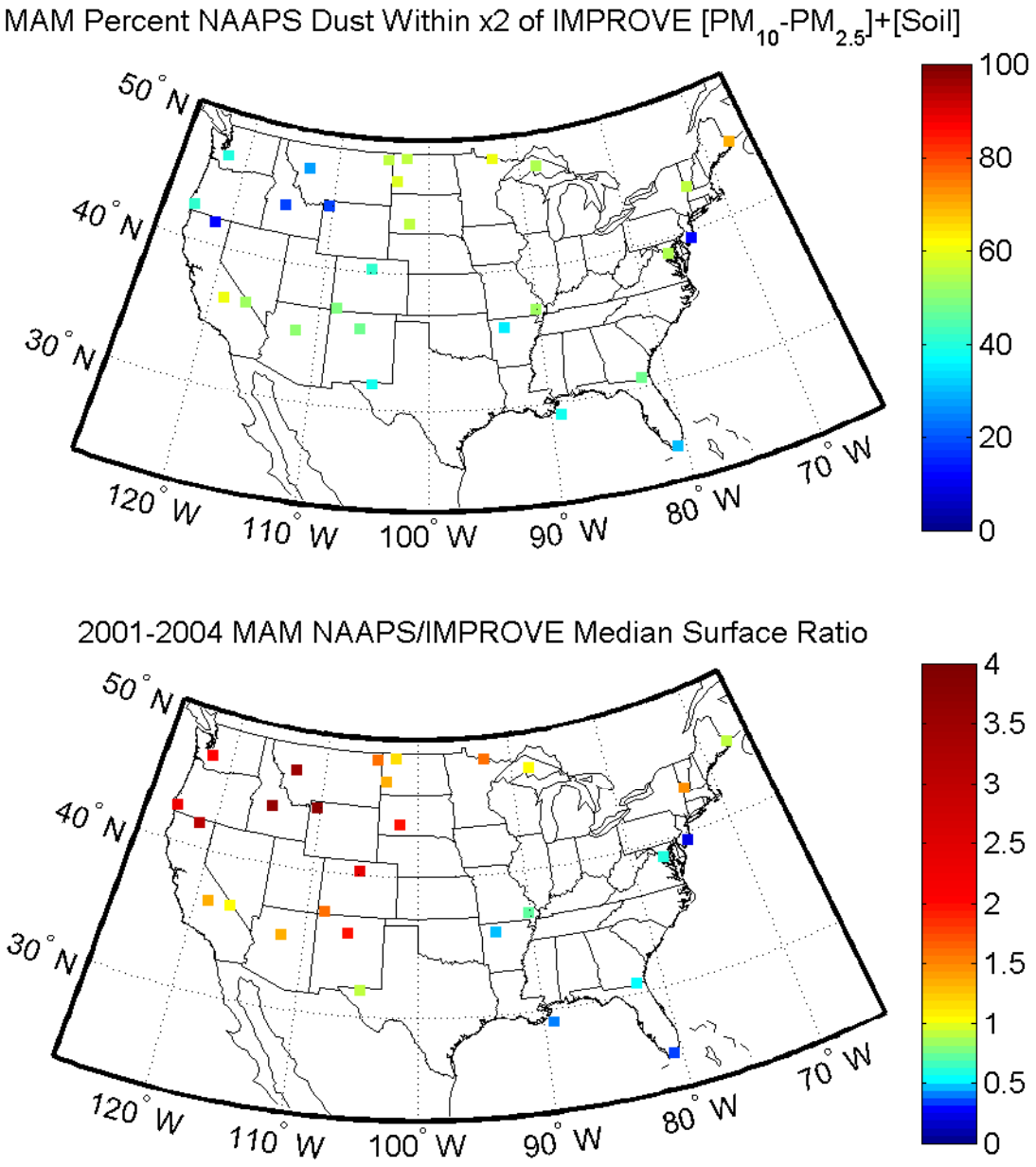


**Figure 4.27: MAM frequency (%) of NAAPS predictions falling within a factor of two of IMPROVE [$PM_{10}$-$PM_{2.5}$]+[Soil] (top) and MAM median ratios of NAAPS to IMPROVE (bottom).**

Since NAAPS predicts almost no local dust influence in this region in spring, this behavior demonstrates the role of elevation in the surface concentrations of long-range dust as predicted by NAAPS, due to the vertical gradient of Asian dust transport in the

boundary layer. Figure 4.28 contains a vertical cross-section of NAAPS predicted dust concentration for an observed dust plume in April 2001 just off the west coast of the U.S. In this event, at this location at least, the dust mass peaked in the free-troposphere, at a height of ~2500 m. Since all of the measurement sites in the northern and central Rockies are located at elevations between 1200 and 2800 meters, these sites would thus receive more Asian dust than surrounding sites at lower elevations, as also discussed by VanCuren and Cahill (2002). Since it has already been suggested that removal processes may be underestimated in NAAPS, it makes sense that these sites are predicted to receive consistently more mass due to long-range transport than is measured by IMPROVE.

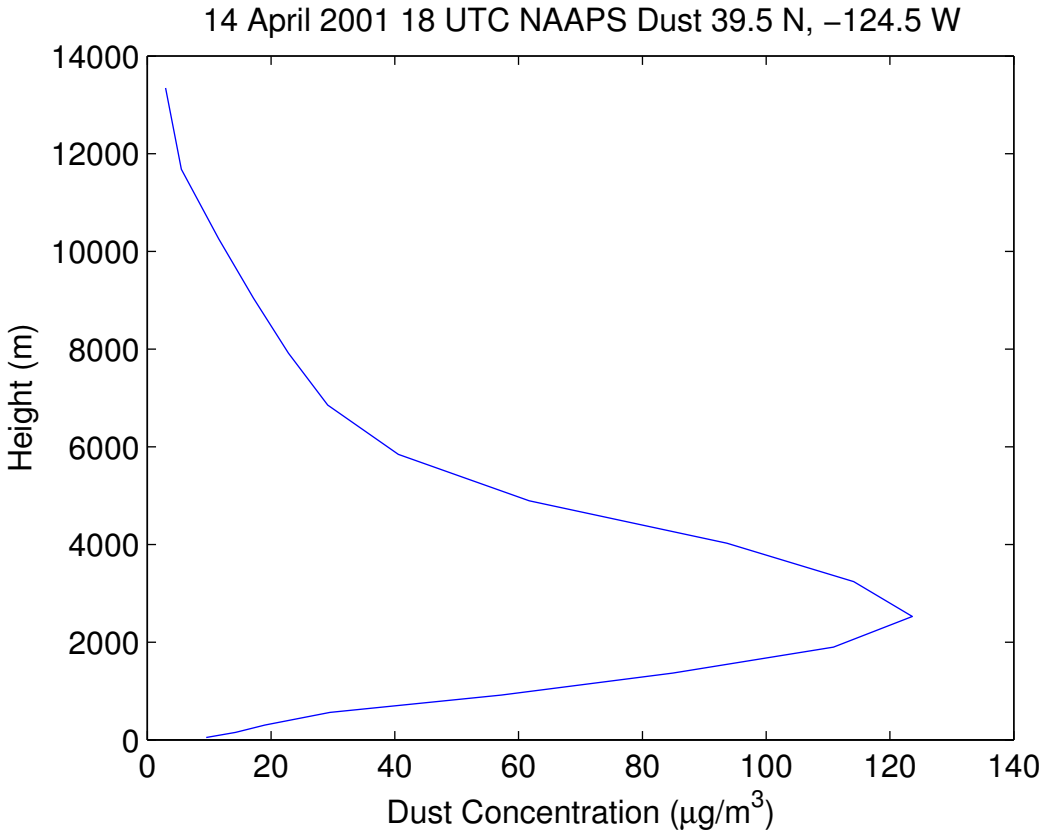


**Figure 4.28: 14 April 2001 18 UTC vertical cross-section of NAAPS predicted dust concentration for 39.5º N, -124.5º W.**

This finding should not, however, serve to discredit NAAPS soil dust predictions over the U.S. in spring. In general, the model shows a high degree of skill in reproducing

the timing of Asian dust peaks that appear in the IMPROVE record. With the northern Rockies and coastal sites removed, the average frequency of NAAPS ratios that fell within a factor of two of IMPROVE increased to just over 51% of the total four-year predictions for springtime.

### 4.3.3 JJA 2001 to 2004

Comparison results for the summer months of 2001-2004 appear in Figure 4.29. On average, the correspondence between NAAPS and IMPROVE [$PM_{10}$-$PM_{2.5}$]+[Soil] was lower in the summer than the spring or winter, with 33% of the NAAPS predictions occurring within a factor of two of the IMPROVE measurements for the 28 IMPROVE sites on average. Frequencies were reasonably high throughout the western U.S. in summer, except at the four southwestern-most sites, whereas frequencies were low throughout the eastern half of the U.S., with the exception of Lye Brook Wilderness, Vermont and Everglades National Park in Florida. Among sites exhibiting low frequencies of agreement with IMPROVE, the median NAAPS/IMPROVE ratios were all well below one.

The persistent presence of sea salt in the aerosol coarse mode is likely still a contributing factor to the low median ratios at sites in the eastern and southeastern U.S. in the summer, however, an under-predicted impact of North African dust sources in NAAPS could also result in the bias of NAAPS/IMPROVE toward very small ratios. Evidence at Brigantine National Wildlife Reserve suggests that at least one Saharan dust event, which resulted in a 24-hour average $PM_{10}$ soil concentration > 20 μg $m^{-3}$ at the site, was not predicted by NAAPS. Other unresolved summer peaks in the IMPROVE record at Brigantine could be due to Saharan dust plumes, given that elevated dust

amounts at the site tend to correspond to elevated Si-to-Ca ratios. Due to the relatively infrequent nature of dust incursions at Brigantine, however, more years of data are necessary to confirm this suspicion.

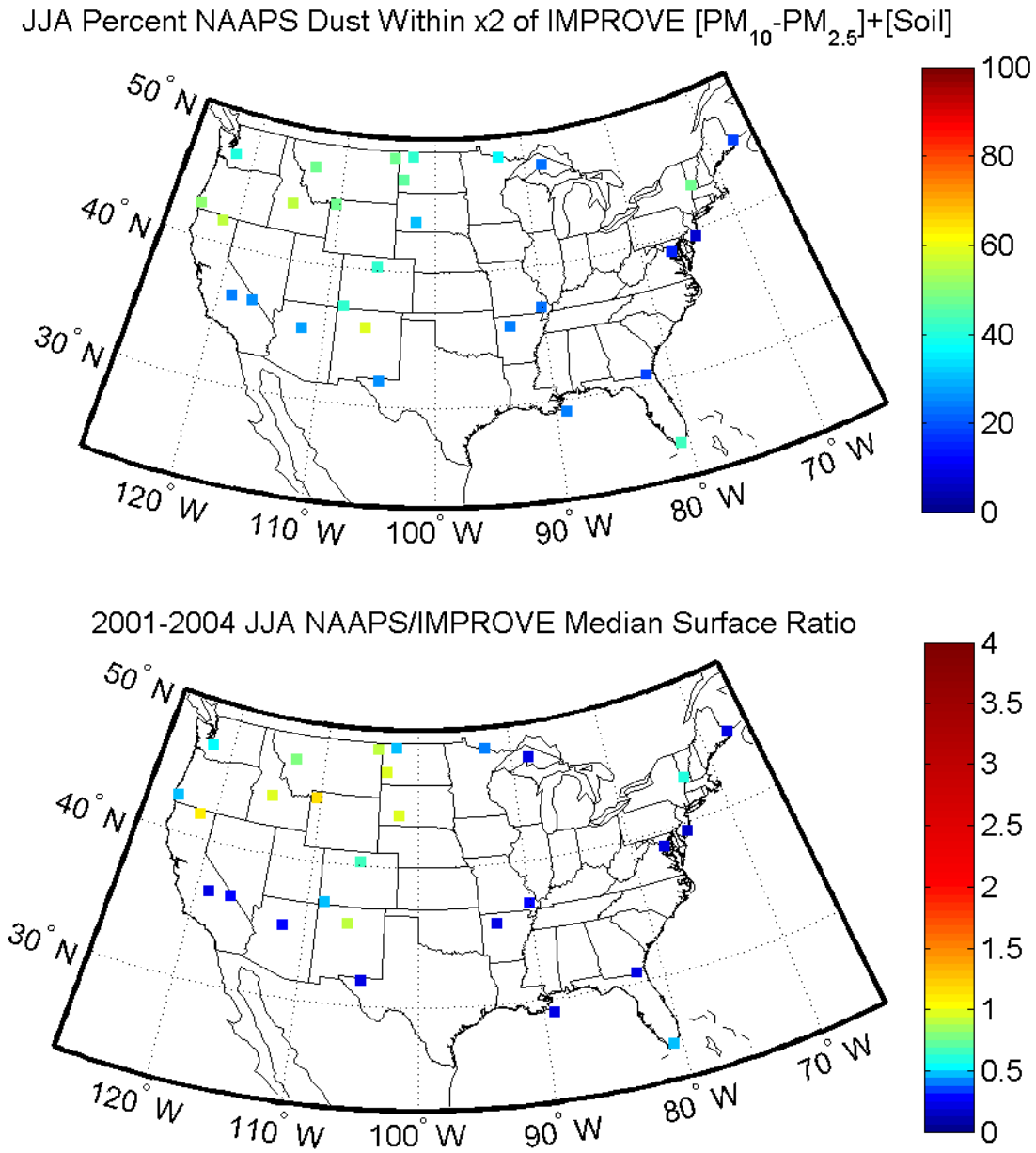


**Figure 4.29: JJA frequency (%) of NAAPS predictions falling within a factor of two of IMPROVE [$PM_{10}$-$PM_{2.5}$]+[Soil] (top) and JJA median ratios of NAAPS to IMPROVE (bottom).**

Another factor that could lead to low NAAPS/IMPROVE ratios throughout the eastern U.S. in the summer is the fact that pollution events are most prevalent during the

season. Strong incident sunlight and stable conditions often result in stagnation periods in which aerosols can be oxidized. In regions of high relative humidity, aerosols can also grow due to water uptake. Thus, the $PM_{10}$ could contain many non-soil species (including residual water mass) that would bias the comparison toward ratios less than one.

In the southwestern U.S., however, the existence of local dust sources and anthropogenic activities are likely to blame for the low median ratios of NAAPS-to-IMPROVE. Studies have shown that Sequoia National Park is heavily influenced by dust emissions from tilling and unpaved roadways during the summer (Chow et al., 1992), which is consistent with the persistently high $PM_{10}$ soil amounts measured at the sites in the summer/early fall of 2003 and 2004. Such an influence may also exist at other southwestern sites like Death Valley National Park in California or Guadelupe Mountains National Park in Texas; however, the episodic nature of high coarse mass at Death Valley (Chapter 3, Section 3.3.1.2) may be more indicative of local, topographically-forced dust storms that are simply not resolved in NAAPS.

### 4.3.4 SON 2001 to 2004

The upper plot in Figure 4.30 indicates that the frequency of NAAPS predictions falling within a factor of two of IMPROVE in the fall months was generally low. 30% of predictions fell in the 2:1/1:2 range of IMPROVE on average during the season. Median ratios were again less than one at the extreme southwestern U.S. sites and throughout the east and southeastern portions of the country. High NAAPS/IMPROVE ratios were realized in the upper Great Plains and once again in the northern Rocky Mountain/Idaho region.

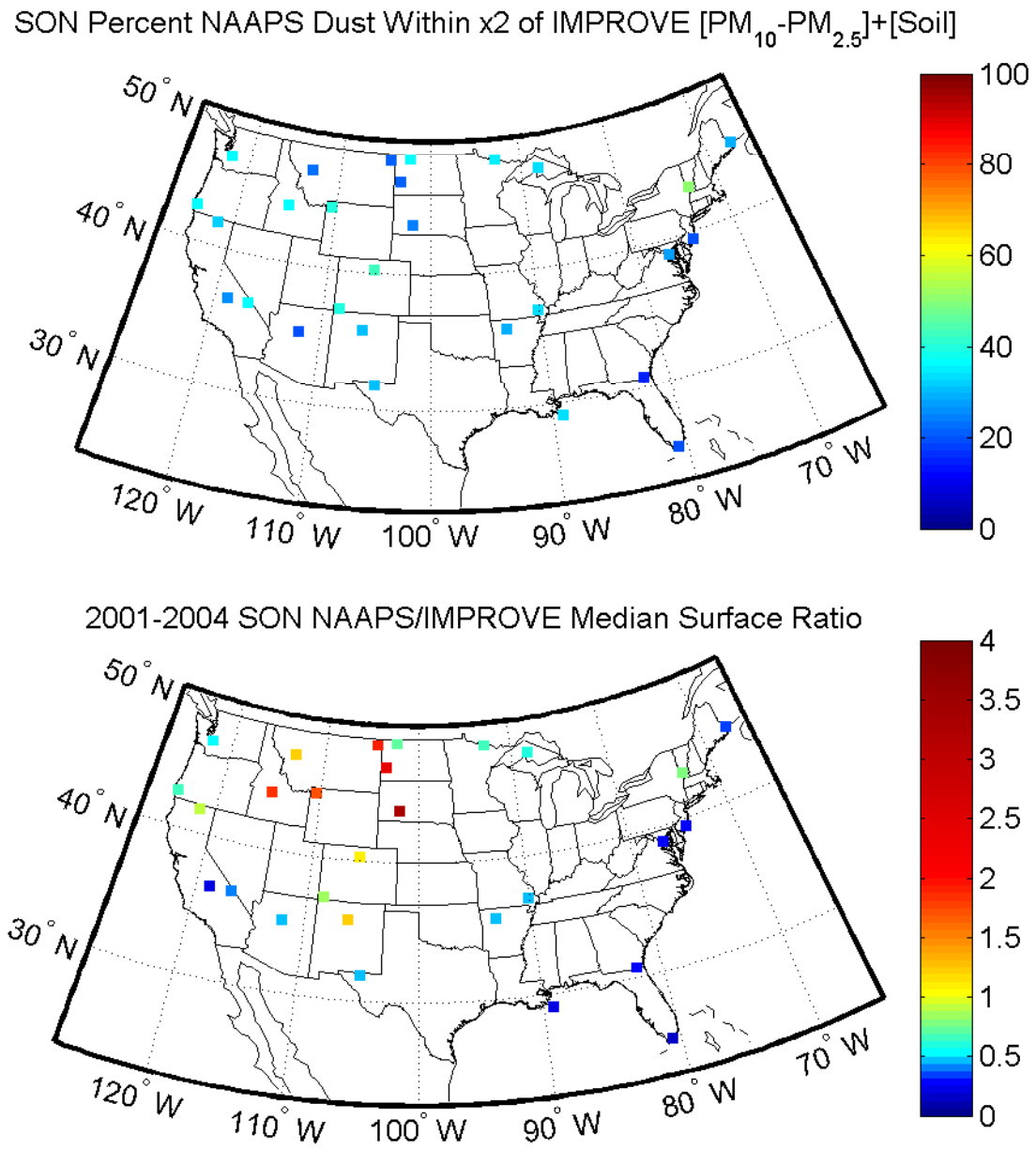


**Figure 4.30: SON frequency (%) of NAAPS predictions falling within a factor of two of IMPROVE [$PM_{10}$-$PM_{2.5}$]+[Soil] (top) and SON median ratios of NAAPS to IMPROVE (bottom).**

The presence of sea salt in the coarse mode aerosol is likely still to blame for low ratios at coastal sites, and also at Upper Buffalo Wilderness and Mingo, Missouri, as southerly flow from the Gulf of Mexico in this season would cause these sites to at least occasionally be impacted by marine air masses. The persistence of high $PM_{10}$ due to agricultural activity was observed into the fall at Sequoia, resulting in a continually low

NAAPS/IMPROVE median ratio. The underestimation of local dust production near other southwestern U.S. sites appears to persist in the fall in NAAPS as well.

NAAPS predicts the most widespread influence of North American dust sources due to vigorous dust production in the High Plains of Montana and southeastern Colorado/northern New Mexico in the fall (Chapter 3, Section 3.2.1). The combination of strong katabatic winds and low surface moisture in these regions results in the generation of frequent, strong pulses of dust in the model. Although such dust production does occur in these regions, as indicated by the spatial pattern of $Ca^{2+}$ ion concentration in rainwater over the U.S. for 2004 (Figure 4.31), the high NAAPS/IMPROVE median ratios during this season indicate that these sources produce more dust in the model than is measured by the IMPROVE network. The addition of snow cover information could help suppress the generation of dust events in Montana in later parts of the year; implementation of a variable threshold friction velocity is probably also necessary to scale down the amount of mass emitted from these sites. However, it is important to note again that the 2001-2004 comparisons were hindered by a lack of IMPROVE measurement sites in the Great Plains states. Several sites in this region were added to the network in/after 2004. Data analysis and comparison of NAAPS to IMPROVE in more recent years would help to clarify the role of regional dust production and transport in this area of the U.S.

NAAPS also mobilizes dust over several smaller sources in Oregon and Idaho during the fall months, resulting in the high NAAPS/IMPROVE median ratios at sites in the northern Rockies. Since these regions are at high elevations, some of this activity could also be suppressed with the addition of snow cover information, although a sensitivity study is needed in order to examine whether this approach would be effective

(or even necessary). It should also be noted that the underestimation of dry deposition processes in the model would result in anomalously high mass concentrations in the vicinity of North American dust source regions.

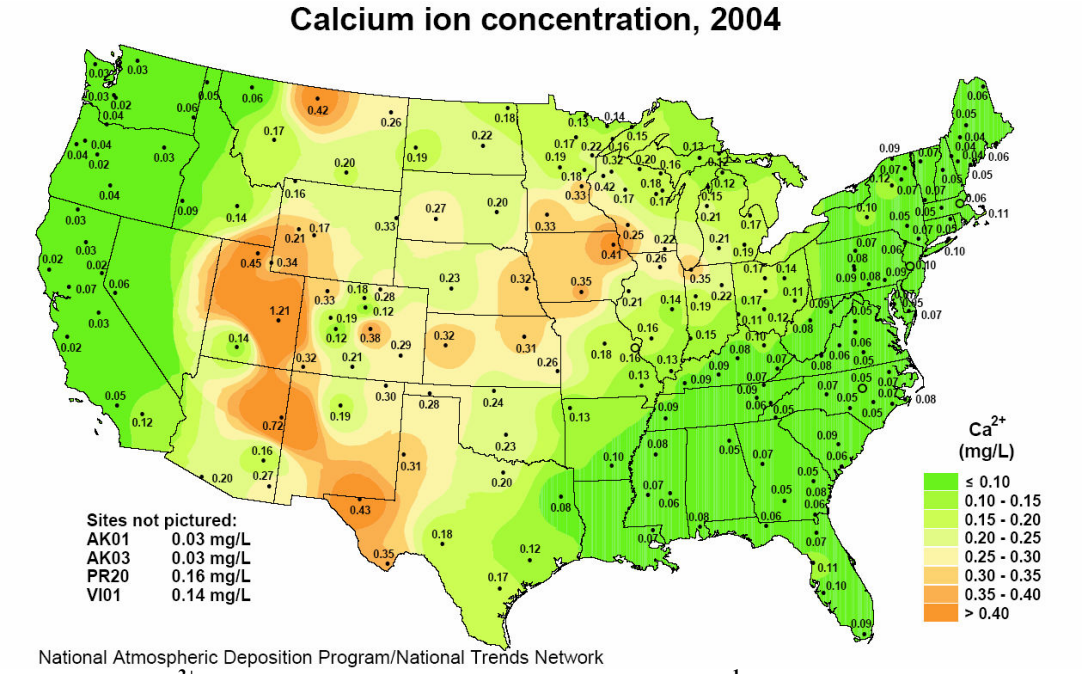


**Figure 4.31: $Ca^{2+}$ ion concentration in rainwater for 2004 (mg $L^{-1}$). (Source: National Atmospheric Deposition Program/National Trends Network (http://nadp.sws.uiuc.edu)).**

# 5 Summary and Future Work

## 5.1 Summary of Findings

This study made use of measurements taken by the Interagency Monitoring of Protected Visual Environments (IMPROVE) network to evaluate NAAPS predictions of surface dust concentrations in the continental U.S. from 2001 to 2004. An examination of the impact of local dust aerosol production and long-range transport over North America was also carried out by running the four-year NAAPS simulation with and without a suppression of North American dust sources.

From 2001 to 2004, NAAPS emitted an average of 1306 Tg of dust annually. This is on the lower end of estimates from six other models, which range from 1019 to 1814 Tg $yr^{-1}$. The bulk of dust emissions in NAAPS occurred in the source regions of North Africa and the Arabian Peninsula, whereas 17 to 19% of annual dust production was simulated over Asia. North American dust sources accounted for less than 2% of the annual atmospheric dust burden in NAAPS; mobilization of North American dust occurred most frequently in the model in eastern Montana, eastern New Mexico/western Texas and southeastern Colorado in total amounts that varied by season. These source regions were predicted to be most active in the fall and winter months, leading to seasonally-averaged mass concentrations above 50 μg $m^{-3}$ in the vicinity of North American sources.

NAAPS predicted the most geographically-widespread influence of non-North American dust sources at the surface over North America in the spring months, in average concentrations ranging from ~5 to 12 μg $m^{-3}$ throughout the western and central U.S. Average concentrations of non-North American dust above 20 μg $m^{-3}$ were predicted in the U.S. in summer, however, these high concentrations were mostly confined to areas of Florida and Texas. These non-North American dust incursions were most likely attributable to Asian sources in the spring, and North African sources in the summer months, although NAAPS predicted some background non-North American dust mass at the surface (≤ 1 μg $m^{-3}$) in the continental U.S. throughout the year. NAAPS seasonally-averaged total column dust predictions revealed that NAAPS predicted a zonal region of trans-Pacific dust transport from 30º to 50º N in spring, which is consistent with a long-term climatological estimate (Zhao et al., 2006). Trans-Atlantic transport of North African dust to the U.S., on the other hand, was simulated south of 30º N, along the southern branch of the semi-permanent Bermuda high in the summer.

The dust flux in NAAPS is scaled to represent the mass attributable to dust particles smaller than 10 μm in diameter. If the aerosol coarse mass concentration, [$PM_{10}$-$PM_{2.5}$], measured by the IMPROVE network is assumed to contain only insoluble crustal material, total $PM_{10}$ soil mass concentrations can be estimated from the IMPROVE data as [$PM_{10}$-$PM_{2.5}$]+[Soil], where [Soil] refers to the mass concentration of soil particles smaller than 2.5 μm in diameter, reconstructed from the measured $PM_{2.5}$ mass concentrations of Al, Ca, Si, Ti and Fe. A dataset containing information on the coarse mode composition measured at a few IMPROVE sites in 2004 provided a means to investigate this method of estimating the $PM_{10}$ soil concentrations and to test our

hypothesis that these assumptions were not universally valid. We confirmed that the method overestimates total $PM_{10}$ soil concentrations at many sites due to the presence of sea salt and organic aerosol in the coarse mode. In the fall and winter months at sites in the western U.S., soil particles actually comprised a very small total of the coarse mass fraction. Since correction factors for the actual soil fraction of the aerosol coarse mass concentration varied widely among sites and seasons, we did not attempt to apply those derived from this small subset of sites to the entire set of IMPROVE data for the purpose of comparisons with NAAPS. However, these biases in the measurements must be kept in mind when evaluating the degree of agreement between NAAPS and the *in situ* data.

Comparisons of NAAPS predictions to the IMPROVE $[PM_{10}\text{-}PM_{2.5}]$+[Soil] were performed at 28 IMPROVE sites throughout the continental U.S. In winter, an average of 39% of NAAPS predictions fell within a factor of two of the IMPROVE measurements. Higher frequencies of agreement (on the order of 50% or higher) occurred throughout the southwestern U.S., the Great Lake states, and the New England states, whereas sites in the northwestern and east/southeastern U.S. exhibited lower frequencies. Median ratios of NAAPS-to-IMPROVE were greater than one at the northwestern sites, but less than one at the eastern and southeastern U.S. sites, for the following possible reasons:

- Very clean overall conditions throughout the western U.S.
- Possible regional dust influences in the central U.S. that are not captured by NAAPS
- Maximum production of sea salt aerosol occurs in winter, contributing to large sea salt loadings in the coarse mode at coastal sites, and perhaps certain inland sites as well

In spring, when Asian dust transport to the U.S. is maximized, NAAPS predictions had the highest degree of agreement with the IMPROVE measurements, as hypothesized. On average, 45% of the predictions were within a factor of two of the IMPROVE measurements during this season for 2001-2004. The lowest frequencies occurred at coastal and southeastern sites, and elevated sites (at altitudes above ~1200 meters) in northern California, Idaho, and the northern Rockies. Median NAAPS/IMPROVE ratios were again low at the coastal and southeastern sites, but were greater than one at the northern Rockies sites, and throughout the western U.S. Some explanations for this behavior include:

- A consistent bias of the IMPROVE measurements at coastal sites due to sea salt aerosol in the coarse mode
- Potential underestimation of removal processes during long-range transport, resulting in high mass concentrations in the free troposphere and high median NAAPS/IMPROVE ratios at elevated measurement sites

Agreement between NAAPS and IMPROVE was lower in the summer than in the spring and winter months. The average frequency of NAAPS predictions that feel within a factor of two of the IMPROVE measurements was 33%. Frequencies were lowest throughout the eastern half of the U.S. and for some sites in the southwestern U.S.; median ratios less than one were realized at all of these sites due to a few potential issues:

- Sea salt in the coarse mode at coastal sites
- A potential underestimation by NAAPS of the spatial extent of Saharan dust transport in the eastern U.S.

- Summer pollution events and high relative humidity in the southeastern U.S., enhancing IMPROVE $PM_{10}$ compositions and leading to an incorrect interpretation of the large coarse fraction as soil dust
- Local topographically-forced dust storms and fugitive dust due to agricultural processes at Sequoia National Park and other sites in the southwestern U.S.

NAAPS and IMPROVE had the lowest correspondence during the fall months of 2001-2004, with an average of 30% of NAAPS predictions falling within a factor of two of the IMPROVE $[PM_{10}\text{-}PM_{2.5}]$+[Soil] measurements. Median ratios below one occurred throughout the eastern and southwestern U.S., and at sites in the High Plains and northern Rocky Mountains due to:

- Sea salt in the coarse mode
- Persistent influence of agricultural activities and/or local dust production at southwestern sites that is unresolved in NAAPS
- Vigorous model dust production in the High Plains and Oregon/Idaho due to a lack of snow cover information in NAAPS and/or the potential need for a higher threshold friction velocity; also a potential underestimation of dry deposition in the vicinity of these source regions

## 5.2 Suggestions for Future Work

Based upon the findings in this study and the continual interest in investigating the behavior of NAAPS in the continental U.S., some suggested areas of future work include:

- **Utilize the Coupled Ocean/Atmosphere Mesoscale Prediction System (COAMPS) to simulate dust lofting in North America.**

The Navy's Coupled Ocean/Atmosphere Mesocale Prediction System (COAMPS) is a non-hydrostatic mesoscale forecast model used to provide the DoD with reliable short-term meteorological forecasts. Preliminary results using COAMPS to generate dust forecasts over the Arabian Peninsula indicate that the model has good skill in resolving the fine-scale variability of dust storms in the region. Due to the complex terrain in the vicinity of North American dust sources, such a tool would be extremely useful in quantifying the relative impacts of local dust production and long-range dust transport over the continental U.S. Implementing new source functions to describe the seasonal cycle of agricultural processes may also be required to resolve the influence of dust mobilization in the southwestern and central U.S., although more observation stations in the Plains states are first necessary to better quantify the magnitudes of regional dust production in this part of the country.

- **Investigate possible unique tracers for Asian and North American dusts.**

Although case studies have confirmed episodic, intense Asian dust events in North America (Husar et al., 2001; Thulasiraman et al., 2002), only a few studies (Jaffe et al., 2005; Liu et al., 2003; VanCuren, 2003; VanCuren and Cahill, 2002) have tried to quantify the impact of Asian aerosols at sites in the continental U.S. on longer timescales and over a broad geographic region. Aluminum-to-calcium and silicon-to-calcium ratios can be used to separate the influence of calcium-depleted North African dust from calcium-enriched Asian or southwestern U.S. dusts at U.S. sites with some confidence; however, VanCuren and Cahill (2002) note that the Al/Ca upper-limit used in their study to identify Asian dust in North America (2.6) has some overlap with source regions in the southwestern U.S. Given that NAAPS appears to predict at least a background amount of

Asian dust throughout the year at several U.S. sites, it will be necessary to investigate other potential means of separating dusts of Asian origin from those of North American origin.

- **Examine variability in the optical properties of dust.**

Currently, the optical depth forecasts in NAAPS are constructed from NAAPS mass predictions using the same mass scattering efficiency for all dust generated in the model. Since dusts from different source regions have different chemical characteristics, different mean sizes, and may potentially be coated with different substances, it would be useful to compile average values of mean size and mass scattering efficiency for the main dust-producing regions of the world to be used in creating forecasts of aerosol optical depth. Since dust that has undergone long-range transport is generally dominated by smaller particles that are more efficient at extinguishing incident light, this is especially important in order to quantify the optical depths associated with Asian and North African dust events over the continental U.S.

- **Study NAAPS predicted dust plume height in the presence of ice clouds.**

It has been mentioned that certain types of dust are potentially good at nucleating ice formation at warmer temperatures. Since satellite products cannot currently be used to infer plume height, and are often not reliable in diagnosing the presence of dust aerosol over land, models provide the only real "data" on the vertical structure of dust aerosol transport in real time, particularly for plumes containing low mass concentrations that could still affect ice cloud formation. Integrating NAAPS predictions with information about ice cloud locations from lidar or the International Satellite Cloud Climatology

Project (ISCCP) could be used to investigate relationships between atmospheric dust concentration and ice cloud occurrence.

- **Find ways to determine sea salt amounts from aerosol measurements and revisit current IMPROVE assumptions about OC, sulfate, and nitrate.**

Sea salt in the coarse mode was found to be a confounding factor in the NAAPS-to-IMPROVE comparisons at many sites in all seasons of this study. Thus, it would be useful to have a robust means of separating sea salt from other $PM_{10}$ species. The IMPROVE network is currently also investigating methods to quantify the amount of sea salt aerosol that is present in the fine mode. Estimating marine mass by differencing measured components of the fine mass from the gravimetric $PM_{2.5}$ has been suggested (Prospero, personal communication); however, this method is only valid if assumptions about the total mass of sulfate, nitrate, and organic compounds are also valid. Studies have shown, however, that the current OC multiplier of 1.4 used by the IMPROVE network may be an underestimate at some urban and most remote sites (Turpin and Lim, 2001). The amount of ammonia present in the aerosol species is also an unknown in the IMPROVE network, leading to uncertainties in the organic, sulfate, and nitrate masses that could very well be on the order of the sea salt mass present at coastal monitoring stations.

- **Examine NAAPS sulfate product in the continental U.S.**

Although this study focused on the production and transport of soil dust aerosol in the U.S., a preliminary comparison of sulfate predictions in NAAPS to measured aerosol sulfur concentrations in IMPROVE was also carried out. After examining a few IMPROVE sites, it appears that NAAPS compares well or slightly overestimates the

mass at sites with higher sulfate amounts (Figure 5.1); whereas it tends to underestimate the sulfate mass at cleaner sites. A more complete investigation of the sulfate transport and chemistry in NAAPS is necessary to confirm these patterns, however.

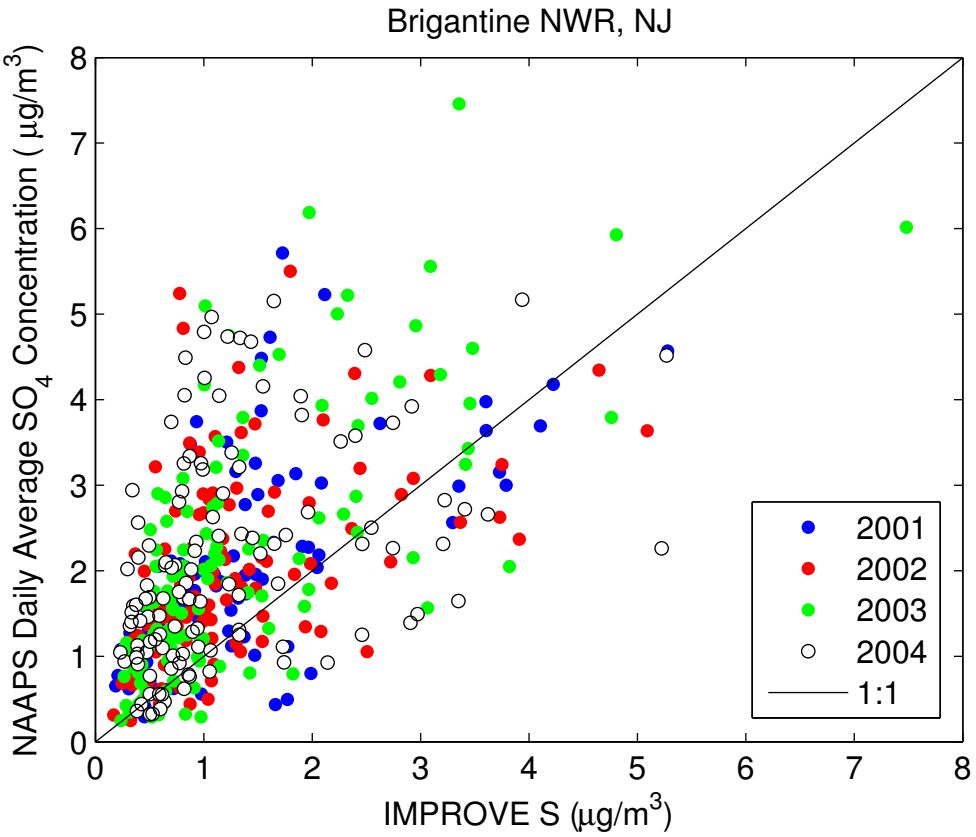


**Figure 5.1: NAAPS daily sulfur concentrations versus IMPROVE aerosol sulfur measured from 2001-2004 at Brigantine National Wildlife Reserve, New Jersey.**

REFERENCES

Biscaye, P. E., F. E. Grousset, M. Revel, S. VanderGaast, G. A. Zielinski, A. Vaars, and G. Kukla, 1997: Asian provenance of glacial dust (stage 2) in the Greenland Ice Sheet Project 2 Ice Core, Summit, Greenland. *Journal of Geophysical Research-Oceans*, **102,** 26765-26781.

California-Davis, cited 2006: IMPROVE Data Guide. [Available online from http://vista.cira.colostate.edu/improve/Publications/OtherDocs/IMPROVEDataGuide/IMPROVEDataGuide.htm.]

Chow, J. C., J. G. Watson, D. H. Lowenthal, P. A. Solomon, K. L. Magliano, S. D. Ziman, and L. W. Richards, 1992: Pm10 Source Apportionment in California San-Joaquin Valley. *Atmospheric Environment Part a-General Topics*, **26,** 3335-3354.

Christensen, J. H., 1997: The Danish Eulerian hemispheric model - A three-dimensional air pollution model used for the Arctic. *Atmospheric Environment*, **31,** 4169-4191.

Danielsen, E. F., 1980: Stratospheric Source for Unexpectedly Large Values of Ozone Measured over the Pacific-Ocean During Gametag, August 1977. *Journal of Geophysical Research-Oceans and Atmospheres*, **85,** 401-412.

Dubovik, O., B. N. Holben, M. D. King, A. Smirnov, T. F. Eck, S. Kinne, and I. Slutsker, 1999: A flexible inversion algorithm for the retrieval of aerosol optical properties from sun and sky radiance measurements. *ALPS '99*, Cent. Natl. d'Etudes Spatiales, Meribel, France.

Duce, R. A., 1995: Sources, distributions, and fluxes of mineral aerosols and their relationship to climate. *Aerosol Forcing of Climate: Report of the Dahlem Workshop on Aerosol Forcing of Climate*, R. J. Charlson and J. Heintzenberg, Eds., John Wiley, 43-72.

Duce, R. A., C. K. Unni, B. J. Ray, J. M. Prospero, and J. T. Merrill, 1980: Long-Range Atmospheric Transport of Soil Dust from Asia to the Tropical North Pacific - Temporal Variability. *Science*, **209,** 1522-1524.

Eck, T. F., B. N. Holben, J. S. Reid, O. Dubovik, A. Smirnov, N. T. O'Neill, I. Slutsker, and S. Kinne, 1999: Wavelength dependence of the optical depth of biomass burning, urban, and desert dust aerosols. *Journal of Geophysical Research-Atmospheres*, **104,** 31333-31349.

Feingold, G., W. R. Cotton, S. M. Kreidenweis, and J. T. Davis, 1999: The impact of giant cloud condensation nuclei on drizzle formation in stratocumulus: Implications for cloud radiative properties. *Journal of the Atmospheric Sciences*, **56,** 4100-4117.

Finlayson-Pitts, B. J. and J. C. Hemminger, 2000: Physical chemistry of airborne sea salt particles and their components. *Journal of Physical Chemistry A*, **104,** 11463-11477.

Gillette, D., 1978: Wind-Tunnel Simulation of Erosion of Soil - Effect of Soil Texture, Sandblasting, Wind Speed, and Soil Consolidation on Dust Production. *Atmospheric Environment*, **12,** 1735-1743.

Ginoux, P., M. Chin, I. Tegen, J. M. Prospero, B. Holben, O. Dubovik, and S. J. Lin, 2001: Sources and distributions of dust aerosols simulated with the GOCART model. *Journal of Geophysical Research-Atmospheres*, **106,** 20255-20273.

Hand, J. L., S. M. Kreidenweis, D. E. Sherman, J. L. Collett, S. V. Hering, D. E. Day, and W. C. Malm, 2002: Aerosol size distributions and visibility estimates during the Big Bend regional aerosol and visibility observational (BRAVO) study. *Atmospheric Environment*, **36,** 5043-5055.

Haywood, J. M., R. P. Allan, I. Culverwell, T. Slingo, S. Milton, J. Edwards, and N. Clerbaux, 2005: Can desert dust explain the outgoing longwave radiation anomaly over the Sahara during July 2003? *Journal of Geophysical Research-Atmospheres*, **110,** D05105, doi:10.1029/2004JD005232.

Heald, C. L., D. J. Jacob, R. J. Park, L. M. Russell, B. J. Huebert, J. H. Seinfeld, H. Liao, and R. J. Weber, 2005: A large organic aerosol source in the free troposphere missing from current models. *Geophysical Research Letters*, **32,** L18809, doi:1029/2005GL023831.

Hillel, D., 1982: *Introduction to Soil Physics*. Academic.

Hogan, T. F. and T. E. Rosmond, 1991: The Description of the Navy Operational Global Atmospheric Prediction Systems Spectral Forecast Model. *Monthly Weather Review*, **119,** 1786-1815.

Husar, R. B., D. M. Tratt, B. A. Schichtel, S. R. Falke, F. Li, D. Jaffe, S. Gasso, T. Gill, N. S. Laulainen, F. Lu, M. C. Reheis, Y. Chun, D. Westphal, B. N. Holben, C. Gueymard, I. McKendry, N. Kuring, G. C. Feldman, C. McClain, R. J. Frouin, J. Merrill, D. DuBois, F. Vignola, T. Murayama, S. Nickovic, W. E. Wilson, K. Sassen, N. Sugimoto, and W. C. Malm, 2001: Asian dust events of April 1998. *Journal of Geophysical Research-Atmospheres*, **106,** 18317-18330.

IPCC, 2001: *Climate Change 2001: The Scientific Basis. Contribution of Working Group to the Third Assessment Report of the Intergovernmental Panel on Climate Change*.

Jaffe, D., S. Tamura, and J. Harris, 2005: Seasonal cycle and composition of background fine particles along the west coast of the US. *Atmospheric Environment*, **39,** 297-306.

Karyampudi, V. M., S. P. Palm, J. A. Reagen, H. Fang, W. B. Grant, R. M. Hoff, C. Moulin, H. F. Pierce, O. Torres, E. V. Browell, and S. H. Melfi, 1999: Validation of the Saharan dust plume conceptual model using lidar, Meteosat, and ECMWF data. *Bulletin of the American Meteorological Society*, **80,** 1045-1075.

Liu, W., P. K. Hopke, and R. A. VanCuren, 2003: Origins of fine aerosol mass in the western United States using positive matrix factorization. *Journal of Geophysical Research-Atmospheres*, **108,** D23, 4716, doi:10.1029/2003JD003678.

Loveland, T. R., B. C. Reed, J. F. Brown, D. O. Ohlen, Z. Zhu, L. Yang, and J. W. Merchant, 2000: Development of a global land cover characteristics database and IGBP DISCover from 1 km AVHRR data. *International Journal of Remote Sensing*, **21,** 1303-1330.

Luo, C., N. M. Mahowald, and J. del Corral, 2003: Sensitivity study of meteorological parameters on mineral aerosol mobilization, transport, and distribution. *Journal of Geophysical Research-Atmospheres*, **108,** D15, 4447, doi:10.1029/2003JD003483.

Malm, W. C., J. F. Sisler, D. Huffman, R. A. Eldred, and T. A. Cahill, 1994: Spatial and Seasonal Trends in Particle Concentration and Optical Extinction in the United-States. *Journal of Geophysical Research-Atmospheres*, **99,** 1347-1370.

Malm, W. C., B. A. Schichtel, M. L. Pitchford, L. L. Ashbaugh, and R. A. Eldred, 2004: Spatial and monthly trends in speciated fine particle concentration in the United States. *Journal of Geophysical Research-Atmospheres*, **109,** D03306, doi:10.1029/2003JD003739.

Merrill, J. T., M. Uematsu, and R. Bleck, 1989: Meteorological Analysis of Long-Range Transport of Mineral Aerosols over the North Pacific. *Journal of Geophysical Research-Atmospheres*, **94,** 8584-8598.

Miller, R. L., I. Tegen, and J. Perlwitz, 2004: Surface radiative forcing by soil dust aerosols and the hydrologic cycle. *Journal of Geophysical Research-Atmospheres*, **109,** D04203, doi:10.1029/2003JD004085.

Myhre, G., F. Stordal, M. Johnsrud, A. Ignatov, M. I. Mischenko, I. V. Geogdzhayev, D. Tanre, J. L. Deuze, P. Goloub, T. Nakajima, A. Higurashi, O. Torres, and B. Holben, 2004: Intercomparison of satellite retrieved aerosol optical depth over the ocean. *Journal of the Atmospheric Sciences*, **61,** 499-513.

Parker, D. J., C. D. Thorncroft, R. R. Burton, and A. Diongue-Niang, 2005: Analysis of the African easterly jet, using aircraft observations from the JET2000 experiment. *Quarterly Journal of the Royal Meteorological Society*, **131,** 1461-1482.

Patterson, E. M., D. A. Gillette, and B. H. Stockton, 1977: Complex Index of Refraction between 300 and 700 Nm for Saharan Aerosols. *Journal of Geophysical Research-Oceans and Atmospheres*, **82,** 3153-3160.

Perry, K. D., T. A. Cahill, R. A. Eldred, D. D. Dutcher, and T. E. Gill, 1997: Long-range transport of North African dust to the eastern United States. *Journal of Geophysical Research-Atmospheres*, **102,** 11225-11238.

Prospero, J. M., P. Ginoux, O. Torres, S. E. Nicholson, and T. E. Gill, 2002: Environmental characterization of global sources of atmospheric soil dust identified with the Nimbus 7 Total Ozone Mapping Spectrometer (TOMS) absorbing aerosol product. *Reviews of Geophysics*, **40,** 1002, doi:10.1029/2000RG000095.

Reid, J. S., R. G. Flocchini, T. A. Cahill, and R. S. Ruth, 1994: Local Meteorological, Transport, and Source Aerosol Characteristics of Late Autumn Owens Lake (Dry) Dust Storms. *Atmospheric Environment*, **28,** 1699-1706.

Sassen, K., 2002: Indirect climate forcing over the western US from Asian dust storms. *Geophysical Research Letters*, **29,** 1465, doi:10.1029/2001GL014051.

Sassen, K., P. J. DeMott, J. M. Prospero, and M. R. Poellot, 2003: Saharan dust storms and indirect aerosol effects on clouds: CRYSTAL-FACE results. *Geophysical Research Letters*, **30,** 1633, doi:10.1029/2003GL017371.

Shaw, G. E., 1980: Transport of Asian Desert Aerosol to the Hawaiian-Islands. *Journal of Applied Meteorology*, **19,** 1254-1259.

Smirnov, A., B. N. Holben, D. Savoie, J. M. Prospero, Y. J. Kaufman, D. Tanre, T. F. Eck, and I. Slutsker, 2000: Relationship between column aerosol optical thickness and in situ ground based dust concentrations over Barbados. *Geophysical Research Letters*, **27,** 1643-1646.

Sokolik, I. N. and O. B. Toon, 1999: Incorporation of mineralogical composition into models of the radiative properties of mineral aerosol from UV to IR wavelengths. *Journal of Geophysical Research-Atmospheres*, **104,** 9423-9444.

Tegen, I. and I. Fung, 1994: Modeling of Mineral Dust in the Atmosphere - Sources, Transport, and Optical-Thickness. *Journal of Geophysical Research-Atmospheres*, **99,** 22897-22914.

——, 1995: Contribution to the Atmospheric Mineral Aerosol Load from Land-Surface Modification. *Journal of Geophysical Research-Atmospheres*, **100,** 18707-18726.

Tegen, I. and A. A. Lacis, 1996: Modeling of particle size distribution and its influence on the radiative properties of mineral dust aerosol. *Journal of Geophysical Research-Atmospheres*, **101,** 19237-19244.

Tegen, I., S. P. Harrison, K. E. Kohfeld, S. Engelstaedter, and M. Werner, 2002: Emission of soil dust aerosol: Anthropogenic contribution and future changes. *Geochimica Et Cosmochimica Acta*, **66,** A766-A766.

Thulasiraman, S., N. T. O'Neill, A. Royer, B. N. Holben, D. L. Westphal, and L. J. B. McArthur, 2002: Sunphotometric observations of the 2001 Asian dust storm over Canada and the US. *Geophysical Research Letters*, **29,** 1255, 10.1029/2001GL014188.

Turpin, B. J. and H. J. Lim, 2001: Species contributions to PM2.5 mass concentrations: Revisiting common assumptions for estimating organic mass. *Aerosol Science and Technology*, **35,** 602-610.

van der Schrier, G., K. R. Briffa, T. J. Osborn, and E. R. Cook, 2006: Summer moisture availability across North America. *Journal of Geophysical Research-Atmospheres*, **111,** D11102, doi:10.1029/2005JD006745.

VanCuren, R. A., 2003: Asian aerosols in North America: Extracting the chemical composition and mass concentration of the Asian continental aerosol plume from long-term aerosol records in the western United States. *Journal of Geophysical Research-Atmospheres*, **108,** 4623, doi:10.1029/2003JD003459.

VanCuren, R. A. and T. A. Cahill, 2002: Asian aerosols in North America: Frequency and concentration of fine dust. *Journal of Geophysical Research-Atmospheres*, **107,** 4804, doi:10.1029/2002JD002204.

Vasconcelos, L. A. D., J. D. W. Kahl, D. S. Liu, E. S. Macias, and W. H. White, 1996: Patterns of dust transport to the Grand Canyon. *Geophysical Research Letters*, **23,** 3187-3190.

Weaver, C. J., P. Ginoux, N. C. Hsu, M. D. Chou, and J. Joiner, 2002: Radiative forcing of Saharan dust: GOCART model simulations compared with ERBE data. *Journal of the Atmospheric Sciences*, **59,** 736-747.

Westphal, D. L., O. B. Toon, and T. N. Carlson, 1988: A Case-Study of Mobilization and Transport of Saharan Dust. *Journal of the Atmospheric Sciences*, **45,** 2145-2175.

Witek, M. L., P. J. Flatau, P. K. Quinn, and D. L. Westphal, in preparation: Global sea salt modeling: results and validation against multi-campaign shipboard measurements. *Journal of Geophysical Research*.

Zender, C. S., H. S. Bian, and D. Newman, 2003: Mineral Dust Entrainment and Deposition (DEAD) model: Description and 1990s dust climatology. *Journal of Geophysical Research-Atmospheres*, **108,** 4416, doi:10.1029/2002JD002775.

Zhao, T. L., S. L. Gong, X. Y. Zhang, J. P. Blanchet, I. G. McKendry, and Z. J. Zhou, 2006: A simulated climatology of Asian dust aerosol and its trans-Pacific transport. Part I: Mean climate and validation. *Journal of Climate*, **19,** 88-103.